

SYNTHETIC IDENTIFICATION OF NOVEL BENZAMIDE ANALOGS INHIBITING ACETYLCHOLINESTERASE BY 2D QSAR ANALYSIS AND INSILICO TECHNIQUES

A Dissertation submitted to
THE TAMILNADU Dr. M.G.R MEDICAL UNIVERSITY
CHENNAI – 600032

In partial fulfillment of the requirements for the award of the degree of

MASTER OF PHARMACY
IN
BRANCH - II (PHARMACEUTICAL CHEMISTRY)

SUBMITTED BY

BHUVANESWARI. S **(261915002)**

Under the Guidance of

Mr. R. VIJAYAKUMAR, M.Pharm.

Associate Professor

Department of Pharmaceutical Analysis



C.L. BAID METHA COLLEGE OF PHARMACY.

(An ISO 9001-2008 certified Institute)

THORAIPAKKAM, CHENNAI-600097

OCTOBER 2021

SYNTHETIC IDENTIFICATION OF NOVEL BENZAMIDE ANALOGS INHIBITING ACETYLCHOLINESTERASE BY 2D QSAR ANALYSIS AND INSILICO TECHNIQUES

A Dissertation submitted to
THE TAMILNADU Dr. M.G.R MEDICAL UNIVERSITY
CHENNAI – 600032

In partial fulfillment of the requirements for the award of the degree of

MASTER OF PHARMACY
IN
BRANCH - II (PHARMACEUTICAL CHEMISTRY)

SUBMITTED BY

BHUVANESWARI. S **(261915002)**

Under the Guidance of

Mr. R. VIJAYAKUMAR, M.Pharm.

Associate Professor

Department of Pharmaceutical Analysis



C.L. BAID METHA COLLEGE OF PHARMACY.

(An ISO 9001-2008 certified Institute)

THORAIPAKKAM, CHENNAI-600097

OCTOBER 2021



Mr. R.VIJAYAKUMAR, M. Pharm,

Associate professor

Department of Pharmaceutical Analysis.

CERTIFICATE

This is to certify that **S. BHUVANESWARI (261915002)**, carried out the dissertation work on “**SYNTHETIC IDENTIFICATION OF NOVEL BENZAMIDE ANALOGS INHIBITING ACETYLCHOLINESTERASE BY 2D QSAR ANALYSIS AND INSILICO TECHNIQUES**” for the award of degree of **MASTER OF PHARMACY** under **THE TAMILNADU Dr. M.G.R. MEDICAL UNIVERSITY, CHENNAI- 600097** in the **academic year 2019-21** under my Supervision and Guidance in the Department of Pharmaceutical Chemistry, **C.L. BAID METHA COLLEGE OF PHARMACY, CHENNAI-600 097** during the academic year 2019-2021.

PLACE: CHENNAI-97.

DATE:

ASSO. Prof. R. VIJAYAKUMAR M.Pharm,
Department of Pharmaceutical Analysis,
C.L. BAID METHA COLLEGE OF PHARMACY
CHENNAI – 600 097.



Prof. Dr. Grace Rathnam, M. Pharm, Ph.D.,

Principal & HOD,

Department of Pharmaceutics.

CERTIFICATE

This is to certify that the project entitled “**SYNTHETIC IDENTIFICATION OF NOVEL BENZAMIDE ANALOGS INHIBITING ACETYLCHOLINESTERASE BY 2D QSAR ANALYSIS AND INSILICO TECHNIQUES**” as submitted by **S. BHUVANESWARI (261915002)**, in partial fulfillment for the award of the degree of **Master of Pharmacy** in the academic year **2019-21**. It was carried out at **C.L. BAID METHA COLLEGE OF PHARMACY, CHENNAI – 600097** under the guidance and supervision of **Mr. R. VIJAYAKUMAR, M.Pharm**, Associate Professor in the Department of Pharmaceutical Analysis during the academic year 2019 – 2021.

PLACE: CHENNAI-97.

DATE:

Dr. Grace Rathnam, M. Pharm, Ph.D.,

Principal & HOD,

Department of Pharmaceutics,

C.L. BAID METHA COLLEGE OF PHARMACY

CHENNAI – 600 097.

DECLARATION

I do hereby declare that the thesis entitled “**SYNTHETIC IDENTIFICATION OF NOVEL BENZAMIDE ANALOGS INHIBITING ACETYLCHOLINESTERASE BY 2D QSAR ANALYSIS AND INSILICO TECHNIQUES**” by **S. BHUVANESWARI (261915002)**, in partial fulfillment of the degree of **MASTER OF PHARMACY** was carried out at **C.L. BAID METHA COLLEGE OF PHARMACY, CHENNAI-600 097** under the guidance and Supervision of **Mr. R. VIJAYAKUMAR, M.Pharm**, during the academic year 2019-2021. The work embodied in this thesis is original & is not submitted in part or full for any other degree of this or any other University.

PLACE: CHENNAI-97.

DATE:

S. BHUVANESWARI

(261915002)

**DEPARTMENT OF PHARMACEUTICAL CHEMISTRY
C.L. BAID METHA COLLEGE OF PHARMACY
CHENNAI – 600 097.**

ACKNOWLEDGEMENT

My deepest gratitude goes to my family for their unflagging love & support throughout my life, they who introduced me to this competitive pharmacy world.

I wish to thank our beloved Principal **Dr. GRACE RATHNAM, M.Pharm., Ph.D.** for providing me great exposure with necessary facilities and scheduled time to do my project in our college premises.

My privilege to express our grateful and sincere gratitude to **Prof. R. VIJAYAKUMAR M.Pharm.**, Associate Professor of Pharmaceutical Analysis Department for his great support and guidance to move my project in a right direction. In addition, his perpetual energy & enthusiasm motivated us to get interest in research.

I especially want to thank **Prof. Dr. N. RAMALAKSHMI, M.Pharm., Ph.D.** Head of Pharmaceutical Chemistry Department for her support & providing us to work in their lab & her advice boosted me.

I would like to thank **Mr. SRINIVASAN & Mrs. SHANTHI** (stores in-charge) who provided the chemicals and supported me to complete our project. Also, I thank the entire **NON-TEACHING STAFFS** who helped us to complete my project.

CONTENTS

PARTICULARS	PAGE NO.
1. INTRODUCTION	1
2. BENZAMIDE AS A CORE	2
3. ACTIVITY	
3.1. ACETYLCHOLINE	3
3.2. CHOLINESTERASE	3
3.3. CHOLINERGIC NEURON AND ALZHEIMER	4
4. QSAR	5
5. DOCKING	6
6. REVIEW OF LITREATURE	7
7. AIM OF THE RESEARCH	13
7.1. OBJECTIVE OF THE RESEARCH	
8. PLAN OF STUDY	14
9. MATERIALS AND METHODS	
9.1. 2D-QSAR APPROACH	15
9.2. COMPOUNDS DESIGNING	33
9.3. <i>INSILICO</i> SCREENING OF LIGANDS	40
9.4. SCHEME	46
9.5. GENERAL PROCEDURE OF SYNTHESIS	47
9.6. CHARACTERISATION	47
10. RESULTS AND DISCUSSION	
10.1. 2D QSAR MODEL	49
10.2. COMPOUNDS DESIGNED	59
10.3. <i>INSILICO</i> SCREENING RESULTS	60
10.4. QSAR RESULT FOR NOVEL COMPOUNDS	65
10.5. DOCKING RESULTS	66
10.6. SYNTHESIS	73
10.7. CHARACTERIZATION	74
11. REFERENCES	75

LIST OF ABREVIATIONS

AD	-	Alzheimer's disease
CNS	-	Central nervous system
NFTs	-	Neuro Fibrillary Tangles
BBB	-	Blood Brain Barrier
AchE	-	Acetylcholinesterase
BchE	-	Butrylcholesterase
APP	-	Amyloid Precursor Protein
TLC	-	Thin Layer Chromatography
IR	-	Infrared
¹H-NMR	-	Proton Nuclear Magnetic Resonance
m.p	-	Melting Point
Mol.For	-	Molecular Formula
Mol.Wt	-	Molecular Weight
Mg	-	Milligram
µg	-	Microgram
Min	-	Minutes

1. INTRODUCTION:

Medicinal chemistry is defined as an interdependent mature science that is a combination of applied (medicine) and basic (chemistry) sciences. It encompasses the discovery, development, identification, and interpretation of the mode of action of biologically active compounds at the molecular level. Discovery is the identification of novel active chemical compounds, often called "hits", which are typically found by assay of compounds for a desired biological activity. The "hit" compound is improved for its pharmacologic, pharmacodynamic and pharmacokinetic properties by chemical or functional group modifications, transforming it into a lead compound. A lead compound should have a known structure and a known mechanism of action. An optimization step, which deals with the improvement of the lead structures. The optimization process takes primarily in to account the increase in potency, selectivity and toxicity. Its characteristics are the establishment of the molecular mode of action. However, an assessment of the pharmacokinetic parameters such as absorption, distribution, metabolism, excretion and oral bioavailability is almost systematically practiced at an early stage of the development in order to eliminate unsatisfactory candidates. A development step, is the continuation of the improvement of the pharmacokinetic properties and the fine tuning of the pharmaceutical properties (chemical formulation) of the active substances in order to render them suitable for clinical use. This chemical formulation process can consist in the preparation of better absorbed compounds, of sustained release formulations, and of water soluble derivatives or in the elimination of properties related to patient's compliance. Molecular modeling, or computational chemistry, has become a well-established part of drug development. In particular, medicinal chemistry in its most common practice-focusing on small organic molecules encompasses synthetic organic chemistry and computational chemistry in close combination with chemical biology, enzymology and structural biology, together aiming at the discovery and development of new therapeutic agents. [1]

2. BENZAMIDE AS A CORE:

Benzamide is a white solid with the chemical formula of $C_6H_5C(O)NH_2$. It is the simplest amide derivative of benzoic acid. It is slightly soluble in water, and soluble in many organic solvents.

Molecular Formula:	C_7H_7NO
Formula Weight:	121.13658
Composition:	C(69.41%) H(5.82%) N(11.56%) O(13.21%)
Molar Refractivity:	$35.18 \pm 0.3 \text{ cm}^3$
Molar Volume:	$108.1 \pm 3.0 \text{ cm}^3$
Parachor:	$281.7 \pm 4.0 \text{ cm}^3$
Index of Refraction:	1.564 ± 0.02
Surface Tension:	$46.0 \pm 3.0 \text{ dyne/cm}$
Density:	$1.120 \pm 0.06 \text{ g/cm}^3$
Dielectric Constant:	Not available
Polarizability:	$13.94 \pm 0.5 \cdot 10^{-24} \text{ cm}^3$
Ring Double Bond Equivalents:	5
Monoisotopic Mass:	121.052764 Da
Nominal Mass:	121 Da
Average Mass:	121.1366 Da

Benzamide derivatives have been reported for a variety of pharmacological activities, such as Acetylcholinesterase inhibition [2-5], antimicrobial [6, 7], antioxidant [8], chymotrypsin [9], antiasthmatic [10], anti-leukotriene [11] and anti-HIV [12] activities. The amide bond is an important pharmacophore group found in a wide variety of therapeutically important drugs e.g. buspirone, ampakine and phosphoramidate compounds. The ampakine compounds containing benzamide core are used to improve learning, memory and in the treatment of neurodegenerative disorders, cognitive impairment, depression, Alzheimer's disease and schizophrenia. The roles of cholinesterase inhibitors in Alzheimer's disease are still not completely unveiled, focus the attention of biologists and chemists on the modification of amide bond for the development of biological, pharmaceutical and clinical compounds. Recently, it was shown that some benzamide derivatives exhibited good inhibitory potency towards acetylcholinesterase.

The benzamide structure is analogous to the indanone structure present in the donepezil. This was pictorially represented by A.Aliabadi, *et. al.* in his research article. In the same way the piperidine

present in the donepezil has more potency in AchE inhibition [12]. Hence the current study involves the benzamide hybridized with 4-piperidone derivative.

3. ACTIVITY:

3.1. ACETYLCHOLINE:

Acetylcholine (Ach) is a messenger in both the central and peripheral nervous systems. [13, 14] It is involved in pre and post-ganglionic parasympathetic and pre-ganglionic sympathetic cholinergic transmission. Acetylcholine is synthesized in the pre-synaptic neurons by the reaction of choline that is supplied from the diet and acetyl CoA produced from the mitochondria, in the presence of an enzyme choline acetyltransferase. These are stored in the synaptic vesicles by the vesicular acetylcholine transporter (VAcHT) with the exchange of two protons for one acetylcholine molecule. These vesicles release acetylcholine by depolarization at the synaptic cleft. [15, 16] Ach activates the muscarinic and the nicotinic receptors of the skeletal muscles at the neuromuscular junction. **(Fig.1)** [17] This Ach can be inactivated by the enzyme acetylcholinesterase that hydrolyzes Ach into acetate and choline. About 5000 molecules of ACh can be hydrolyzed by one molecule of acetylcholinesterase per second. Choline after hydrolysis is taken back to the presynaptic neuron by choline transporter. But this is a rate-limiting step. [15]

3.2. CHOLINESTERASE:

Cholinesterase (ChE) belonging to the esterase family, hydrolyze the choline-based enzymes. It contains two different types of enzymes, namely acetylcholinesterase, and butyrylcholinesterase.[17] Acetylcholinesterase (EC 3.1.1.7) present in the conducting tissues in nerve and muscle, central and peripheral tissues, motor and sensory fibers, and cholinergic and non-cholinergic fibers.[18, 19] Butyrylcholinesterase (EC 3.1.1.8) present in the liver, kidney, and blood serum. It is mainly involved in the hydrolysis of dietary esters. [18, 20] It has a classical role in the terminating neurotransmission involving acetylcholine. Both are large moieties capable of producing other physiological actions. [17] Shreds of evidence show that both acetylcholinesterase (AchE) and butyrylcholinesterase (BchE) have a major effect on amyloidogenesis. Even AchE forms complexes with the Amyloid-beta ($A\beta$) plaques to increase neurotoxicity. It also induces astrocytosis. ChE contributes to the phosphorylation of microtubule-associated protein tau, which further worsens the condition of degeneration of neurons in Alzheimer's disease (AD) patients.

Other non-classical roles include the growth of the neurons, changes in the cerebral blood flow, glial cell activation and proliferation, and lipid homeostasis. [21]

3.3. CHOLINERGIC NEURON AND ALZHEIMER:

Cholinergic neurons are the nerve cell that transmits messages using Ach as a neurotransmitter. It is found in the basal forebrain and brainstem where the pedunclopontine nucleus and laterodorsal tegmental nucleus serves as the region for Ach production. It is a part of the thalamus and the striatum. [22] Cholinergic neurons project from the basal forebrain to the cerebral cortex and hippocampus of the brain. This helps in the cognitive activity of the brain. Evidence shows that the neurodegenerative disease called Alzheimer's was found from the observation of a reduction in the number of neurons in the basal forebrain and loss in cholinergic markers in the cortex. These effects lead to Mild Cognitive Impairment (MCI) in the patients. It served a prodromal of AD. This basal forebrain, a potential biomarker, atrophies associated with the age of the patients. [22-26] Due to this disruptive and delayed cholinergic signaling paved towards several deficits and dementia. Patients experience memory loss, altered sleep awake cycle, confusion, difficulty concentrating, aggression, agitation, depression, hallucination, retarding muscle movements, dysarthria, and loss of appetite. Conditions worsen with the severity of symptoms. When they are treated with cholinesterase inhibitors, improvement in symptoms were seen.[27] Drugs such as Donepezil, galantamine, rivastigmine, memantine, tacrine, ginkgo biloba, and physostigmine were used to treat Alzheimer's disease in a dose-dependent manner.[18, 19]

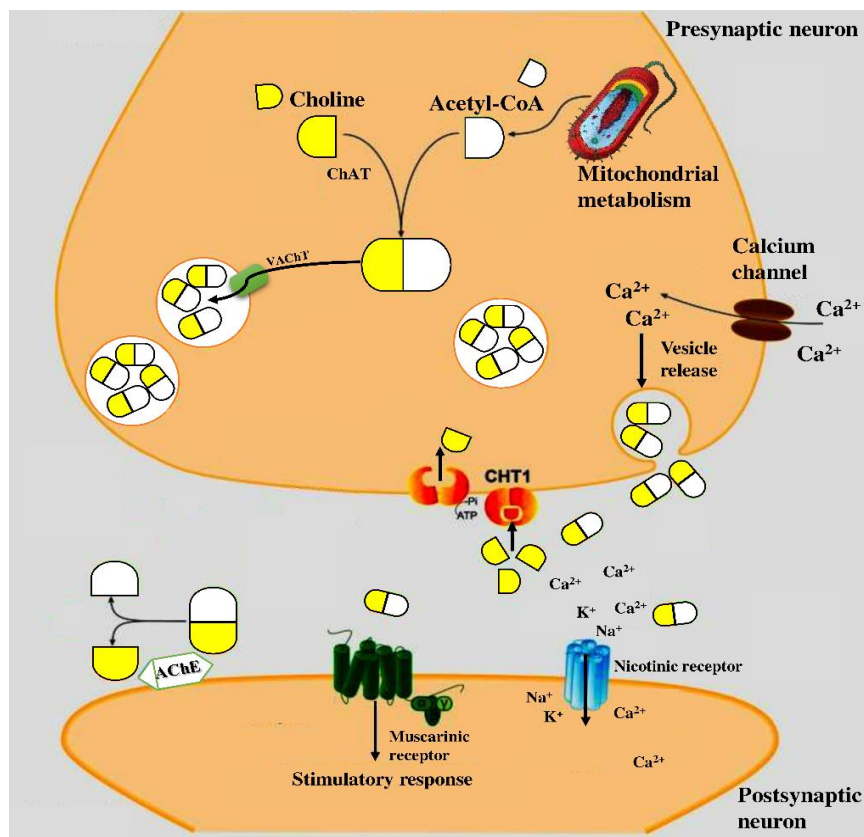


Fig.1. Acetylcholine formation and hydrolysis depiction at the synapse.

4. QSAR:

Quantitative Structural Activity Relationship (QSAR) is a computational method of statistics, to determine the relationship between the structures of the compounds with their targets. It is a tool to define the best fit ligands designed by mathematical models. Stages of QSAR involve data selection, extraction of descriptors, variable selection, construction of the model, and validation. QSAR regression models relate a set of "predictor" variables (X) to the potency of the response variable (Y), while classification QSAR models relate the predictor variables to a categorical value of the response variable. In QSAR modeling, the predictors consist of physico-chemical properties or theoretical molecular descriptors of chemicals; the QSAR response-variable could be a biological activity of the chemicals. QSAR models first summarize a supposed relationship between chemical structures and biological activity in a data-set of chemicals. Second, QSAR models predict the activities of new chemicals. [28]

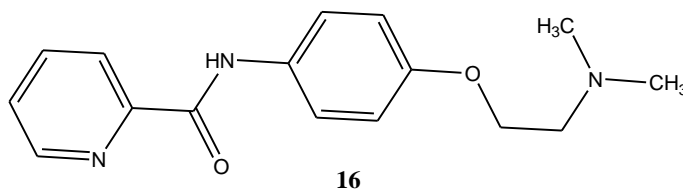
5. DOCKING:

Molecular docking is a technique which predicts the favoured introduction of one particle to second when bound to one another to form a stable complex. It used to foresee the quality of partiality between two particles by utilizing scoring function. It helps to achieve relative orientation between ligand and protein such that free energy of overall system is minimized.

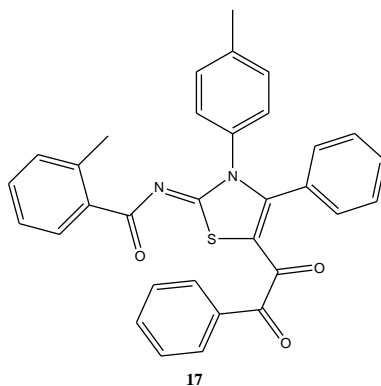
Structure based drug design is based on the principles in which small molecule ligands identify and interact with macromolecules is great importance in pharmaceutical research and development. The availability of the three dimensional macromolecules structure enables a constant examination of the coupling site topology including the presence of clefts, cavities and sub- pockets. Selective modulation of a validated drug target by high affinity ligands interferes with specific cellular processer ultimately leading to the desired pharmacological and therapeutic effect. The compound database is docked into a previously selected target binding state. It provides a result of the docked molecule. These docked molecules were ranked that can be used for sole criteria for selected promising molecule. It is evaluated to determine their biological activity on the molecular target under investigation. [29]

6. REVIEW OF LITREATURE:

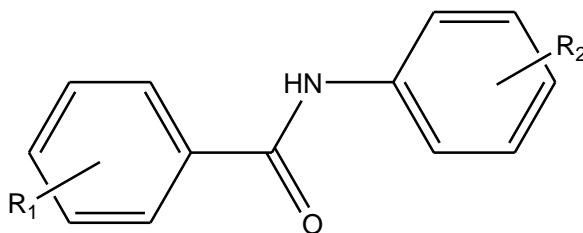
1. A series of benzamide and picolinamide derivatives with dimethylamine side chain as an AchE inhibitor was reported by Xiao-hui Gao *et al*. These compounds were assayed by Ellman's method. The compound in Fig.1 that has para dimethylamine substituted picolinamide was more potent with 2.49 μ M as IC₅₀ value and exhibited a mixed type of inhibition with increasing K_m and increasing concentration. Docking studies with AchE (PDB ID 1EVE) gave binding energy of -22.75kcal/mol. The compound binds with the target at the side chain which forms conformation as the shape of the active site. But this conformation was not seen in docking with BchE. This shows selectivity towards AchE. [2]



2. Amara Mumtaz *et al* synthesized tetra substituted thiazole by reacting benzamide and various aryl moieties. Domino synthesis was carried out by refluxing thiourea and acetophenone in the presence of iodine and tosic acid in DMSO. The structures were characterized by FTIR, ¹HNMR, ¹³CNMR, and EIMS. The compound 2-Methyl-N-(5-(2-oxo-2-phenylacetyl)-4-phenyl-3-(p-tolyl) thiazol-2(3H)-ylidene) benzamide Fig.2 was found to be more active against AchE in the enzymatic assay by Ellman's method. Galanthamine and donepezil were the standard drugs. Compound was dimethyl substituted but when it is replaced by chlorine, fluorine or methoxy group the activity was decreased. It showed competitive type of inhibition. Docking with AchE (PDB ID 4BDT) reveals the formation of hydrogen bonding and π - π interaction in the compound. Cytotoxicity studies by MTT assay using cervical cancer lines (HeLa cell line) and cell viability by measurement of purple formazan were reported. This compound inhibited 78.3% against HeLa cell lines. [3]



3. Martin Kratky *et al* developed a series of novel halogenated 2-hydroxy-N-phenyl benzamide derivatives. These were synthesized by microwave conditions under phosphorous trichloride. The compounds were reported to be moderate in inhibition of AchE in the range of 33.1-85.8 μ M by Ellman's method. The compounds exhibited more inhibition than the standard rivastigmine. The compound 5-Bromo-N-(3,5-dichlorophenyl)-2-hydroxybenzamide (**18**), 5-Bromo-N-(3,4,5-trichlorophenyl)-2-hydroxybenzamide (**19**), and 5-Bromo-N-(3-trifluoro methyl phenyl)-2-hydroxybenzamide (**20**) (**Fig.3**) showed IC₅₀ value of 33.1, 42.08, and 42.67 μ M respectively. They were the most potent derivatives. The reactivity of halogens was in the order trifluoro methyl > fluoro > bromo > chloro. The compounds exhibited pseudo-irreversible inhibition mechanism in the kinetic study. Physiochemical parameters were also reported to find out the blood-brain barrier permeability. [4]



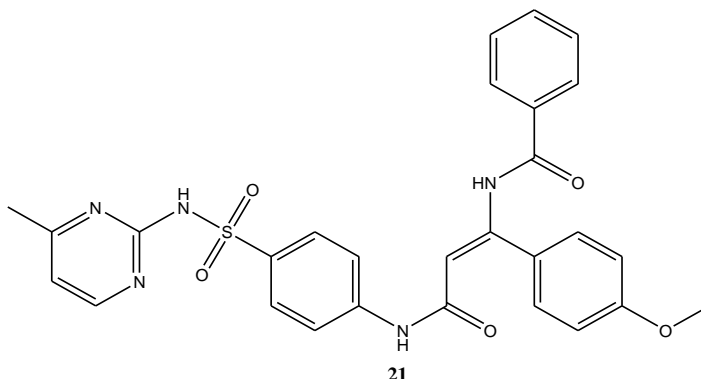
18 - R₁ - 5-Br, R₂ - 3,5-diCl

19 - R₁ - 5-Br, R₂ - 3,4,5-triCl

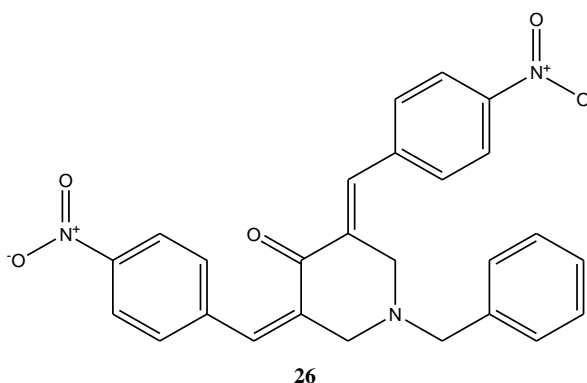
20 - R₁ - 5-Br, R₂ - 3 - CF₃

4. Mehtap Tugrak *et al* designed a series of benzamides. The synthesis was done by refluxing 4-(4-methoxy benzylidene)-2-phenyloxazol-5(4H)-one and a sulfonamide in glacial acetic acid at 100°C for 18-22hours. These compounds found to be 1.2 to 2.8 fold increase in potency than standard tacrine. The compound N-(1-(4-methoxyphenyl)-3-((4-(N-(4-methylpyrimidin-2-yl)sulfamoyl)phenyl)amino)-3-oxoprop-1-en-1-yl)benzamide (**21**)

(Fig.4) was more potent against AchE with IC₅₀ value of 9.11nM and lowest Ki value of 8.91nM. [5]

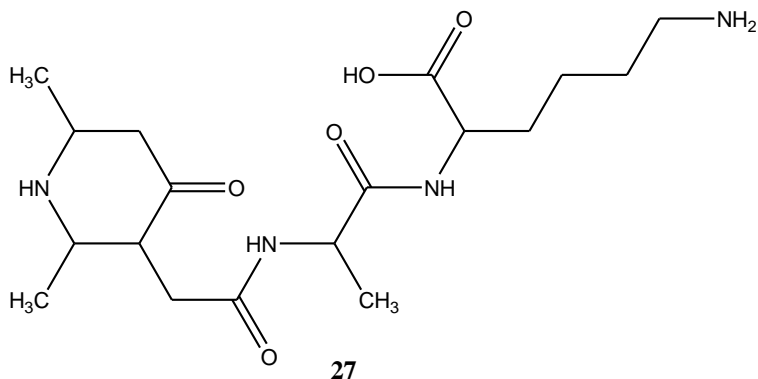


5. Sulunay Parlar evaluated a series of piperidinone derivatives as AchE inhibitors. The derivatives were synthesized by Claisen-schmidt condensation between N-benzyl-4-piperidinone and aryl aldehydes in the presence of potassium hydroxide and methanol solvent. The AchE inhibition assay revealed that the compound (26) (Fig.5) 1-benzyl-3,5-bis(4-nitrobenzylidene)piperidin-4-one gave IC₅₀ value of 12.55μM and compared to rivastigmine. The compounds with para-substituted were found to be more potent and the substituted halogens show reactivity in the manner as Fluoro > Chloro > Bromo. Also, the compounds were found to bind with both catalytic active site (CAS) and peripheral anionic site (PAS) of the AchE enzyme. [30]

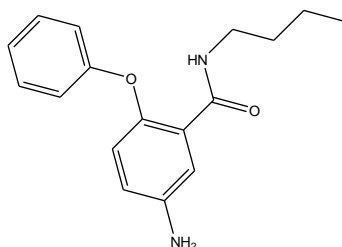


6. Parasuraman Pavadai *et al* designed and synthesized a novel dipeptide fused piperidinone (DPPS) as AchE and β-amyloid inhibitors. Dipeptide was synthesized by solid-phase peptide synthesis in the presence of Fmoc protection for coupling of amino acids and piperidine-4-one derivative. The product was cleaved from the resin. Then it was purified and characterized by mass spectroscopy. Inhibition assay by Ellman's method was done for

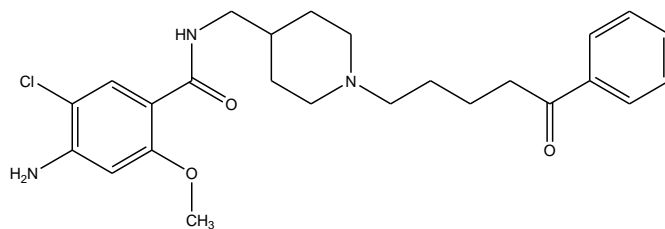
the compound DPPS (**27**) (**Fig.6**). It resulted in IC₅₀ value of 0.479μM/ml and compared to donepezil as a standard drug. [31]



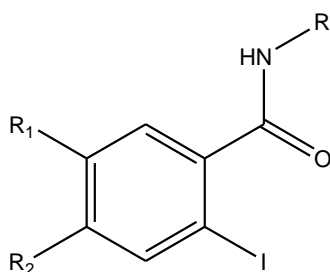
7. A series of novel substituted benzamides, similar to Parsalmide were designed and evaluated for *in vitro* activity on COX-1 and COX-2 as well as *in vivo* in the Carragenan induced rat paw edema, a classical *in vivo* anti-inflammatory assay. Compound 11b (Fig.7) showed a favorable profile *in vitro* and *in vivo*, were screened and compared with parsalmide for gastrointestinal (GI) tolerability *in vivo* in the rats. Results obtained showed that Parsalmide and compound 11b inhibited both COX-1 and COX-2 *in vitro* as well as they were active *in vivo*. Both compounds were devoid of gastric effect at the efficacious dose. In addition, both prevented indomethacin induced gastric damage [32]



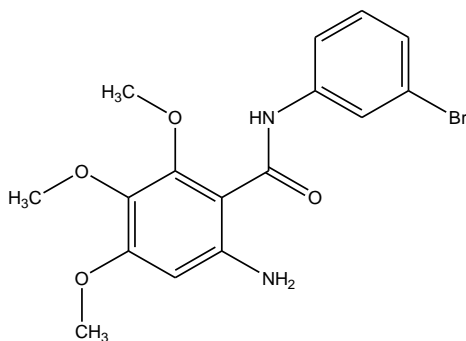
8. Many gastrointestinal prokinetics such as benzamides have binding affinity for 5-HT₄ receptors and behave as 5-HT₄ receptor agonist. A set of benzamide derivatives were tested as selective 5-HT₄ receptor agonists. They performed modification of the parent compound 4-amino-5-chloro-2-methoxy-N-[1-(6-oxo-6-phenylhexyl)piperidin-4-yl methyl] benzamide which enhance both upper and lower gastrointestinal motility without any significant adverse effects. [33]



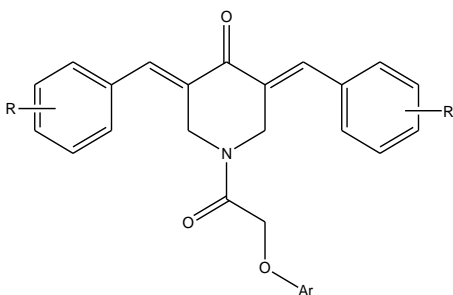
9. The *N*-(1-Phenyl-4-carboxypyrazol-5-yl)-, *N*-(indazol-3-yl)-and *N*-(indazol-5-yl)-2-iodobenzamides, with benodanillike structure, were synthesized by reflux method in acetic acid with the corresponding benzotriazinones with potassium iodide for 1hr. The antifungal activity of the *N*-substitution with an aromatic heterocyclic system on benzamide moiety were reported. Among the tested iododerivatives, some of the compounds possessed interesting activities toward some phytopathogenic fungal strains. [6]



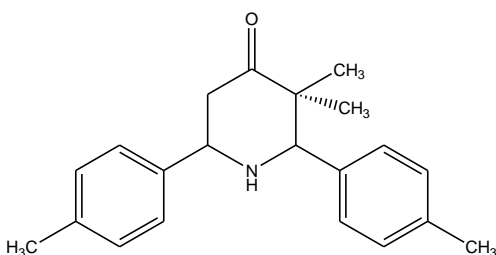
10. The benzamides and the benzamidines and the cyclic benzamidines were designed as the mimics of 4-anilino quinazolines for an inhibitor of EGFR tyrosine kinase. The specific inhibitions of *v*-Src kinase were observed in the benzamides, and the benzamidine. The compound 1j and 2d shows specific inhibitions of *v*-Src kinase in the benzamide and benzamidine at a 10 $\mu\text{g/ml}$. but the cyclic benzamidines show potent activity at 1.0 $\mu\text{g/ml}$. [34]



11. Amit anthwal et. al., synthesized 4-piperidone based curcuminoids against human myeloid leukemia (KBM5) and colon cancer (HCT116) cell lines. All the designed compounds were evaluated for the anti-inflammatory activity by down regulation of tumour necrosis factor- α -induced nuclear factor- κ B. compounds showed were found to be potential in activity. [35]



12. Karthick N *et al.*, Proposed a synthesis method by condensation 4-piperidone benzaldehyde and also spectral analysis for characterization. Evaluation of the antioxidant activity by DPPH assay were also reported. Hence proved to be a good anti-scavenger. [36]



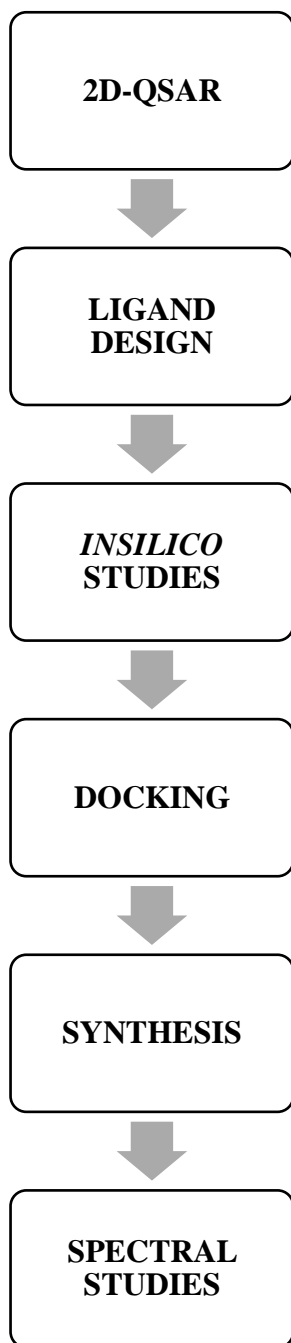
7. AIM OF THE RESEARCH:

Acetylcholine (Ach) is the main neurotransmitter in the nervous system. Ach transmits signals at the synapses. This transmission is interrupted when a cholinesterase enzyme hydrolyses the acetylcholine into acetyl CoA and choline. This leads to the degeneration of neurons in the brain. Degeneration causes dementia, Alzheimer, Parkinson, schizophrenia, etc. The inhibition of acetylcholinesterase can improve the neurotransmission in the brain. The AchE enzyme is the potent target in the Alzheimer's disease. The work is aimed to design and evaluate the benzamide derivatives to inhibit the acetylcholinesterase enzyme. This improves the neuronal transmission. This study involves the 2D-QSAR methodologies to analyze the structural relationship with the activity. Followed by the design of novel ligands and screening of insilico activities like physiochemical properties, ADME parameters, toxicity, and molecular docking. Docking of a novel ligand with acetylcholinesterase enzyme was performed and compared to donepezil. The compounds were characterized using FT-IR, ¹H NMR, ¹³C NMR, and MASS spectroscopy. The activity is carried out by Ellman's assay.

7.1. OBJECTIVE OF THE STUDY:

- A. To derive the 2D-QSAR model using QSARINS software.
- B. To design benzamide derivatives using CHEMDRAW software.
- C. To evaluate toxicity, ADME properties for the designed compounds.
- D. To perform docking studies for the designed compounds.
- E. To synthesize the designed compounds.
- F. To characterize and evaluate the acetylcholinesterase enzyme inhibition activity.

8. PLAN OF STUDY:

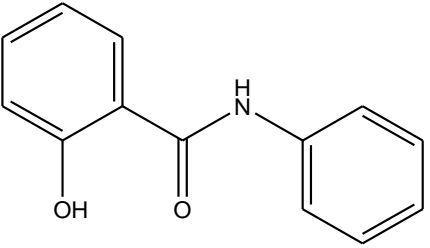
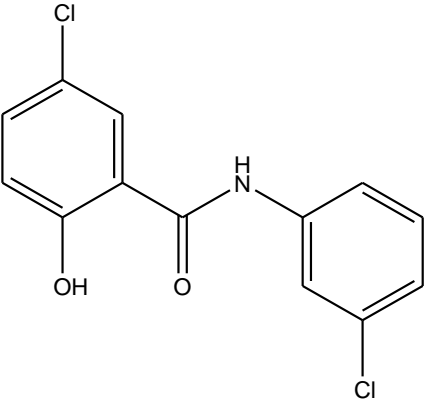
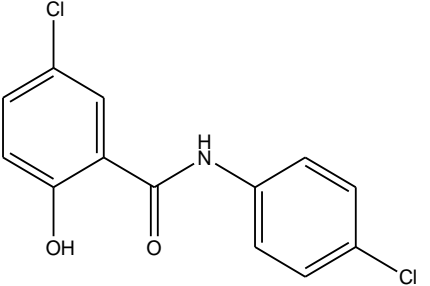
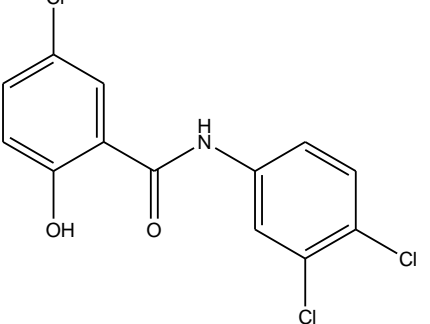


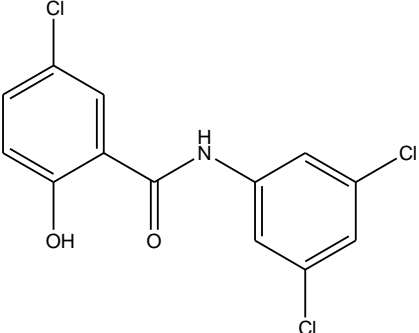
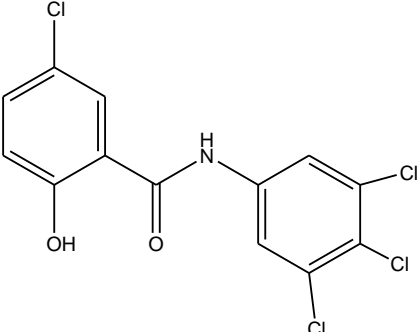
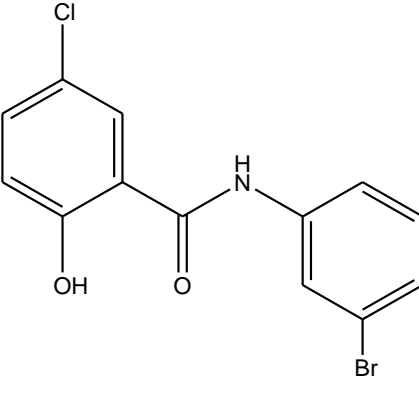
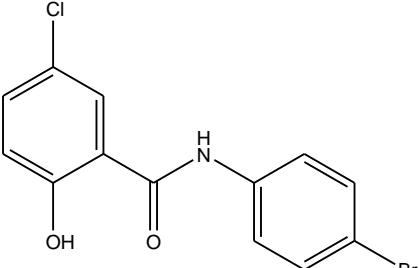
9. MATERIALS AND METHODS:

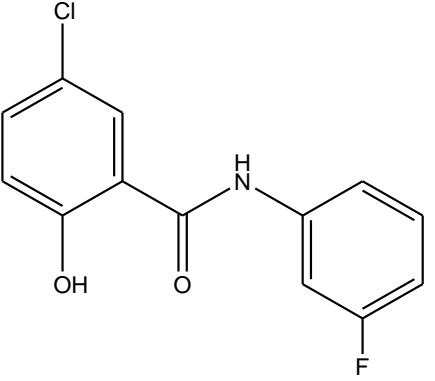
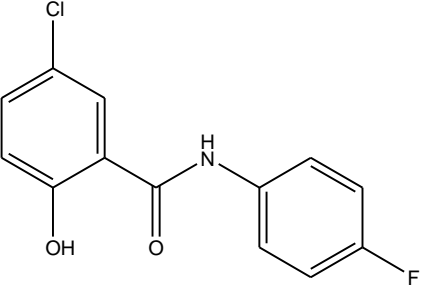
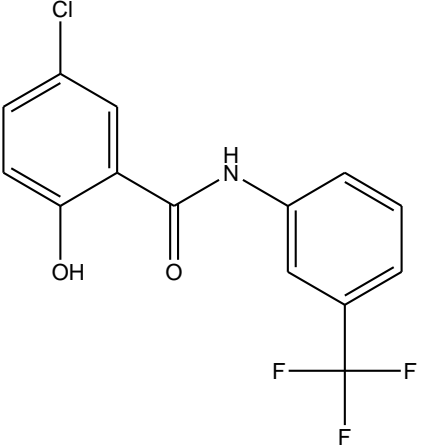
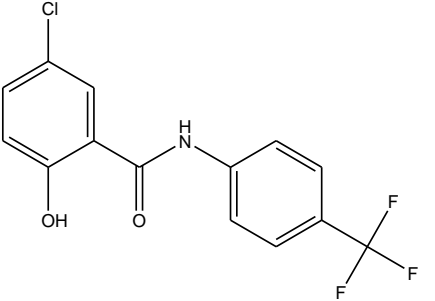
9.1. 2D-QSAR APPROACH:

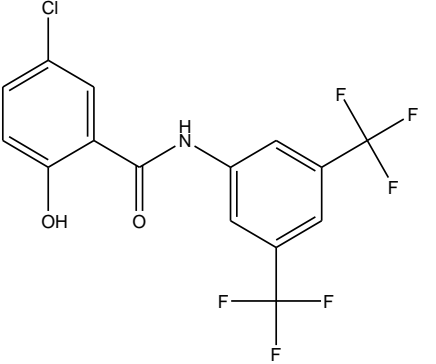
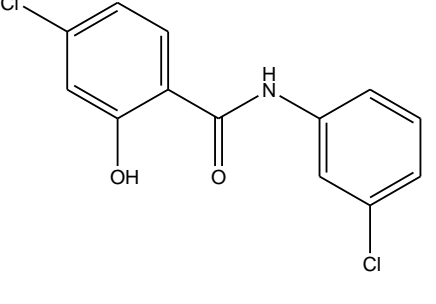
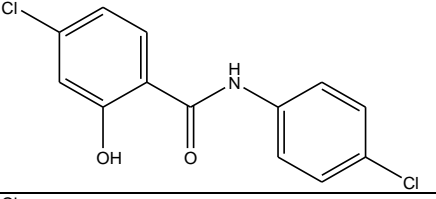
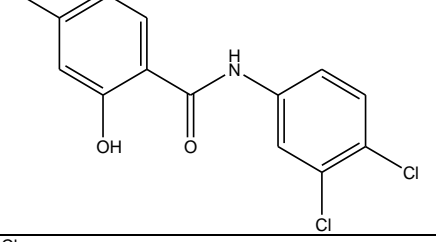
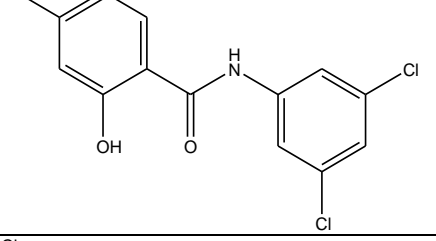
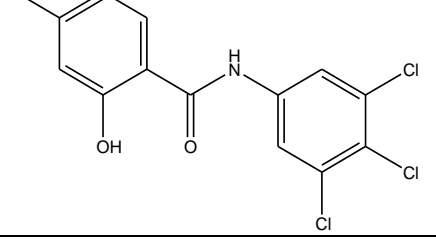
Quantitative structure activity relationship (QSAR) relates the chemical structure to biological and other activities by developing a QSAR model. Using such an approach one could predict the activities of newly designed compounds before a decision is being made whether these compounds should be really synthesized and tested. The data set used for the QSAR analyses contains 79 molecules belonging to benzamide derivatives as acetylcholinesterase inhibitors. The compounds were taken from the research work of Martin Kratky, et al. [4], Martin Kratky, et al. [37], Aliabadi, A, et al. [12], and Amara Mumtaz, et al. [3] All the structures of the compounds were drawn in ChemDraw software. The structures of all the compounds along with their actual and predicted biological activities are presented in Table 1. A set of 79 molecules were selected and divided into training and test set in the ratio of 4:1. The negative logarithm of IC₅₀ values (PIC₅₀) were calculated using the IC₅₀ values of reported compounds. The compounds were run in the Padel software for descriptors generation. The descriptors along with the activity were proceeded for QSAR studies. QSARINS software is used for QSAR study. The data set is prepared by removing the constant variables greater than 80% and other correlated variables greater than 95% in the independent variables. Using genetic algorithm the QSAR model was developed. The models were validated in both internal and external validation. The models were verified by Applicability domain. The applicability domain is used to identify the most influencing compound to the model. The leverage method and the insurbia graphs helps in identifying the outliers in this QSARINS software. Then the outliers were found and removed from the 1st model. Then the remaining compounds were proceeded for next model generation in the same way. [38]

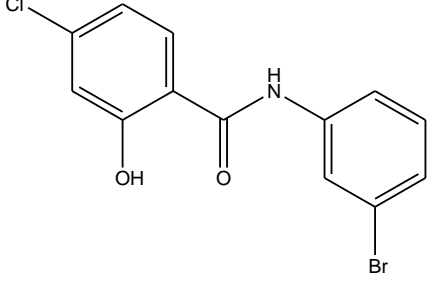
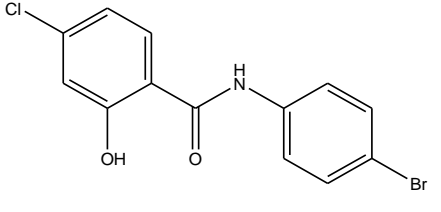
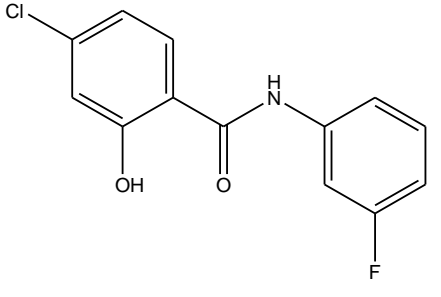
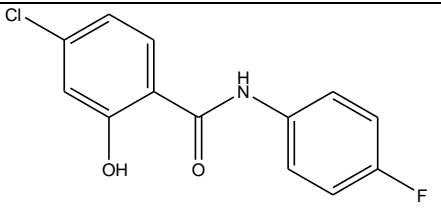
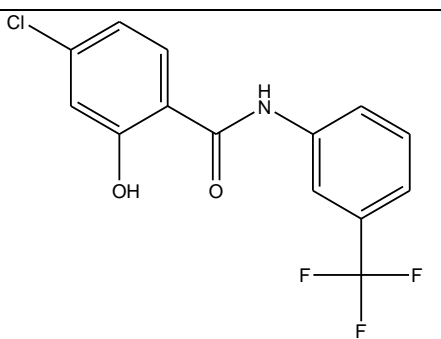
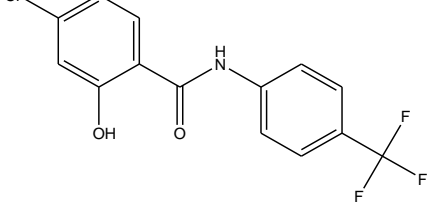
Table 1. The structures of all the compounds along with their actual and predicted biological activities.

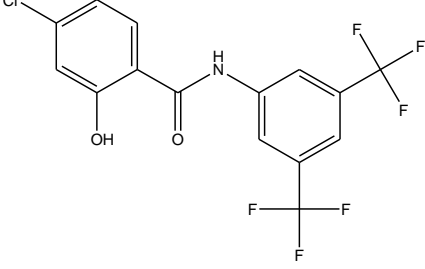
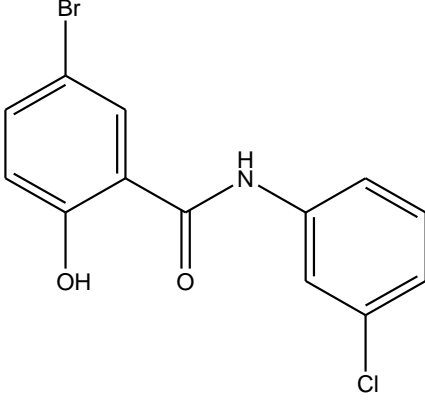
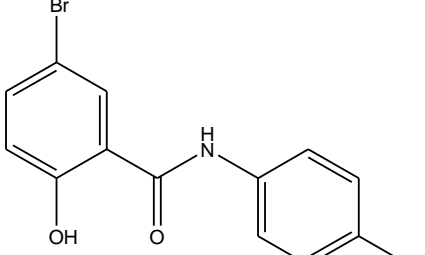
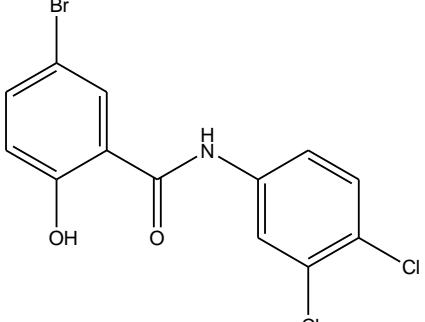
Compound Name	Structure	Molecular Formula	IC ₅₀ VALUE (μM)	<i>p</i> K _i = -Log(IC ₅₀)
1		C ₁₃ H ₁₁ NO ₂	49.71	-1.69644
2		C ₁₃ H ₉ Cl ₂ NO ₂	59.5	-1.77452
3		C ₁₃ H ₉ Cl ₂ NO ₂	76.53	-1.88383
4		C ₁₃ H ₈ Cl ₃ NO ₂	60.79	-1.78383

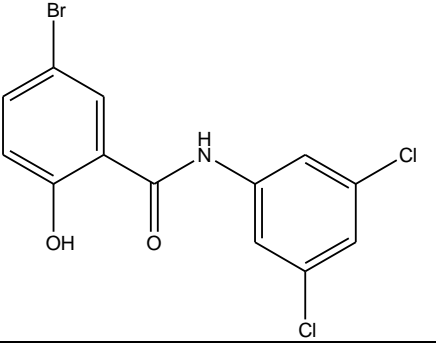
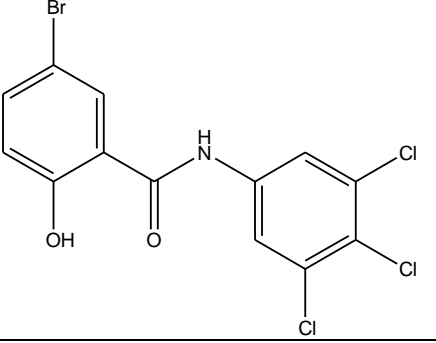
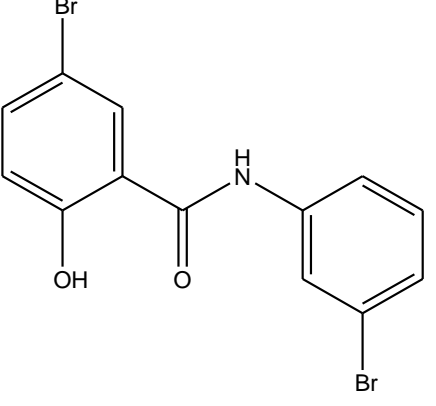
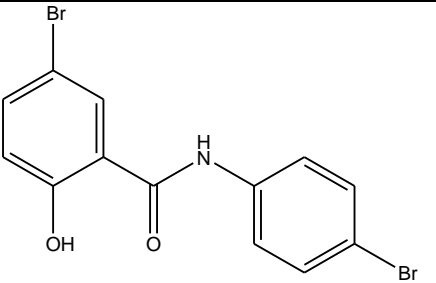
5	 <p>Chemical structure of 2-(3,5-dichlorophenyl)acetamide: A benzene ring with a hydroxyl group (-OH) at the 1-position and an acetamide group (-NH-C(=O)-CH₂-) at the 2-position. The benzene ring is substituted with chlorine atoms (-Cl) at the 3 and 5 positions.</p>	$C_{13}H_8Cl_3NO_2$	46.21	-1.66474
6	 <p>Chemical structure of 2-(2,3,5-trichlorophenyl)acetamide: A benzene ring with a hydroxyl group (-OH) at the 1-position and an acetamide group (-NH-C(=O)-CH₂-) at the 2-position. The benzene ring is substituted with chlorine atoms (-Cl) at the 2, 3, and 5 positions.</p>	$C_{13}H_7Cl_4NO_2$	51.06	-1.70808
7	 <p>Chemical structure of 2-(4-bromophenyl)acetamide: A benzene ring with a hydroxyl group (-OH) at the 1-position and an acetamide group (-NH-C(=O)-CH₂-) at the 2-position. The benzene ring is substituted with a chlorine atom (-Cl) at the 3-position and a bromine atom (-Br) at the 4-position.</p>	$C_{13}H_9ClBrNO_2$	50.03	-1.69923
8	 <p>Chemical structure of 2-(3-bromophenyl)acetamide: A benzene ring with a hydroxyl group (-OH) at the 1-position and an acetamide group (-NH-C(=O)-CH₂-) at the 2-position. The benzene ring is substituted with a chlorine atom (-Cl) at the 3-position and a bromine atom (-Br) at the 4-position.</p>	$C_{13}H_9ClBrNO_2$	58.25	-1.7653

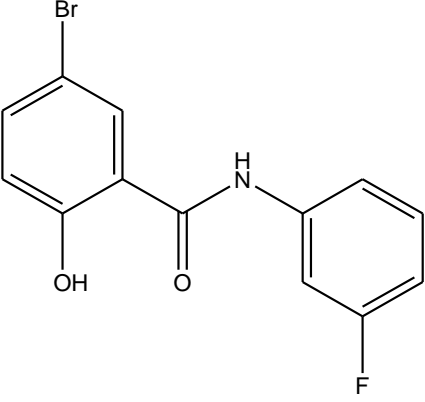
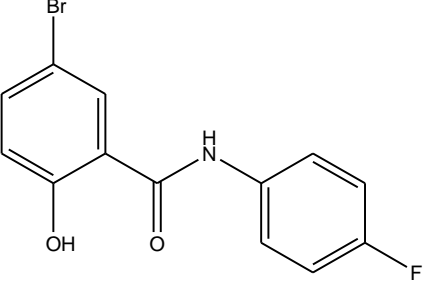
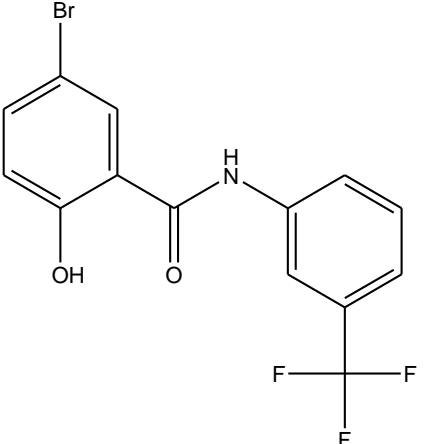
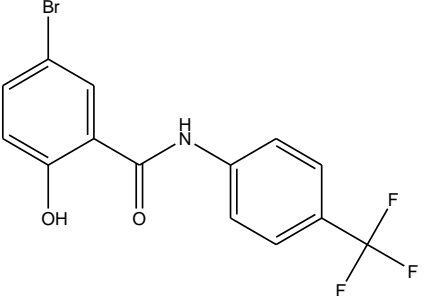
9	 <p>Chemical structure of 2-(3-chloro-4-hydroxyphenyl)acetamide, N-(4-fluorophenyl)-. It consists of a benzamide core where the phenyl ring is substituted with a chlorine atom at the 3-position and a hydroxyl group at the 4-position. The nitrogen atom is substituted with a 4-fluorophenyl group.</p>	$C_{13}H_9ClFNO_2$	58.65	-1.76827
10	 <p>Chemical structure of 2-(3-chloro-4-hydroxyphenyl)acetamide, N-(3-fluorophenyl)-. It consists of a benzamide core where the phenyl ring is substituted with a chlorine atom at the 3-position and a hydroxyl group at the 4-position. The nitrogen atom is substituted with a 3-fluorophenyl group.</p>	$C_{13}H_9ClFNO_2$	48.27	-1.68368
11	 <p>Chemical structure of 2-(3-chloro-4-hydroxyphenyl)acetamide, N-(4-(trifluoromethyl)phenyl)-. It consists of a benzamide core where the phenyl ring is substituted with a chlorine atom at the 3-position and a hydroxyl group at the 4-position. The nitrogen atom is substituted with a 4-(trifluoromethyl)phenyl group.</p>	$C_{14}H_9ClF_3NO_2$	54.41	-1.73568
12	 <p>Chemical structure of 2-(3-chloro-4-hydroxyphenyl)acetamide, N-(3-(trifluoromethyl)phenyl)-. It consists of a benzamide core where the phenyl ring is substituted with a chlorine atom at the 3-position and a hydroxyl group at the 4-position. The nitrogen atom is substituted with a 3-(trifluoromethyl)phenyl group.</p>	$C_{14}H_9ClF_3NO_2$	58.47	-1.76693

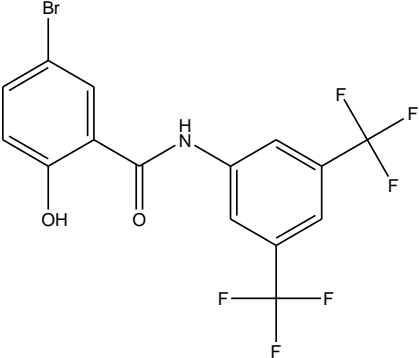
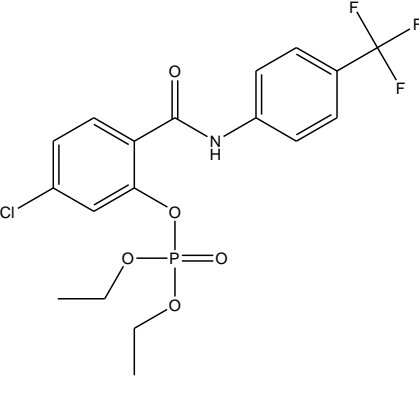
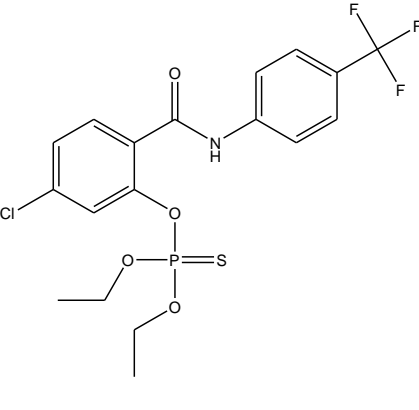
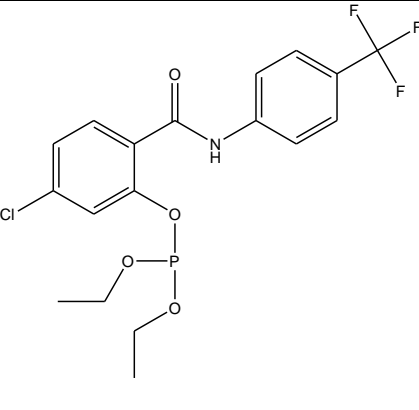
13		C ₁₅ H ₈ ClF ₆ NO ₂	50.18	-1.70053
14		C ₁₃ H ₉ Cl ₂ NO ₂	58.08	-1.76403
15		C ₁₃ H ₉ Cl ₂ NO ₂	56.19	-1.74966
16		C ₁₃ H ₈ Cl ₃ NO ₂	46.26	-1.66521
17		C ₁₃ H ₈ Cl ₃ NO ₂	50.15	-1.70027
18		C ₁₃ H ₇ Cl ₄ NO ₂	57.78	-1.76178

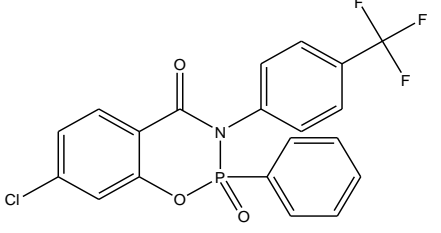
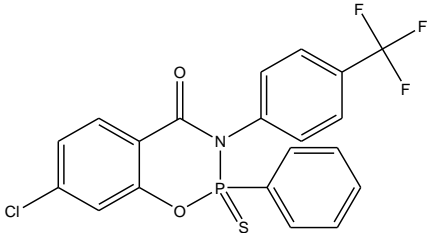
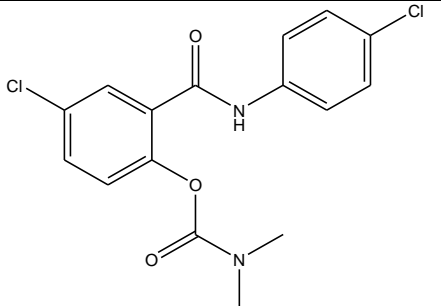
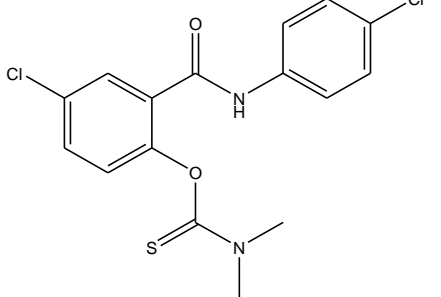
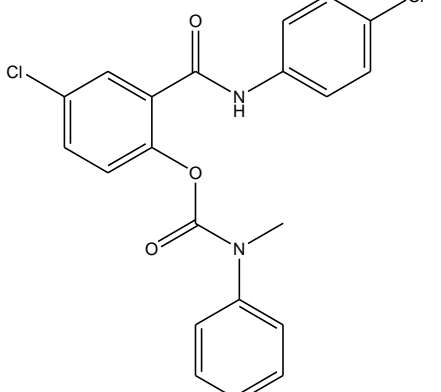
19		$C_{13}H_9BrClNO_2$	60.03	-1.77837
20		$C_{13}H_9BrClNO_2$	58.32	-1.76582
21		$C_{13}H_9ClFNO_2$	60.79	-1.78383
22		$C_{13}H_9ClFNO_2$	62.85	-1.79831
23		$C_{14}H_9ClF_3NO_2$	68.28	-1.83429
24		$C_{14}H_9ClF_3NO_2$	60.29	-1.78025

25	 <p>Chemical structure of 2-(3,5-bis(trifluoromethyl)phenylamino)-4-chlorophenol. It consists of a central benzamide core where the phenyl ring is substituted with a chlorine atom at the para position and a hydroxyl group at the ortho position. The nitrogen atom is attached to a 3,5-bis(trifluoromethyl)phenyl group.</p>	$C_{15}H_8ClF_6NO_2$	54.72	-1.73815
26	 <p>Chemical structure of 2-(4-chlorophenylamino)-3-bromophenol. It consists of a central benzamide core where the phenyl ring is substituted with a bromine atom at the meta position and a hydroxyl group at the ortho position. The nitrogen atom is attached to a 4-chlorophenyl group.</p>	$C_{13}H_9BrClNO_2$	62.04	-1.79267
27	 <p>Chemical structure of 2-(3-chlorophenylamino)-4-bromophenol. It consists of a central benzamide core where the phenyl ring is substituted with a bromine atom at the para position and a hydroxyl group at the ortho position. The nitrogen atom is attached to a 3-chlorophenyl group.</p>	$C_{13}H_9BrClNO_2$	85.75	-1.93323
28	 <p>Chemical structure of 2-(2,4-dichlorophenylamino)-3-bromophenol. It consists of a central benzamide core where the phenyl ring is substituted with a bromine atom at the meta position and a hydroxyl group at the ortho position. The nitrogen atom is attached to a 2,4-dichlorophenyl group.</p>	$C_{13}H_8BrCl_2NO_2$	60.83	-1.78412

29	 <p>Chemical structure of 2-(3,5-dibromo-4-hydroxyphenyl)acetamide. It consists of a benzene ring with a bromine atom at the 3-position, a hydroxyl group at the 4-position, and an acetamide group at the 2-position. The acetamide group is further substituted with a 3,5-dichlorophenyl ring.</p>	$C_{13}H_8BrCl_2NO_2$	33.13	-1.52022
30	 <p>Chemical structure of 2-(2,4,6-trichlorophenyl)acetamide. It consists of a benzene ring with a bromine atom at the 3-position, a hydroxyl group at the 4-position, and an acetamide group at the 2-position. The acetamide group is further substituted with a 2,4,6-trichlorophenyl ring.</p>	$C_{13}H_7BrCl_3NO_2$	42.08	-1.62408
31	 <p>Chemical structure of 2-(4-bromophenyl)acetamide. It consists of a benzene ring with a bromine atom at the 3-position, a hydroxyl group at the 4-position, and an acetamide group at the 2-position. The acetamide group is further substituted with a 4-bromophenyl ring.</p>	$C_{13}H_9Br_2NO_2$	69.72	-1.84336
32	 <p>Chemical structure of 2-(3-bromophenyl)acetamide. It consists of a benzene ring with a bromine atom at the 3-position, a hydroxyl group at the 4-position, and an acetamide group at the 2-position. The acetamide group is further substituted with a 3-bromophenyl ring.</p>	$C_{13}H_9Br_2NO_2$	70.3	-1.84696

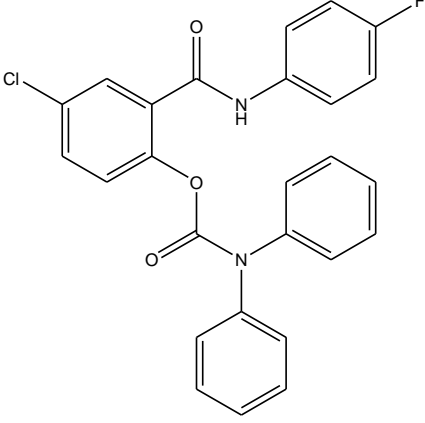
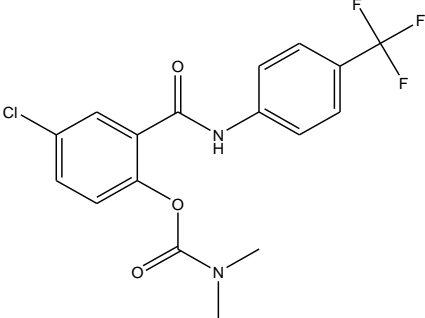
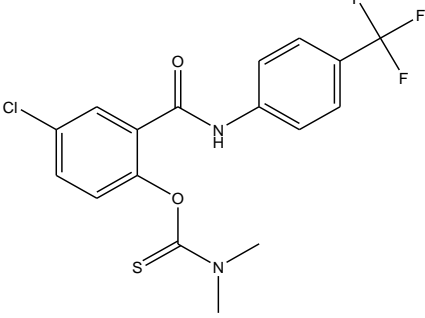
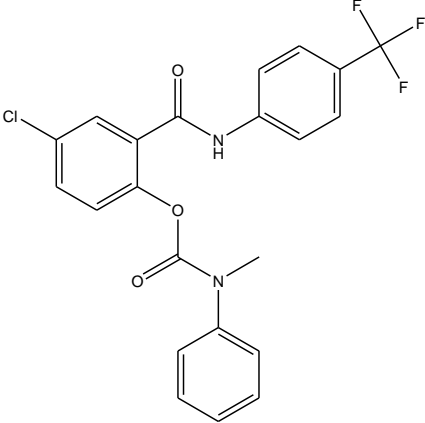
33	 <p>Chemical structure of 3-bromo-4-hydroxybenzamide N-(4-fluorophenyl). It consists of a benzamide core with a bromine atom at the 3-position and a hydroxyl group at the 4-position of the benzamide ring. The nitrogen atom is substituted with a 4-fluorophenyl group.</p>	$C_{13}H_9BrFNO_2$	54.44	-1.73592
34	 <p>Chemical structure of 3-bromo-4-hydroxybenzamide N-(3-fluorophenyl). It consists of a benzamide core with a bromine atom at the 3-position and a hydroxyl group at the 4-position of the benzamide ring. The nitrogen atom is substituted with a 3-fluorophenyl group.</p>	$C_{13}H_9BrFNO_2$	61.22	-1.78689
35	 <p>Chemical structure of 3-bromo-4-hydroxybenzamide N-(4-(trifluoromethyl)phenyl). It consists of a benzamide core with a bromine atom at the 3-position and a hydroxyl group at the 4-position of the benzamide ring. The nitrogen atom is substituted with a 4-(trifluoromethyl)phenyl group.</p>	$C_{14}H_9BrF_3NO_2$	42.67	-1.63012
36	 <p>Chemical structure of 3-bromo-4-hydroxybenzamide N-(3-(trifluoromethyl)phenyl). It consists of a benzamide core with a bromine atom at the 3-position and a hydroxyl group at the 4-position of the benzamide ring. The nitrogen atom is substituted with a 3-(trifluoromethyl)phenyl group.</p>	$C_{14}H_9BrF_3NO_2$	44.79	-1.65118

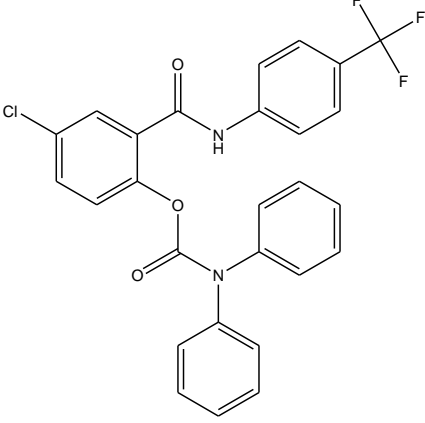
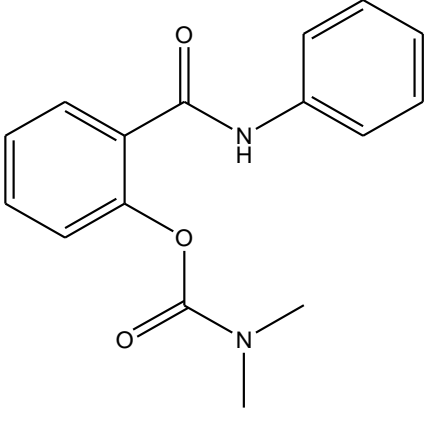
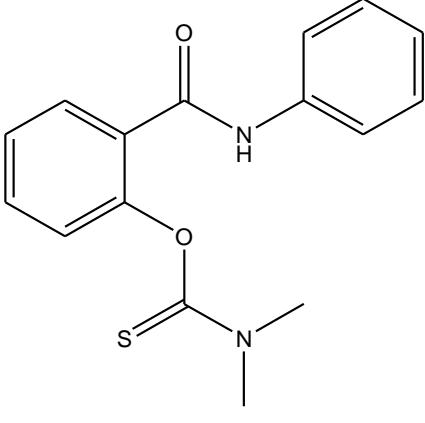
37		$C_{15}HBrF_6NO_2$	48.46	-1.68538
38		$C_{18}H_{18}ClF_3NO_5P$	86.3	-1.93601
39		$C_{18}H_{18}ClF_3NO_4P$ S	9.16	-0.9619
40		$C_{18}H_{18}ClF_3NO_4P$	66.37	-1.82197

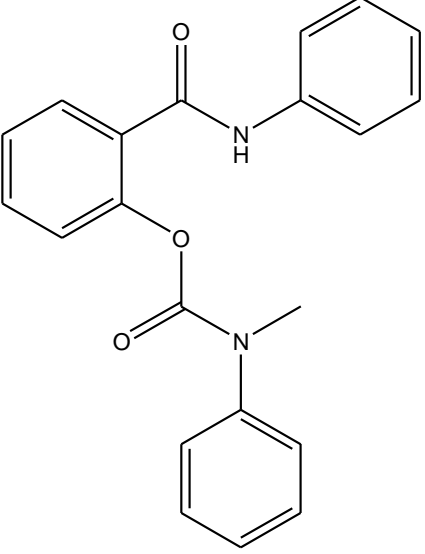
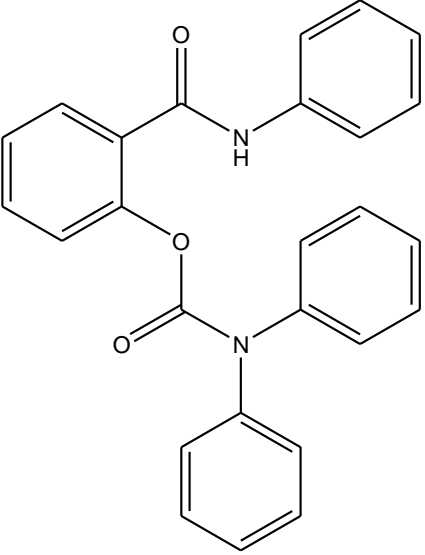
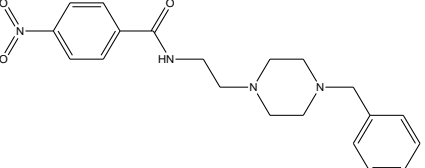
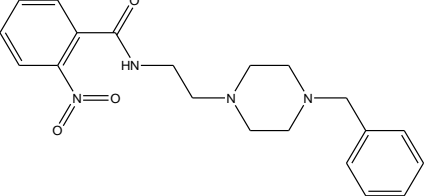
41		$C_{20}H_{21}ClF_3NO_3P$	48.3	-1.68395
42		$C_{20}H_{21}ClF_3NO_2PS$	63.48	-1.80264
43		$C_{16}H_{14}Cl_2N_2O_3$	72.87	-1.86255
44		$C_{16}H_{14}Cl_2N_2O_2S$	38.98	-1.59084
45		$C_{21}H_{16}Cl_2N_2O_3$	74.83	-1.87408

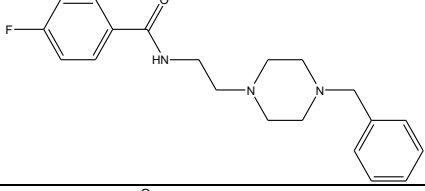
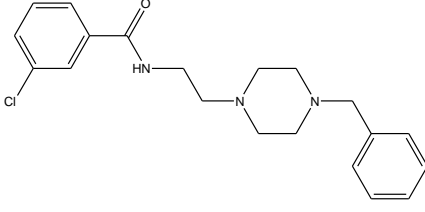
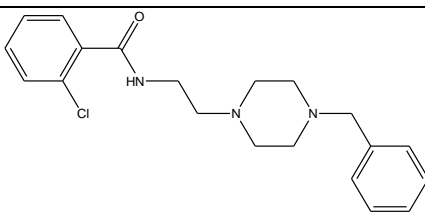
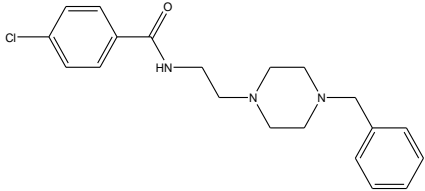
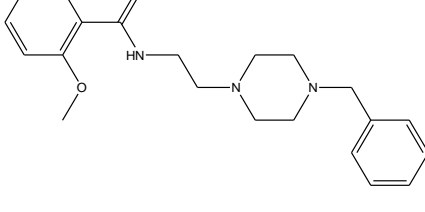
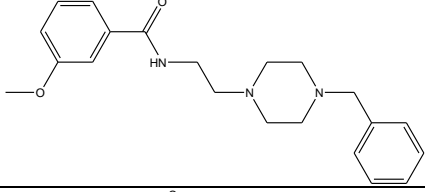
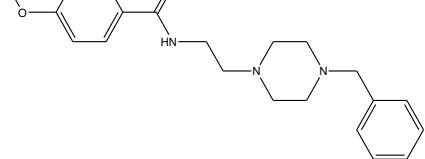
46		$C_{26}H_{18}Cl_2N_2O_3$	54.81	-1.73886
47		$C_{16}H_{14}BrClN_2O_3$	62.38	-1.79505
48		$C_{16}H_{14}BrClN_2O_2$ S	59.05	-1.77122
49		$C_{21}H_{16}BrClN_2O_3$	81.6	-1.91169

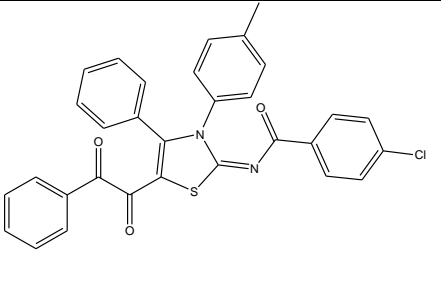
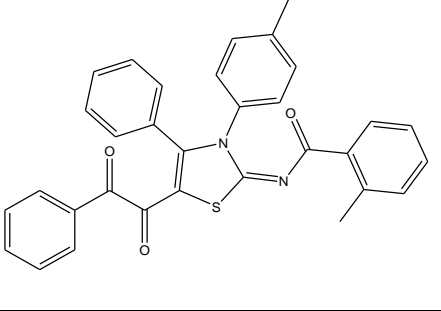
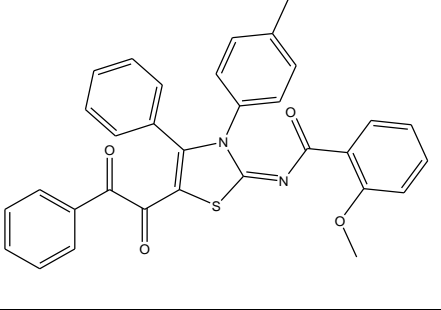
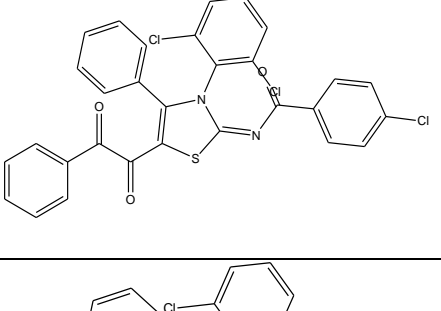
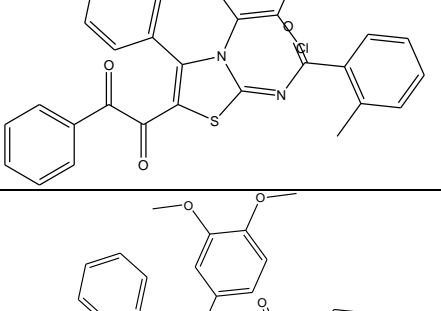
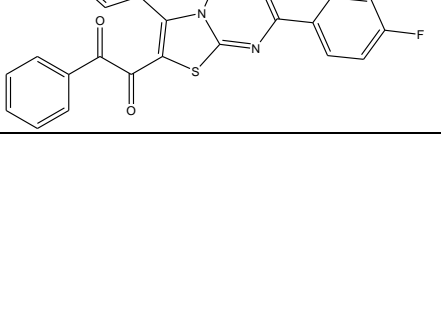
50		$C_{26}H_{18}BrClN_2O_3$	63.29	-1.80134
51		$C_{16}H_{14}ClFN_2O_3$	76.17	-1.88178
52		$C_{16}H_{14}ClFN_2O_2S$	89.74	-1.95299
53		$C_{21}H_{16}ClFN_2O_3$	62.54	-1.79616

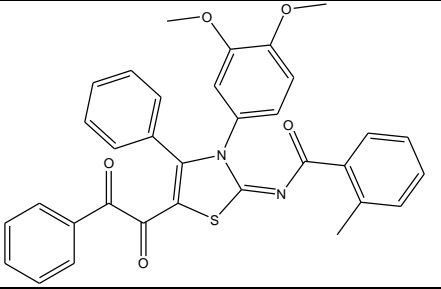
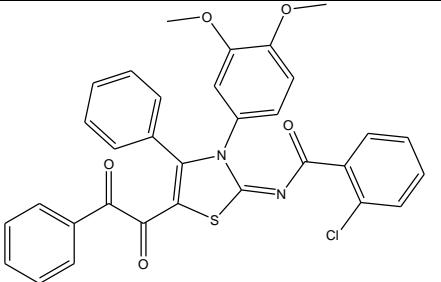
54		$C_{26}H_{18}ClFN_2O_3$	49.03	-1.69046
55		$C_{17}H_{14}ClF_3N_2O_3$	49.04	-1.69055
56		$C_{17}H_{14}ClF_3N_2O_2$ S	41.98	-1.62304
57		$C_{22}H_{16}ClF_3N_2O_3$	49.85	-1.69767

58	 <p>Chemical structure of 2-(3-chloro-4-(trifluoromethyl)phenyl)propanoic acid N,N-diphenylamide. It features a central benzene ring with a chlorine atom at the 3-position and a trifluoromethyl group at the 4-position. The 1-position of this ring is connected to the alpha-carbon of a propanoic acid chain. The carboxylic acid group is in its neutral form. The nitrogen of the amide group is substituted with two phenyl rings.</p>	$C_{27}H_{18}ClF_3N_2O_3$	47.39	-1.67569
59	 <p>Chemical structure of 2-phenylpropanoic acid N,N-dimethylamide. It consists of a benzene ring attached to the alpha-carbon of a propanoic acid chain. The carboxylic acid group is in its neutral form. The nitrogen of the amide group is substituted with two methyl groups.</p>	$C_{16}H_{16}N_2O_3$	57.74	-1.76148
60	 <p>Chemical structure of 2-phenylpropanoic acid N,N-dimethylthioamide. It is similar to structure 59, but the carbonyl oxygen is replaced by a sulfur atom.</p>	$C_{16}H_{16}N_2O_2S$	61.94	-1.79197

61		$C_{21}H_{18}N_2O_3$	55.01	-1.74044
62		$C_{26}H_{20}N_2O_3$	53.79	-1.7307
63		$C_{20}H_{24}N_4O_3$	6.9	-0.83885
64		$C_{20}H_{24}N_4O_3$	23	-1.36173

65		$C_{20}H_{24}FN_3O$	4	-0.60206
66		$C_{20}H_{24}ClN_3O$	9	-0.95424
67		$C_{20}H_{24}ClN_3O$	9.7	-0.98677
68		$C_{20}H_{24}ClN_3O$	0.44	0.356547
69		$C_{21}H_{27}N_3O_2$	21	-1.32222
70		$C_{21}H_{27}N_3O_2$	7.2	-0.85733
71		$C_{21}H_{27}N_3O_2$	27	-1.43136

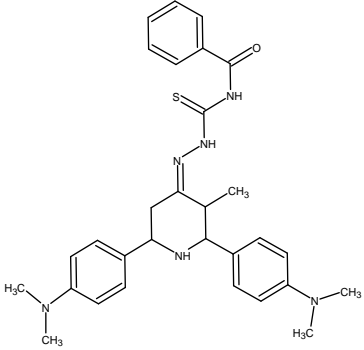
72		$C_{31}H_{21}ClN_2O_3S$	30.1	-1.47857
73		$C_{32}H_{24}N_2O_3S$	1.03	-0.01284
74		$C_{32}H_{24}N_2O_4S$	1.69	-0.22789
75		$C_{30}H_{17}Cl_3N_2O_3S$	2.25	-0.35218
76		$C_{31}H_{20}Cl_2N_2O_3S$	3.37	-0.52763
77		$C_{32}H_{23}FN_2O_5S$	3.32	-0.52114

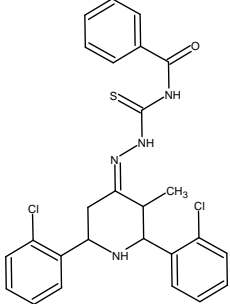
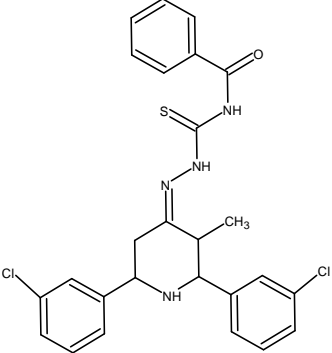
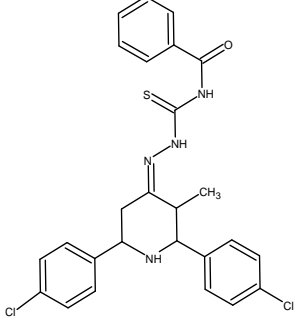
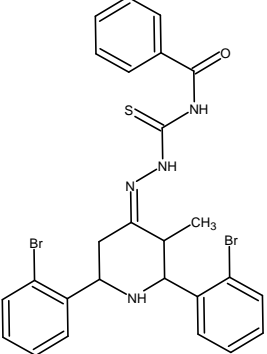
78		$C_{33}H_{26}N_2O_5S$	3.88	-0.58883
79		$C_{32}H_{23}ClN_2O_5S$	5.98	-0.7767

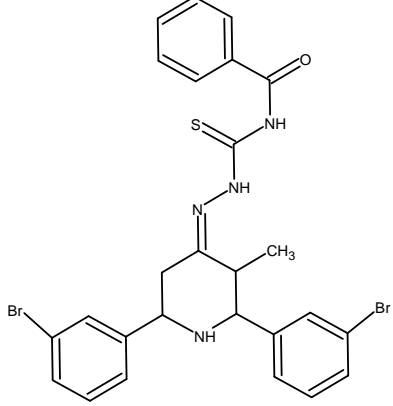
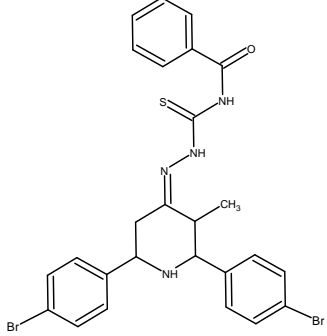
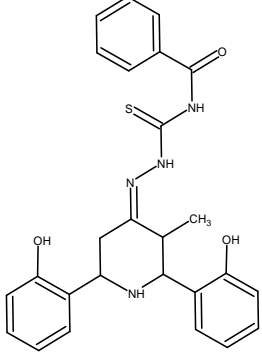
9.2. COMPOUNDS DESIGNING:

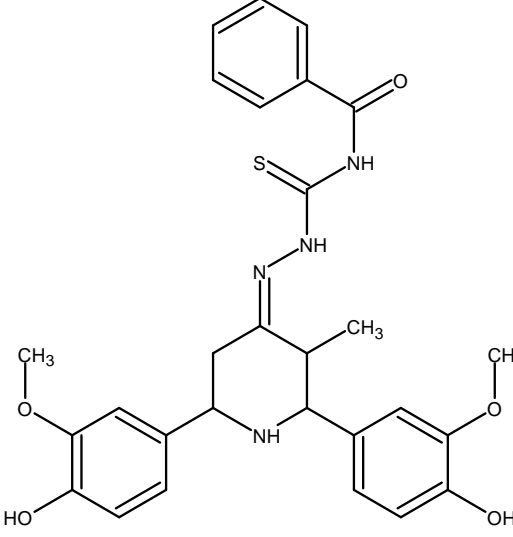
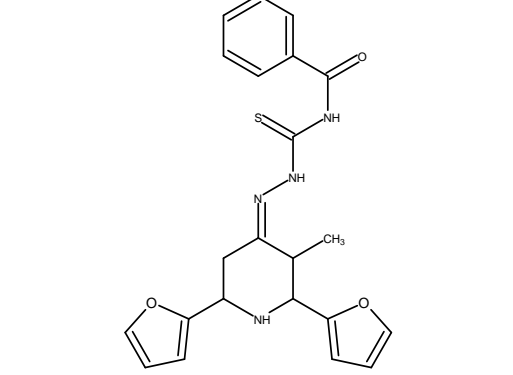
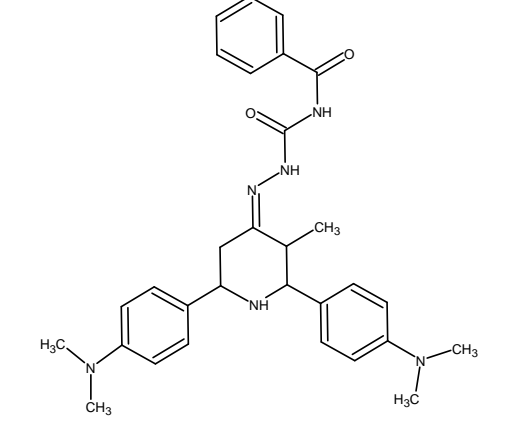
About 20 novel compounds containing benzamide attached to thiosemicarbazide fused with 4-piperidone were designed using CHEMDRAW software (Table.2). CHEMDRAW is a drawing tool that allows you to draw chemical structures including organics, organometallics, polymers and Markush structures. It also includes features such as calculation of molecular properties (e.g. molecular weight, density, molar refractivity, etc.) 2D and 3D structure cleaning and viewing and functionality for naming structures.

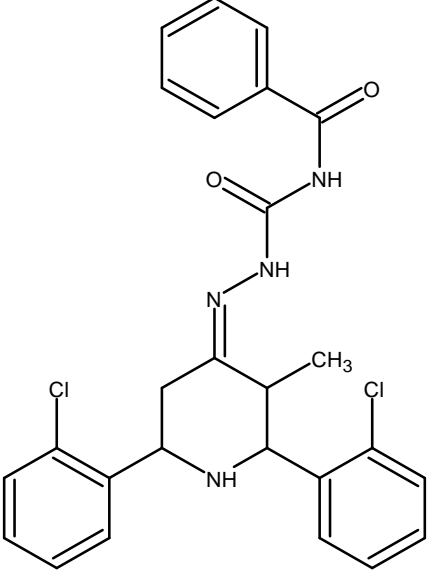
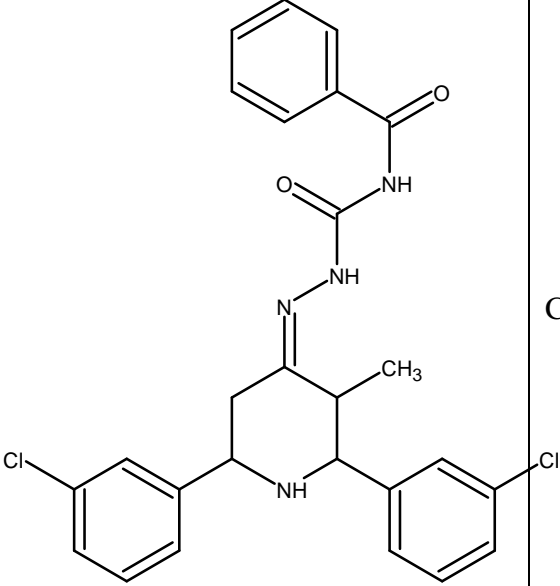
Table. 2. Designed compounds with their IUPAC name.

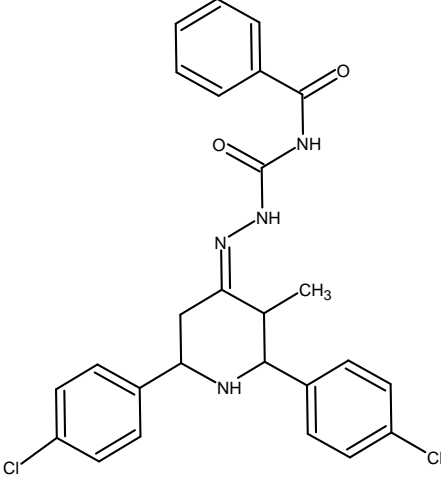
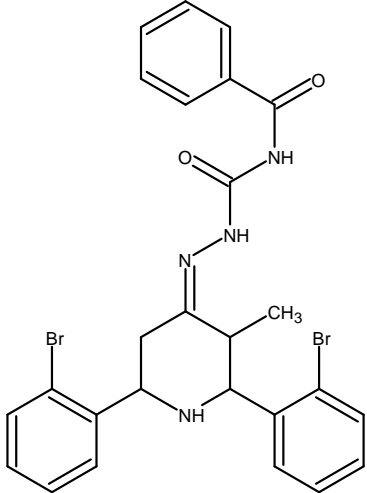
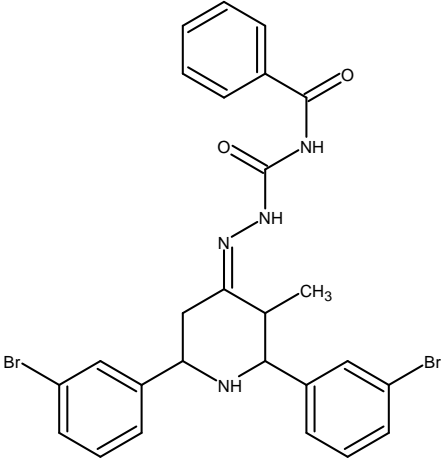
Compound No	Derivative Name	Structure	Molecular Formula	IUPAC Name
1a	P-Dimethylamino Benzaldehyde		$C_{30}H_{36}N_6OS$	1-benzoyl-3-[[[(4Z)-2,6-bis[4-(dimethylamino)phenyl]-3-methylpiperidin-4-ylidene]amino]thiourea

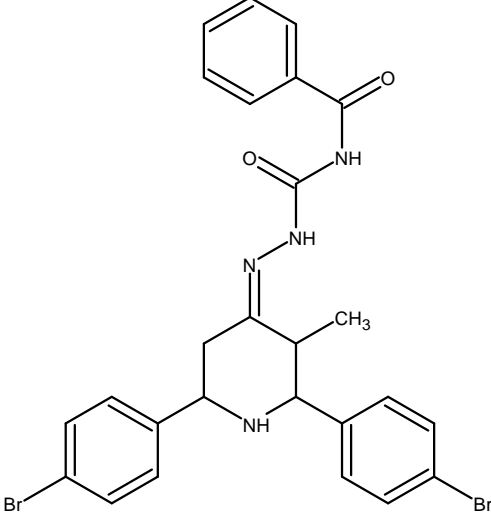
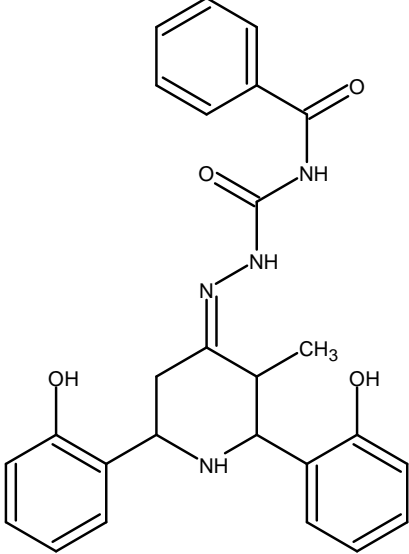
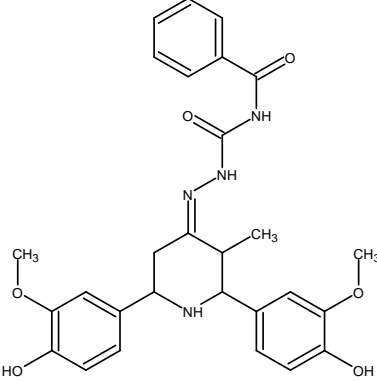
1b	2-Chloro Benzaldehyde		C ₂₆ H ₂₄ Cl ₂ N ₄ O S	1-benzoyl-3-[[4Z)- 2,6-bis(2- chlorophenyl)-3- methylpiperidin-4- ylidene]amino]thiou rea
1c	3-Chloro Benzaldehyde		C ₂₆ H ₂₄ Cl ₂ N ₄ O S	1-benzoyl-3-[[4Z)- 2,6-bis(3- chlorophenyl)-3- methylpiperidin-4- ylidene]amino]thiou rea
1d	P-Chloro Benzaldehyde		C ₂₆ H ₂₄ Cl ₂ N ₄ O S	1-benzoyl-3-[[4Z)- 2,6-bis(4- chlorophenyl)-3- methylpiperidin-4- ylidene]amino]thiou rea
1e	2-Bromo Benzaldehyde		C ₂₆ H ₂₄ Br ₂ N ₄ O S	1-benzoyl-3-[[4Z)- 2,6-bis(2- bromophenyl)-3- methylpiperidin-4- ylidene]amino]thiou rea

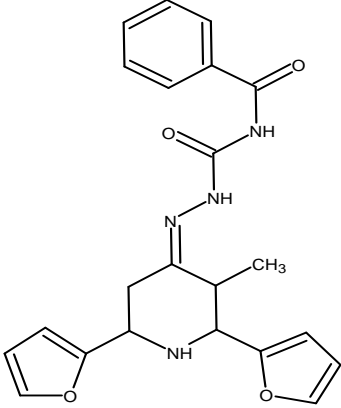
1f	3-Bromo Benzaldehyde		$C_{26}H_{24}Br_2N_4O$ S	1-benzoyl-3-[[[(4Z)-2,6-bis(3-bromophenyl)-3-methylpiperidin-4-ylidene]amino]thiourea
1g	4-Bromo Benzaldehyde		$C_{26}H_{24}Br_2N_4O$ S	1-benzoyl-3-[[[(4Z)-2,6-bis(4-bromophenyl)-3-methylpiperidin-4-ylidene]amino]thiourea
1h	Salicylaldehyde (2-Hydroxy Benzaldehyde)		$C_{26}H_{26}N_4O_3S$	1-benzoyl-3-[[[(4Z)-2,6-bis(2-hydroxyphenyl)-3-methylpiperidin-4-ylidene]amino]thiourea

1i	Vanillin (4-Hydroxy-3-Methoxy Benzaldehyde)		C ₂₈ H ₃₀ N ₄ O ₅ S	1-benzoyl-3-[[(4Z)-2,6-bis(4-hydroxy-3-methoxyphenyl)-3-methylpiperidin-4-ylidene]amino]thiourea
1j	Furfural (Furan-2-Carbaldehyde)		C ₂₂ H ₂₂ N ₄ O ₃ S	1-benzoyl-3-[[(4Z)-2,6-bis(furan-2-yl)-3-methylpiperidin-4-ylidene]amino]thiourea
2a	P-Dimethylamino Benzaldehyde		C ₃₀ H ₃₆ N ₆ O ₂	1-benzoyl-3-[[(4Z)-2,6-bis[4-(dimethylamino)phenyl]-3-methylpiperidin-4-ylidene]amino]thiourea

2b	2-Chloro Benzaldehyde		$C_{26}H_{24}Cl_2N_4O_2$	1-benzoyl-3-([(4Z)- 2,6-bis(2- chlorophenyl)-3- methylpiperidin-4- ylidene]amino)urea
2c	3-Chloro Benzaldehyde		$C_{26}H_{24}Cl_2N_4O_2$	1-benzoyl-3-([(4Z)- 2,6-bis(3- chlorophenyl)-3- methylpiperidin-4- ylidene]amino)urea

2d	P-Chloro Benzaldehyde		$C_{26}H_{24}Cl_2N_4O_2$	1-benzoyl-3-[[4(Z)- 2,6-bis(4- chlorophenyl)-3- methylpiperidin-4- ylidene]amino]urea
2e	2-Bromo Benzaldehyde		$C_{26}H_{24}Br_2N_4O_2$	1-benzoyl-3-[[4(Z)- 2,6-bis(2- bromophenyl)-3- methylpiperidin-4- ylidene]amino]urea
2f	3-Bromo Benzaldehyde		$C_{26}H_{24}Br_2N_4O_2$	1-benzoyl-3-[[4(Z)- 2,6-bis(3- bromophenyl)-3- methylpiperidin-4- ylidene]amino]urea

2g	4-Bromo Benzaldehyde		$C_{26}H_{24}Br_2N_4O_2$	1-benzoyl-3-([(4Z)-2,6-bis(4-bromophenyl)-3-methylpiperidin-4-ylidene]amino)urea
2h	Salicylaldehyde (2-Hydroxybenzaldehyde)		$C_{26}H_{26}N_4O_4$	1-benzoyl-3-([(4Z)-2,6-bis(2-hydroxyphenyl)-3-methylpiperidin-4-ylidene]amino)urea
2i	Vanillin (4-Hydroxy-3-Methoxybenzaldehyde)		$C_{28}H_{30}N_4O_6$	1-benzoyl-3-([(4Z)-2,6-bis(4-hydroxy-3-methoxyphenyl)-3-methylpiperidin-4-ylidene]amino)urea

2j	Furfural (Furan-2-Carbaldehyde)		C ₂₂ H ₂₂ N ₄ O ₄	1-benzoyl-3-[[[(4Z)-2,6-bis(furan-2-yl)-3-methylpiperidin-4-ylidene]amino]urea
----	---------------------------------	---	---	--

9.3. *In silico* screening of ligands:

The physiochemical properties were evaluated using Molinspiration software. Molinspiration is an online tool used to calculate the physiochemical properties, bioactivity scores of any compounds that are already known or novel in identity. [39]

The lead molecules are optimized in terms of potency, selectivity, pharmacokinetics (i.e.) absorption, distribution, metabolism and excretion (ADME) and toxicology before they can become candidates for drug development. *In silico* approaches to predict pharmacokinetic parameters (ADME) were pioneered by Lipinski *et al.* The ADME properties of the designed compounds were evaluated using Swiss ADME and PreADMET online softwares.

SWISS ADME:

Swiss ADME allows you to compute physiochemical descriptors as well as to predict ADME parameters. Pharmacokinetic properties, drugs like nature and medicinal chemistry friendliness of one or multiple small molecules to support drug discovery. There are different methods of log p identification from fragment approaches to topological methods. p- glycoprotein substrate, CYP450 inhibitors are used for pharmacokinetics predictions. And Lipinski's rule are calculated by this swiss adme. Synthetic accessibility value is also calculated which is a score based on the fragmental analysis of structure then molecular size and complexity are observed. Finally, a score is normalized between 1)easy synthesis(and 10)very difficult synthesis(. [40]

Lipinski's rule of five

Lipinski's rule of five also known as the Pfizer's rule of five or simply the rule of five is a rule of thumb to evaluate drug likeness or determine if a chemical compound with a certain pharmacological or biological activity has chemical properties and physical properties that would make it a likely orally active drug in humans. Lipinski's rule states that, in general, an orally active drug has no more than one violation of the following criteria:

- No more than 5 hydrogen bond donors (the total number of nitrogen– hydrogen and oxygen–hydrogen bonds)
- No more than 10 hydrogen bond acceptors (all nitrogen or oxygen atoms)
- A molecular mass less than 500 daltons
- An octanol-water partition coefficient log P not greater than 5

Ghose Filter

This filter defines drug-likeness constraints as follows:

- Calculated log P is between -0.4 and 5.6
- Molecular weight is between 160 and 480
- Molar refractivity is between 40 and 130
- The total number of atoms is between 20 and 70.

Veber Filter

The molecules fitting to these two properties have a high probability of good oral bioavailability.

- Rotatable bond: max. 12
- Polar Surface Area: max. 140 Å²

Egan Rule

Predicts good or bad oral bioavailability.

- $0 \geq \text{TPSA} \leq 132$
- $-1 \geq \log P \leq 6$.

Molar Refractivity

It is a measure of the total polarizability of a mole of a substance and is dependent on the temperature, the index of refraction, and the pressure.

The molar refractivity is defined as

$$A = \frac{4\pi}{3} N_A \alpha$$

Where $N_A = 6.022 \times 10^{23}$ is the Avogadro constant and α is the mean polarizability of a molecule

Polar surface area (PSA) or topological polar surface area (TPSA)

It is a measure of apparent polarity of a molecule is defined as the surface sum overall polar atoms, primarily oxygen and nitrogen, also including their attached hydrogen atoms. PSA is a commonly used for the optimization of a drug's ability to permeate cells. Molecules with a polar surface area of greater than 140 angstroms squared tend to be poor at permeating cell membranes.

Lipophilicity

Lipophilicity is the ability of a molecule to mix with an oily phase rather than with water, is usually measured as partition coefficient, P , between the two phases and is often expressed as $\log P$. Lipophilicity has also been found to affect a number of pharmacokinetic parameters: higher lipophilicity ($\log P > 5$) gives, in general, lower solubility, higher permeability in the gastrointestinal tract, across the blood–brain barrier and other tissue membranes, higher affinity to metabolizing enzymes and efflux pumps, and higher protein binding. Low lipophilicity can also negatively impact permeability and potency and thus results in low BA and efficacy.

Partition coefficient, P

It is defined as a particular ratio of the concentrations of a solute between the two solvents (a biphasic system of liquid phases), specifically for un-ionized solutes, and the logarithm of the ratio is thus $\log P$. When one of the solvents is water and the other is a non-polar solvent, then the $\log P$ value is a measure of lipophilicity or hydrophobicity.

$$\log P_{oct/wat} = \log \frac{[\text{solute}]_{\text{unionized octanol}}}{[\text{solute}]_{\text{unionized water}}}$$

$$\log P_{oct/wat} = \log C_{O/CW}$$

Lipophilicity not only impacts solubility but also influences permeability, potency, selectivity, absorption, distribution, metabolism, and excretion (ADME) properties and toxicity. A desired logP value (octanol-water partition coefficient) is no more than 5.

Water Solubility

Water solubility is a measure of the amount of chemical substance that can dissolve in water at a specific temperature. Solubility is common physicochemical parameter for drug discovery compounds. Determination of the aqueous solubility of the drug candidate is an important analysis as it reflects the bioavailability of the compound.

Log S

The aqueous solubility of a compound significantly affects its absorption and distribution characteristics. Typically, a low solubility goes along with a bad absorption and therefore the general aim is to avoid poorly soluble compounds.

Log S value is a unit stripped logarithm (base10) of the solubility measured in mol/liter. Log S value should be greater than -4.

Rotatable Bonds

The bioavailability of a drug like molecule is related with its rotatable bond number. Less than seven rotatable bonds are essential for good bioavailability. Many highly potent molecules carried more than 10 rotatable bonds and still administered through oral route.

Hydrogen bond acceptors and donors

12 or fewer H-bond donors and acceptors will have a high probability of good oral bioavailability.

PREADMET:

Predmet, is an online web server is also used for the prediction of pharmacokinetic properties and the prediction values for determination of blood-brain barrier (BBB) (permeation, buffer solubility receptor inhibition and substrates are also identified. [41, 42]

ADME Prediction

Numerous *in vitro* methods have been used in the drug selection process for assessing the intestinal absorption of drug candidates. Among them, Caco2-cell model and MDCK (Madin-Darby canine kidney) cell model has been recommended as a reliable *in vitro* model for the prediction of oral drug absorption. In absorption, this module provides prediction models for *in vitro* Caco2-cell and MDCK cell assay. Additionally, *in silico* HIA (human intestinal absorption) model and skin permeability model can predict and identify potential drug for oral delivery and transdermal delivery. In distribution, BBB (blood brain barrier) penetration can give information of therapeutic drug in the central nervous system (CNS), plasma protein binding model in its disposition and efficacy.

PROTOX II:

Animal's trials are currently the major method for determining the possible toxic effects of drug candidates and other methods represent cosmetic. *In silico* prediction methods represent an alternative approach and aim to rationalize preclinical drug development. Protox, a web server for prediction of rodent toxicity analysis the similarity of compounds with known median lethal doses (LD50) and identification of toxic fragments. The reports are regenerated within seconds.

There are two parts of the reports:

- Acute oral toxicity
- Possible toxicity targets indication.

With the prediction LD 50 in mg/kg also the toxicity class of compounds is calculated for I to VI by Global Harmonization System. Toxic doses are often given as LD50 values in mg/kg body weight. The LD50 is the median lethal dose meaning the dose at which 50% of test subjects die upon exposure to a compound. Toxicity classes are defined according to the globally harmonized system of classification of labeling of chemicals (GHS). LD50 values are given in [mg/kg]:

- Class I: fatal if swallowed $LD50 \geq 5$
- Class II: fatal if swallowed $5 < LD50 \leq 50$
- Class III: toxic if swallowed $50 < LD50 \leq 300$
- Class IV: harmful if swallowed $300 < LD50 \leq 2000$
- Class V: may be harmful if swallowed $2000 < LD50 \leq 5000$

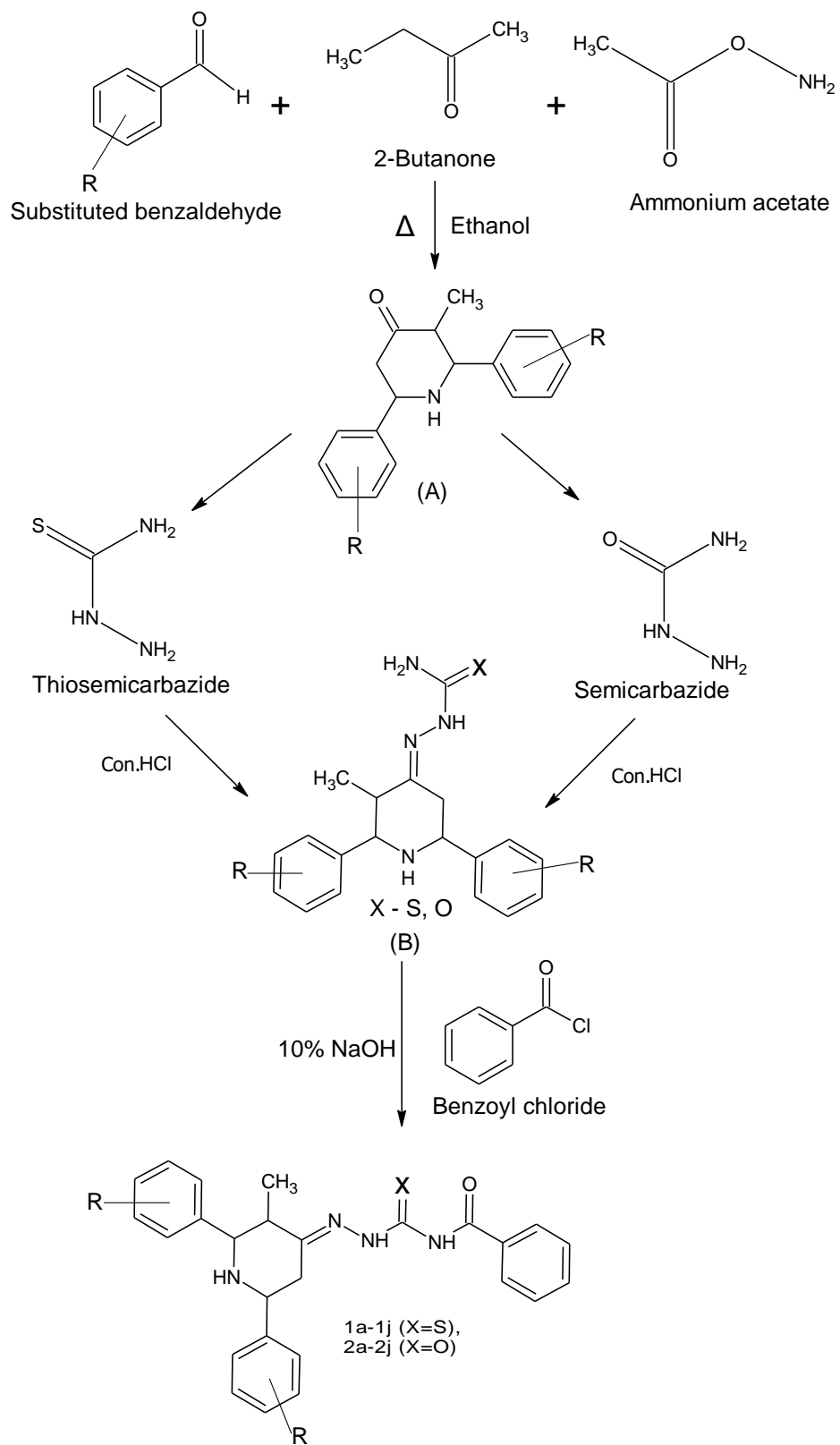
- Class VI: non-toxic (LD50 > 5000)
- Toxicity targets
- Hepatotoxicity
- Carcinogenicity
- Mutagenicity
- Cytotoxicity
- Immunotoxicity

And toxicity predictions of nuclear response signaling, stress response pathway. So these are the advantages of the protox web server. [43]

DOCKING:

All the 20 designed compounds were executed for *insilico* molecular docking studies. The target enzyme acetylcholinesterase was downloaded from the protein data bank (PDB ID: 4EY7). The protein was prepared using the Molegro Molecular Viewer 7.0 software. Preparation was done by removing ligands, cofactors, and water molecules. These ligands were minimized using Chem3DUltra software. The ligands were saved in .pdb format. Then the docking was performed for all the compounds using Autodock 4.0 software [44]. The results were visualized by Biovia discovery studio.

9.4. SCHEME:



9.5. GENERAL PROCEDURE FOR THE SYNTHESIS:

Step.1

Dry ammonium acetate (0.1 mole), substituted benzaldehyde (0.2 mole) and butane-2-one (0.1 mole) were dissolved in 50 mL ethanol. The mixture was heated to boiling until the colour changes from yellow to orange and allowed to stand at room temperature overnight. 30ml of concentrated ammonia and 30 ml concentrated hydrochloric acid was added. Then cooled by keeping in refrigerator. The precipitated hydrochloride salt was neutralized with 30ml dry ether. The product (A) was filtered, dried, and recrystallized from ethanol. [45, 46]

Step.2

The product (A) 0.01 mole was mixed with thiosemicarbazide or semicarbazide 0.01mole in 30ml of ethanol in a round bottomed flask. The flask was fitted with a reflux. Then the contents were refluxed continuously for 3hours. Then kept undisturbed overnight. The precipitate (B) was filtered, dried, and recrystallized with ethanol. [45, 46]

Step.3

The product (B) and the benzoyl chloride was taken in equimolar quantities (0.01mole). The compound was mixed with 10% sodium hydroxide solution followed by slow addition of benzoyl chloride with continuous stirring in ice. Then the contents were kept for seeding overnight in refrigerator. The product (1a-1j, 2a-2j) was filtered, dried, and recrystallized with ethanol. [47]

9.6. CHARACTERIZATION:

All the synthesized compounds were characterized by using FT-IR, ^1H -NMR, ^{13}C -NMR, MASS Spectroscopy.

Infrared Spectroscopy

The infrared spectroscopy is one of the most powerful analytical techniques, this offers the possibility of chemical identification. The advantage of infrared spectroscopy over the other usual methods of structural analysis is that it provides useful information about the functional groups present in the molecule quickly. The technique is based upon the simple fact that a chemical substance shows marked selectable absorption in the infrared region. After absorbing IR radiations the molecules of a chemical compound exhibit small vibrations, giving rise to closely packed

absorption bands called as IR absorption spectrum which may extend over a wide wavelength range. Various bands will be present in IR spectrum which corresponds to the characteristic functional groups and bonds present in a chemical substance. Thus an IR spectrum of a chemical compound is a fingerprint for its identification.

Nuclear Magnetic Resonance Spectroscopy

It is the branch of spectroscopy in which radiofrequency waves induces transitions between magnetic energy levels of nuclei of a molecule. The magnetic energy levels are created by keeping nuclei in a magnetic field. Without the magnetic field the spin states of nuclei are degenerated i.e., possess the same energy and the energy level transition is not possible. The energy level transition is possible with the application of external magnetic field which requires different Rf radiation to put them into resonance. This is a measurable phenomenon. It is a powerful tool for the investigation of nuclei structure.

Mass spectroscopy

Mass spectrometer performs three essential functions. First, it subjects molecules to bombardment by a stream of more amounts of energy electrons, converting some of the molecules to ions, which are then accelerated in a field of electric. Second, the ions which are accelerated are divided according to their ratios of mass to charge in an electric or magnetic field. Finally the ions that have particular mass-to-charge ratio are detected by a device which can count the number of ions striking it. The detector's output is amplified and fed to a recorder. The trace from the recorder is a mass spectrum a graph of particles detected as a function of mass-to- charge ratio. The Mass spectra of the synthesized compounds were taken using Agilent spectrometer.

10. RESULTS AND DISCUSSION:

10.1. 2D QSAR MODEL:

2D QSAR models were generated to determine the structural relationship between the compounds and the acetylcholinesterase inhibition activity. The structures with their pIC₅₀ value were given in the table. 1. About 3 models were generated and were listed below. The model 3 was found with the minimum number of outliers. So it was considered as the best. All the models were validated by both internal and external validation parameters. The experimental, predicted activities and leverage values were given in the table. 3. The internal and external parameters were given in the table.4.

MODEL 1

$$\text{pIC}_{50} = -1.3496 + 0.0162 (\text{ATSC3i}) - 0.7325 (\text{GATS4i}) - 0.0509 (\text{VE3_Dze}) + 0.4199 (\text{C3SP2})$$

R2: 0.8431 R2adj: 0.8327 R2-R2adj: 0.0105 LOF: 0.0553

Kxx: 0.3553 Delta K: 0.1138 RMSE tr: 0.2062 MAE tr: 0.1224

RSS tr: 2.7639 CCC tr: 0.9149 s: 0.2146 F: 80.6326

MODEL 2

$$\text{pIC}_{50} = -2.0963 + 0.1883 (\text{AATSC4i}) - 26.4482 (\text{VE2_Dzi}) + 0.3572 (\text{nBase}) + 0.2309 (\text{C3SP2}) + 0.7007 (\text{ETA_dBetaP})$$

R2: 0.9559 R2adj: 0.9517 R2-R2adj: 0.0042 LOF: 0.0125

Kxx: 0.3137 Delta K: 0.1292 RMSE tr: 0.0928 MAE tr: 0.0716

RSS tr: 0.5077 CCC tr: 0.9774 s: 0.0979 F: 229.5083

MODEL 3

$$\text{pIC}_{50} = -1.9584 - 0.0694 (\text{nBr}) - 0.0001 (\text{ATSC6m}) - 0.0074 (\text{ATSC3i}) + 0.8757 (\text{MATS4e}) + 5734 (\text{nBase})$$

R2: 0.9646 R2adj: 0.9610 R2-R2adj: 0.0036 LOF: 0.0076

Kxx: 0.3890	Delta K: 0.0778	RMSE tr: 0.0713	MAE tr: 0.0564
RSS tr: 0.2798	CCC tr: 0.9820	s: 0.0756	F: 267.06

The model 3 is found to be best in statistical parameters. The R^2 value is 0.96 which is the coefficient of correlation. This determines that the model is robust. The R^2_{adj} value is 0.9610 reveals that the model is convenient for the addition of another descriptor. The Friedman's Lack of fit is least saying that the model is not of chance correlation. The model 3 developed in QSARINS undergo rigorous validation both internal and external according to the OECD principles. The OECD principles involve a defined endpoint, an unambiguous algorithm, a defined domain of applicability, goodness of fit, and mechanistic interpretation of the model. The experimental and the predicted activities were calculated using the model. The residual value are also determined. The graph is constructed between experimental and the predicted values for the model. The best model 3 is given in the Figure.1. Internal validation by cross validation leave-one-out (Q2LOO) was carried out and the value stood nearer to R^2 value of the model (Figure.2). Cross validation leave-many-out (Q2LMO) was also done. All the validation results were tabulated in table 3 and 4. This validation result that the model 3 is robust and fit. (Figure.3)

External validation by Q2-F1, Q2-F2, and Q2-F3, and CCC were applied on selected models. Golbraikh and Tropsha was also verified. The values are recorded in the table 4.

The applicability domain was done by calculating leverage values. The William's plot for the model 3 is given in Figure. The critical leverage HAT value h^* is 0.327. The limits of standard deviation is ± 2.5 . The compound 74 lies beyond this limit is considered as outlier. The outlier compounds are 74, 27, 67, 79 in the model 3. (table.3) (Figure.4)

The Y-scrambling is a technique where the responses are shuffled randomly and output of the model should drastically decline. In model 3, the R^2_{Yscr} and Q^2_{Yscr} value are 0.0926 and -0.1513 respectively. These values are in decreased state to that of the R^2 and Q^2 value of the model 3. Thus model 3 is not by chance correlation. (Table.3) (Figure.5). In the same manner the descriptors were varied randomly and model was calculated. This is known as the Y-scramble for the descriptors. r^2_{Yrnd} and Q^2_{Yrnd} values are 0.0905 and -0.1540 respectively, which is decreased than the model r^2 and Q^2 values (model 3). (Figure.6) [38, 48]

Table.3. Experimental, predicted activities, leverage values of all the models and their residues.

Name	Exp. endpoint	Pred. activity model 1	Residual value: model 1	Pred. activity model 2	Residual value: model 2	Pred. activity model 3	Residual value: model 3	HAT value model 1 (h*=0.3273)	HAT value model 2 (h*=0.3051)	HAT value model 3 (h*=0.3273)
1	-1.6964	-1.8171	-0.1206	-1.7618	-0.0654	-1.6601	0.0364	0.0389	0.064	0.1143
2	-1.7745	-1.8008	-0.0262	-1.7924	-0.0178	-1.7489	0.0257	0.0363	0.0354	0.0586
3	-1.8838	-1.8251	0.0587	-1.8362	0.0477	-1.7844	0.0994	0.0414	0.0598	0.0692
4	-1.7838	-1.7545	0.0293	-1.7863	-0.0025	-1.8145	-0.0307	0.0365	0.0317	0.0594
5	-1.6647	-1.7127	-0.048	-1.7568	-0.092	-1.6752	-0.0105	0.0411	0.0486	0.1039
6	-1.7081	-1.5426	0.1655	-1.7579	-0.0498	-1.745	-0.0369	0.123	0.0617	0.0635
7	-1.6992	-1.8292	-0.13	-1.7963	-0.0971	-1.833	-0.1337	0.0464	0.0444	0.1129
8	-1.7653	-1.8423	-0.077	-1.8375	-0.0722	-1.7896	-0.0243	0.0465	0.0749	0.0576
9	-1.7683	-1.6697	0.0986	-1.7544	0.0138	-1.7444	0.0239	0.0691	0.0344	0.0555
10	-1.6837	-1.7226	-0.039	-1.8099	-0.1262	-1.8195	-0.1358	0.0593	0.041	0.0594
11	-1.7357	-1.6421	0.0935	-1.6747	0.061	-1.6962	0.0395	0.062	0.1138	0.0622
12	-1.7669	-1.7652	0.0017	-1.7388	0.0281	-1.7359	0.031	0.0489	0.0561	0.052
13	-1.7005	-1.6711	0.0295	-1.7176	-0.017	-1.6416	0.0589	0.1481	0.2159	0.1424
14	-1.764	-1.7822	-0.0182	-1.7622	0.0019	-1.7073	0.0568	0.0375	0.0433	0.1425
15	-1.7497	-1.8169	-0.0673	-1.8058	-0.0562	-1.7428	0.0069	0.0408	0.0394	0.0731
16	-1.6652	-1.7108	-0.0456	-1.7585	-0.0933	-1.7894	-0.1242	0.0486	0.0524	0.0764
17	-1.7003	-1.5856	0.1147	-1.7436	-0.0434	-1.6502	0.0501	0.1026	0.0681	0.2316
18	-1.7618	-1.7111	0.0507	-1.7945	-0.0328	-1.7325	0.0293	0.062	0.0369	0.1175
19	-1.7784	-1.8126	-0.0342	-1.7659	0.0124	-1.7841	-0.0057	0.0499	0.0478	0.2968
20	-1.7658	-1.8351	-0.0693	-1.807	-0.0411	-1.7407	0.0251	0.0472	0.0486	0.0993
21	-1.7838	-1.6417	0.1421	-1.7248	0.0591	-1.7312	0.0526	0.0594	0.0533	0.1062
22	-1.7983	-1.7071	0.0912	-1.7803	0.018	-1.8063	-0.008	0.049	0.0361	0.0604
23	-1.8343	-1.1455	0.6888	Excluded	Excluded	Excluded	Excluded	0.6141	Excluded	Excluded
24	-1.7803	-1.7349	0.0454	-1.715	0.0653	-1.7674	0.0128	0.0478	0.0709	0.1027

25	-1.7382	-1.6979	0.0403	-1.7481	-0.01	-1.696	0.0422	0.156	0.2424	0.1918
26	-1.7927	-1.7829	0.0098	-1.7662	0.0265	-1.7075	0.0851	0.0316	0.0359	0.0691
27	-1.9332	-1.8087	0.1245	-1.8102	0.1231	-1.7513	0.1819	0.0372	0.0543	0.0869
28	-1.7841	-1.7364	0.0477	-1.7617	0.0224	-1.7682	0.0159	0.0315	0.0351	0.0818
29	-1.5202	-1.6888	-0.1686	-1.7319	-0.2117	-1.6137	-0.0935	0.0382	0.0559	0.13
30	-1.6241	-1.5803	0.0438	-1.7474	-0.1233	-1.6784	-0.0543	0.0881	0.0557	0.102
31	-1.8434	-1.8168	0.0266	-1.7705	0.0728	-1.7712	0.0722	0.04	0.0427	0.2362
32	-1.847	-1.8312	0.0157	-1.8119	0.035	-1.7351	0.1119	0.0414	0.0679	0.2326
33	-1.7359	-1.6411	0.0948	-1.7268	0.0092	-1.7216	0.0143	0.081	0.0419	0.0635
34	-1.7869	-1.6956	0.0913	-1.7824	0.0045	-1.8038	-0.0169	0.0689	0.0391	0.0746
35	-1.6301	-1.6054	0.0247	-1.6495	-0.0194	-1.6851	-0.055	0.0629	0.1109	0.0993
36	-1.6512	-1.7412	-0.09	-1.7141	-0.0629	-1.7222	-0.071	0.0449	0.0471	0.0869
37	-1.6854	-1.6498	0.0356	-1.7043	-0.0189	-1.617	0.0684	0.142	0.195	0.1976
38	-1.936	-1.6948	0.2412	-1.8216	0.1144	-1.9386	-0.0026	0.056	0.1119	0.15
39	-0.9619	-1.4822	-0.5203	Excluded	Excluded	Excluded	Excluded	0.0427	Excluded	Excluded
40	-1.822	-1.6118	0.2102	-1.7822	0.0398	-1.8963	-0.0744	0.0573	0.18	0.0943
41	-1.684	-1.781	-0.0971	-1.7651	-0.0812	-1.6619	0.022	0.0663	0.1271	0.0665
42	-1.8026	-1.4712	0.3315	-1.7309	0.0717	-1.7619	0.0408	0.0797	0.1774	0.0498
43	-1.8626	-1.8509	0.0117	-1.849	0.0135	-1.8484	0.0142	0.1216	0.1216	0.0769
44	-1.5908	-1.7975	-0.2067	-1.8567	-0.2659	Excluded	Excluded	0.0352	0.072	Excluded
45	-1.8741	-1.7433	0.1308	-1.7666	0.1074	-1.8337	0.0404	0.087	0.0474	0.0486
46	-1.7389	-1.7801	-0.0413	-1.8444	-0.1055	-1.753	-0.0142	0.0297	0.0912	0.088
47	-1.7951	-1.8619	-0.0668	-1.8474	-0.0523	-1.8747	-0.0797	0.1167	0.1185	0.117
48	-1.7712	-1.8149	-0.0437	-1.8567	-0.0855	-1.8296	-0.0584	0.0332	0.0671	0.076
49	-1.9117	-1.7605	0.1511	-1.7654	0.1462	-1.8648	0.0469	0.0835	0.0451	0.0832
50	-1.8013	-1.7896	0.0118	-1.8437	-0.0424	-1.7766	0.0247	0.0318	0.0986	0.0619
51	-1.8818	-1.8211	0.0607	-1.8361	0.0457	-1.8465	0.0353	0.166	0.1108	0.0678
52	-1.953	-1.7106	0.2424	-1.8375	0.1155	-1.8384	0.1146	0.0856	0.0758	0.065

53	-1.7962	-1.6417	0.1544	-1.7531	0.043	-1.8433	-0.0471	0.0989	0.0571	0.0485
54	-1.6905	-1.6963	-0.0058	-1.8311	-0.1406	-1.7795	-0.089	0.0358	0.0795	0.0718
55	-1.6906	-1.9016	-0.211	-1.7794	-0.0888	-1.7102	-0.0197	0.0937	0.1042	0.1009
56	-1.623	-1.762	-0.139	-1.771	-0.148	-1.7153	-0.0923	0.0554	0.0924	0.0607
57	-1.6977	-1.8333	-0.1356	-1.6848	0.0129	-1.6981	-0.0004	0.0843	0.0395	0.0898
58	-1.6757	-1.8396	-0.1639	-1.7206	-0.0449	-1.6279	0.0478	0.0608	0.1001	0.0851
59	-1.7615	-1.8249	-0.0634	-1.7764	-0.0149	-1.7961	-0.0347	0.1208	0.1085	0.0378
60	-1.792	-1.7579	0.0341	-1.7805	0.0115	-1.7588	0.0332	0.0364	0.0747	0.0396
61	-1.7404	-1.7366	0.0038	-1.7361	0.0043	-1.7699	-0.0294	0.0843	0.0599	0.0345
62	-1.7307	-1.7923	-0.0616	-1.8342	-0.1035	-1.6902	0.0405	0.0294	0.1221	0.0842
63	-0.8389	-0.9976	-0.1587	-1.0349	-0.196	-0.874	-0.0351	0.0708	0.1488	0.2267
64	-1.3617	-1.1391	0.2226	-1.1103	0.2514	Excluded	Excluded	0.0965	0.2141	Excluded
65	-0.6021	-0.7713	-0.1692	-1.0173	-0.4153	Excluded	Excluded	0.1094	0.169	Excluded
66	-0.9542	-0.8479	0.1063	-1.0247	-0.0704	-0.8574	0.0968	0.0834	0.1624	0.2151
67	-0.9868	-0.8721	0.1147	-1.0457	-0.0589	-0.7081	0.2787	0.0964	0.1601	0.1767
68	0.3565	-0.7899	-1.1465	Excluded	Excluded	Excluded	Excluded	0.0822	Excluded	Excluded
69	-1.3222	-0.9694	0.3528	-1.0958	0.2265	Excluded	Excluded	0.1116	0.1734	Excluded
70	-0.8573	-0.9371	-0.0798	-1.0717	-0.2144	-0.8565	0.0008	0.0975	0.1705	0.2164
71	-1.4314	-0.8705	0.5608	Excluded	Excluded	Excluded	Excluded	0.0842	Excluded	Excluded
72	-1.4786	0.0172	1.4958	Excluded	Excluded	Excluded	Excluded	0.3877	Excluded	Excluded
73	-0.0128	-0.0204	-0.0076	-0.12	-0.1071	Excluded	Excluded	0.2289	0.3469	Excluded
74	-0.2279	-0.2262	0.0017	-0.3231	-0.0953	-0.352	-0.1241	0.1659	0.2156	0.3855
75	-0.3522	-0.4193	-0.0671	Excluded	Excluded	Excluded	Excluded	0.2536	Excluded	Excluded
76	-0.5276	-0.4139	0.1137	-0.3677	0.16	-0.4883	0.0394	0.1256	0.1944	0.2298
77	-0.5211	-0.4714	0.0497	-0.5855	-0.0644	-0.6472	-0.126	0.1451	0.1207	0.1525
78	-0.5888	-0.424	0.1648	-0.4202	0.1686	-0.5782	0.0107	0.136	0.165	0.1737
79	-0.7767	-0.7721	0.0046	-0.6319	0.1448	-0.5997	0.177	0.0552	0.1183	0.1705

Table.4 Internal and external validation parameters.

MODEL	1	2	3
Q^2_{loo}	0.08156	0.9395	0.9523
$R^2-Q^2_{loo}$	0.0276	0.0164	0.0123
Q^2_{LMO}	0.8094	0.9351	0.9489
R^2_{Yscr}	0.0625	0.0855	0.0926
Q^2_{Yscr}	-0.1029	-0.1389	-0.1513
R^2_{Yrnd}	0.0617	0.0865	0.0905
Q^2_{Yrnd}	-0.1041	-1.384	-0.154
$RMSE_{ext}$	0.4552	0.1628	0.0895
MAE_{ext}	0.2358	0.1215	0.0562
$PRESS_{ext}$	2.9006	0.371	0.1041
R^2_{ext}	0.341	0.8703	0.9703
CCC_{ext}	0.4299	0.8978	0.9738
Q^2-F1	-1.2756	0.7968	0.942
Q^2-F2	-2.0045	0.7953	0.9414
Q^2-F3	0.2357	0.8641	0.9443
$Avg.r^2_m$	0.0614	0.7872	0.8489
Δr^2_m	0.4738	0.1218	0.0429

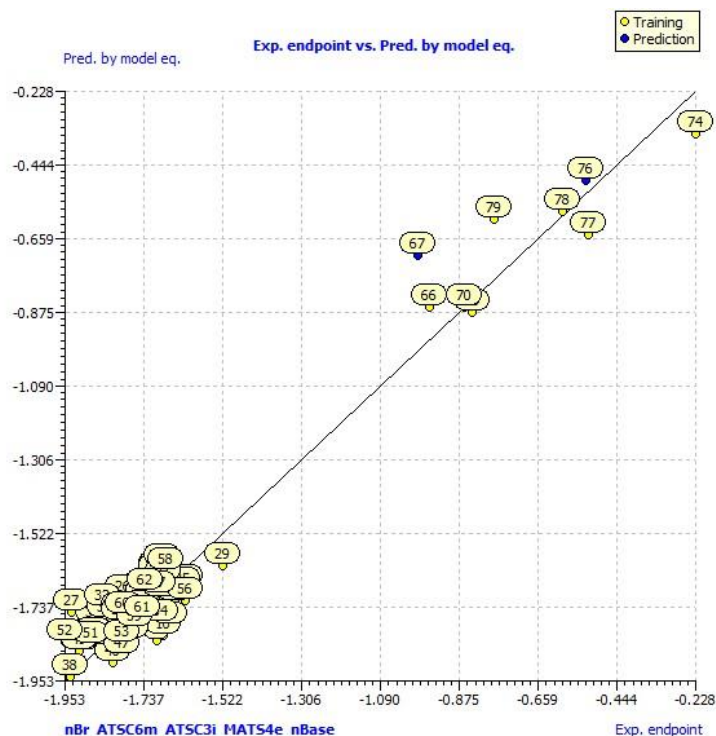


Figure.2. Plot of experimental and predicted activities of the model 3.

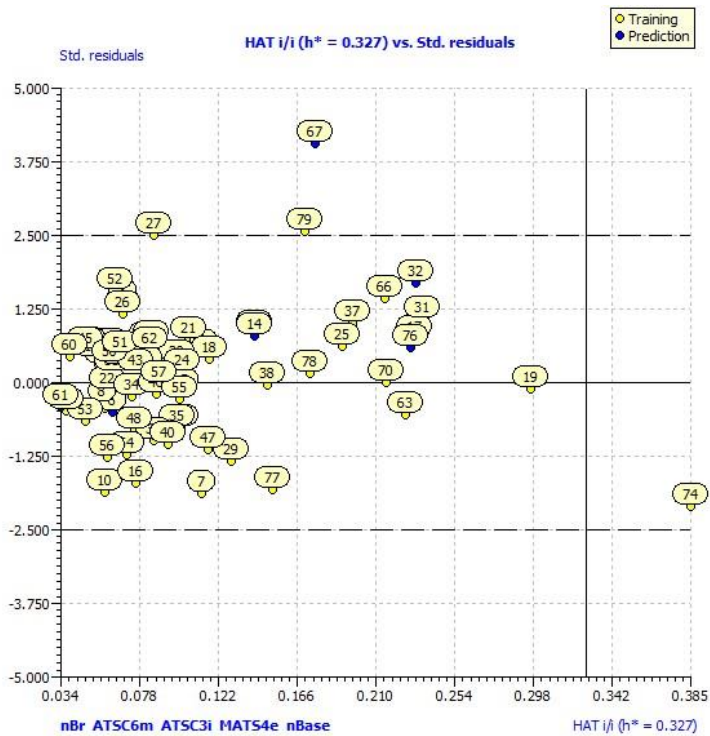


Figure.3. Leverage plot (Williams graph) of the model 3.

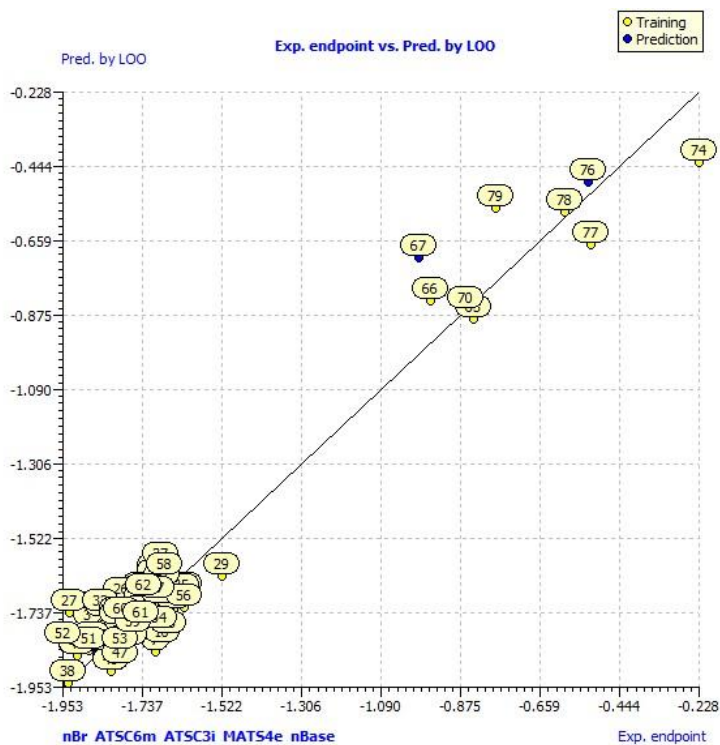


Figure.4. Plot of internal validation by Leave One Out method for the model 3.

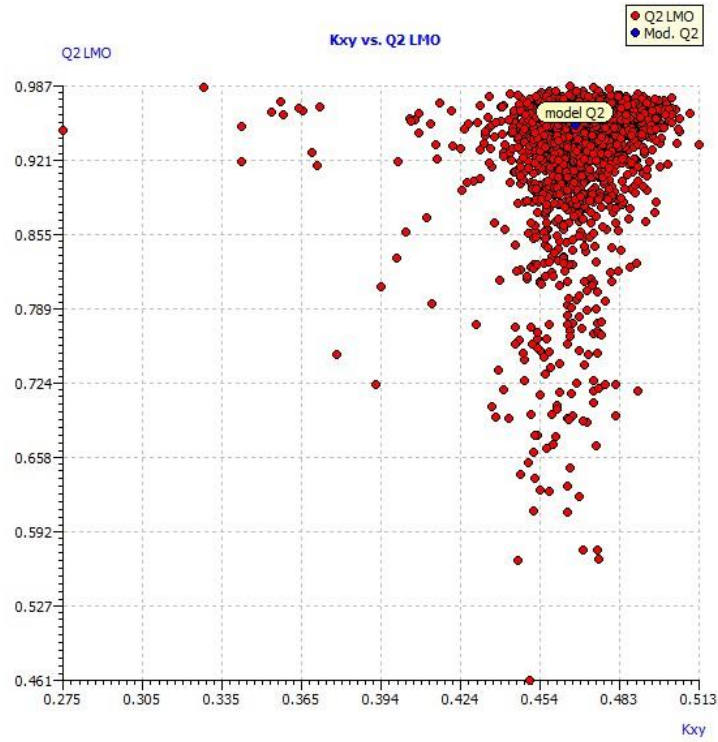


Figure.5. Plot of internal validation by Leave Many Out method for the model 3

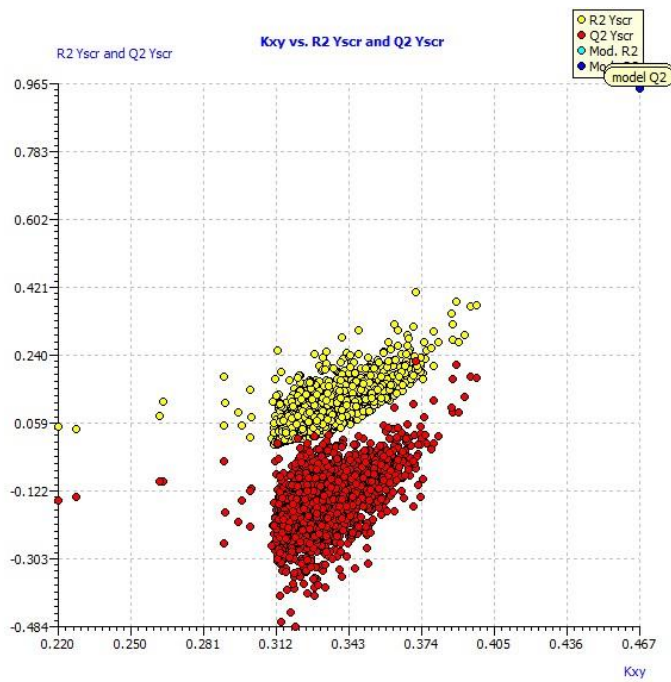


Figure.6. Plot for the Y-scrambling for the model 3.

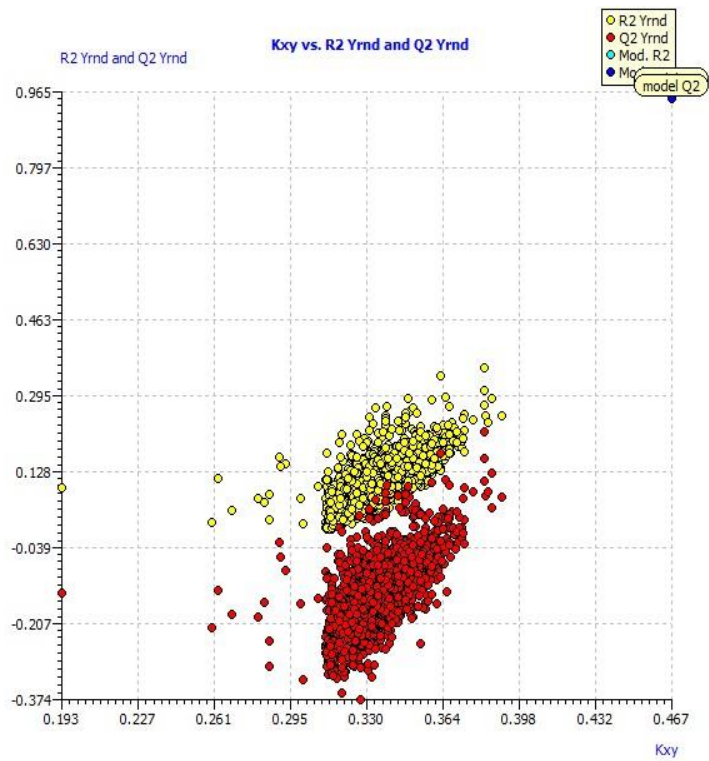


Figure 7. Y-scrambling by varying the descriptors for the model 3.

10.2. COMPOUNDS DESIGNED:

The novel 20 compounds designed were given in the table.2. These compounds were analysed for their physiochemical properties using Molinspiration software and provided in the table.5.

Table.5. Physiochemical properties of the designed compounds.

Compound no.	LogP	TPSA	natoms	Mol. Wt.	nON	nOHNH	nRotb	Volume	No. of H bond donors	No. of H bond acceptor	Molecular Refractivity
1a	4.36	71.99	38	528.73	7	3	8	498.99	3	3	164.55
1b	5.42	65.52	34	511.48	5	3	6	434.25	3	3	146.15
1c	5.47	65.52	34	511.48	5	3	6	434.25	3	3	146.15
1d	5.51	65.52	34	511.48	5	3	6	434.25	3	3	146.15
1e	5.68	65.52	34	600.38	5	3	6	442.95	3	3	151.53
1f	5.73	65.52	34	600.38	5	3	6	442.95	3	3	151.53
1g	5.78	65.52	34	600.38	5	3	6	442.95	3	3	151.53
1h	4.04	105.97	34	474.97	7	5	6	423.21	5	5	140.18
1i	2.84	124.44	38	534.64	9	5	8	474.3	5	7	153.16
1j	3.57	91.8	30	422.51	7	3	6	370.31	3	5	120.67
2a	3.82	89.06	38	512.66	8	3	6	490.11	3	4	157.35
2b	4.88	82.59	34	495.41	6	3	4	425.37	3	4	138.95
2c	4.92	82.59	34	495.41	6	3	4	425.37	3	4	138.95
2d	4.97	82.59	34	495.41	6	3	4	425.37	3	4	138.95
2e	5.14	82.59	34	584.31	6	3	4	434.07	3	4	144.33
2f	5.19	82.59	34	584.31	6	3	4	434.07	3	4	144.33
2g	5.24	82.59	34	584.31	6	3	4	434.07	3	4	144.33
2h	3.5	123.04	34	458.52	8	5	4	414.33	5	6	132.98
2i	2.29	141.51	38	518.57	10	5	6	465.43	5	8	145.96
2j	3.03	108.87	30	406.44	8	3	4	361.44	3	6	113.46

10.3. *IN SILICO* SCREENING RESULTS

- The Swiss ADME results were provided in the table.6. The ADME results from preADMET software were tabulated in the Table.7. The toxicity results were provided in the table.8.
- The compounds 1h, 1j, 2j passed the Lipinski rule of five. Remaining compounds did not pass the Lipinski rule. They mostly violated the molecular weight > 500daltons. Most of compounds passed Veber and Egan rules.
- The Blood Brain Barrier penetration value ranges from 0.07 to 3.4. The standard donepezil shows the BBB value of 0.187. So the compounds were found to penetrate efficiently into the BBB.
- All the compounds showed more than 90% of human intestinal absorption.
- All the compounds except 1j and 2j exhibited an inhibitor of Pgp glycoprotein. This Pgp glycoprotein regulates the intestinal absorption and urinary excretion.
- The compounds shows more than 84% of plasma protein binding. The compounds 1e, f, 1g, 2e, 2f, 2g were found with more than 98% of plasma protein binding.
- The toxicity resulted in the class of 4 and 5 which denotes may or may not be harmful if swallowed.
- All the compounds showed inactive in mutagenicity, immunogenicity and cytotoxicity.
- Except 1a and 2a, compounds showed active in hepatotoxicity at the lethal dose of 1500 – 2500 mg/kg.

Table.6. Swiss ADME results for examining the passing of rules.

Compound no.	Lipinski no. of violations	Ghose no. of violations	Veber no. of violations	Egan no. of violations	Muegge no. of violations	Bioavailability Score	Synthetic Accessibility
1a	1	3	0	0	1	0.55	5.04
1b	2	2	0	0	1	0.17	4.55
1c	2	2	0	0	1	0.17	4.53
1d	2	2	0	0	1	0.17	4.5
1e	2	2	0	0	2	0.17	4.65
1f	2	2	0	0	2	0.17	4.61
1g	2	2	0	0	2	0.17	4.54
1h	0	1	0	1	0	0.55	4.55
1i	1	2	1	1	1	0.55	4.87

1j	0	0	0	0	0	0.55	4.51
2a	1	3	0	0	0	0.55	4.93
2b	1	2	0	0	1	0.55	4.45
2c	1	2	0	0	1	0.55	4.43
2d	1	2	0	0	1	0.55	4.39
2e	2	2	0	0	1	0.17	4.55
2f	2	2	0	0	1	0.17	4.51
2g	2	2	0	0	1	0.17	4.43
2h	0	1	0	0	0	0.55	4.45
2i	1	2	1	1	0	0.55	4.77
2j	0	0	0	0	0	0.55	4.43

Table.7. ADME results of all the compounds designed using Pre ADMET software.

Compound no.	1a	1b	1c	1d	1e	1f	1g	1h	1i	1j
AlogP98 value	5.3875	6.3919	6.3919	6.3919	6.5599	6.5599	6.5599	4.5283	4.4955	3.6401
AMolRef	160.4953	141.2477	141.2477	141.2477	146.8837	146.8837	146.8837	135.0263	147.9527	116.2697
BBB	1.05107	2.81972	3.13952	2.93252	3.13912	3.4388	3.25281	0.24095	0.218408	0.074378
Buffer solubility mgL	18.0335	14.7251	16.6978	46.9071	2.96619	3.36356	9.44884	245.893	237.264	1284.36
Caco2	28.7517	30.8004	29.4757	29.7181	33.6693	32.4796	32.6798	20.6125	20.659	22.3748
CYP_2C19 inhibition	Non	Non	Non	Non	Non	Non	Non	Non	Non	Non
CYP_2C9 inhibition	Inhibitor	Inhibitor	Inhibitor	Inhibitor	Inhibitor	Inhibitor	Inhibitor	Inhibitor	Inhibitor	Inhibitor
CYP_2D6 inhibition	Non	Non	Non	Non	Non	Non	Non	Non	Non	Non
CYP_2D6 substrate	Weakly	Weakly	Weakly	Weakly	Weakly	Weakly	Weakly	Weakly	Weakly	Substrate
CYP_3A4 inhibition	Non	Non	Non	Non	Non	Non	Non	Inhibitor	Inhibitor	Non
CYP_3A4 substrate	Substrate	Substrate	Substrate	Substrate	Substrate	Substrate	Substrate	Weakly	Weakly	Substrate
HIA	96.19506	96.36896	96.36899	96.36899	96.60164	96.60166	96.60167	90.8658	90.01404	93.42031
MDCK	0.043502	0.0447331*	0.0451931*	0.0435102*	0.0182319*	0.0183021*	0.0180546*	0.047243	0.04344	0.064467
Pgp inhibition	Inhibitor	Inhibitor	Inhibitor	Inhibitor	Inhibitor	Inhibitor	Inhibitor	Inhibitor	Inhibitor	Non

Plasma Protein Binding	88.65461	93.67188	93.32756	94.28907	99.39824	99.63768	100	94.10524	84.40718	89.86259
Pure water solubility mgL	0.026166	0.002158	0.001228	0.001109	0.000829	0.000472	0.000426	0.224748	0.055328	0.513331
Skin Permeability	-2.38822	-2.65498	-2.64505	-2.66677	-2.62376	-2.62537	-2.6213	-3.23998	-3.5566	-3.7786
Solvation Free Energy	- 25.820000 **	- 12.100000 **	- 12.100000 **	- 12.100000 **	- 13.100000 **	- 13.100000 **	- 13.100000 **	- 22.700000 **	- 25.540000 **	- 6.440000 **

Compound no.	2a	2b	2c	2d	2e	2f	2g	2h	2i	2j
AlogP98 value	5.3875	6.3919	6.3919	6.3919	6.5599	6.5599	6.5599	4.5283	4.4955	3.6401
AMolRef	160.4953	141.2477	141.2477	141.2477	146.8837	146.8837	146.8837	135.0263	147.9527	116.2697
BBB	1.05107	2.81972	3.13952	2.93252	3.13912	3.4388	3.25281	0.24095	0.218408	0.074378
Buffer solubility mgL	18.0335	14.7251	16.6978	46.9071	2.96619	3.36356	9.44884	245.893	237.264	1284.36
Caco2	28.7517	30.8004	29.4757	29.7181	33.6693	32.4796	32.6798	20.6125	20.659	22.3748
CYP_2C19 inhibition	Non	Non	Non	Non	Non	Non	Non	Non	Non	Non
CYP_2C9 inhibition	Inhibitor	Inhibitor	Inhibitor	Inhibitor	Inhibitor	Inhibitor	Inhibitor	Inhibitor	Inhibitor	Inhibitor

CYP_2D6 inhibition	Non	Non	Non	Non	Non	Non	Non	Non	Non	Non
CYP_2D6 substrate	Weakly	Weakly	Weakly	Weakly	Weakly	Weakly	Weakly	Weakly	Weakly	Substrate
CYP_3A4 inhibition	Non	Non	Non	Non	Non	Non	Non	Inhibitor	Inhibitor	Non
CYP_3A4 substrate	Substrate	Substrate	Substrate	Substrate	Substrate	Substrate	Substrate	Weakly	Weakly	Substrate
HIA	96.19506	96.36896	96.36899	96.36899	96.60164	96.60166	96.60167	90.8658	90.01404	93.42031
MDCK	0.043502	0.0447331*	0.0451931*	0.0435102*	0.0182319*	0.0183021*	0.0180546*	0.047243	0.04344	0.064467
Pgp inhibition	Inhibitor	Inhibitor	Inhibitor	Inhibitor	Inhibitor	Inhibitor	Inhibitor	Inhibitor	Inhibitor	Non
Plasma Protein Binding	88.65461	93.67188	93.32756	94.28907	99.39824	99.63768	100	94.10524	84.40718	89.86259
Pure water solubility mgL	0.026166	0.002158	0.001228	0.001109	0.000829	0.000472	0.000426	0.224748	0.055328	0.513331
Skin Permeability	-2.38822	-2.65498	-2.64505	-2.66677	-2.62376	-2.62537	-2.6213	-3.23998	-3.5566	-3.7786
Solvation Free Energy	-25.820000**	-12.100000**	-12.100000**	-12.100000**	-13.100000**	-13.100000**	-13.100000**	-22.700000**	-25.540000**	-6.440000**

Table.8. Toxicity predictions of all the compounds using PROTOX-II software.

Compound No.	Predicted LD₅₀ Mg\Kg	Class Of Toxicity	Hepato Toxicity	Carcino Genicity	Immuno Genicity	Muta Genicity	Cyto Toxicity
1a	2500	5	INACTIVE	ACTIVE	INACTIVE	INACTIVE	INACTIVE
1b	2500	5	ACTIVE	INACTIVE	INACTIVE	INACTIVE	INACTIVE
1c	2500	5	ACTIVE	INACTIVE	INACTIVE	INACTIVE	INACTIVE
1d	2500	5	ACTIVE	INACTIVE	INACTIVE	INACTIVE	INACTIVE
1e	1500	4	ACTIVE	INACTIVE	INACTIVE	INACTIVE	INACTIVE
1f	2500	5	ACTIVE	INACTIVE	INACTIVE	INACTIVE	INACTIVE
1g	1500	4	ACTIVE	INACTIVE	INACTIVE	INACTIVE	INACTIVE
1h	1500	4	ACTIVE	ACTIVE	INACTIVE	INACTIVE	INACTIVE
1i	1000	4	ACTIVE	ACTIVE	INACTIVE	INACTIVE	INACTIVE
1j	1860	4	ACTIVE	ACTIVE	INACTIVE	INACTIVE	INACTIVE
2a	2500	5	INACTIVE	ACTIVE	INACTIVE	INACTIVE	INACTIVE
2b	2500	5	ACTIVE	INACTIVE	INACTIVE	INACTIVE	INACTIVE
2c	2500	5	ACTIVE	INACTIVE	INACTIVE	INACTIVE	INACTIVE
2d	2500	5	ACTIVE	INACTIVE	INACTIVE	INACTIVE	INACTIVE
2e	2000	4	ACTIVE	INACTIVE	INACTIVE	INACTIVE	INACTIVE
2f	2500	5	ACTIVE	INACTIVE	INACTIVE	INACTIVE	INACTIVE
2g	1500	4	ACTIVE	INACTIVE	INACTIVE	INACTIVE	INACTIVE
2h	1500	4	ACTIVE	ACTIVE	INACTIVE	INACTIVE	INACTIVE
2i	2500	5	ACTIVE	ACTIVE	INACTIVE	INACTIVE	INACTIVE
2j	2500	5	ACTIVE	ACTIVE	INACTIVE	INACTIVE	INACTIVE
Donepezil	505	4	INACTIVE	ACTIVE	ACTIVE	INACTIVE	ACTIVE

10.4. QSAR RESULT FOR NOVEL COMPOUNDS:

The descriptors were generated for the 20 designed compounds using PADEL software. Then predicted activity was calculated using model 3. (Table. 9) The results obtained were compared with the predicted activity of the compounds used in the QSAR study and also the predicted activity of the standard donepezil. The predicted activity resulted in the range of -1.36 to -1.06. The compounds 1g, 2g, 2j, and 2i exhibited -1.3064, -1.3636, -1.3353, and -1.2018 respectively as the predicted activity value in the model 3. Thus these compounds shows good activity.

Table.9 Predicted activity calculated using model 3 for the designed novel compounds.

Compound Name	nBr	ATSC6m	ATSC3i	MATS4e	nBase	Predicted Activity (Model 3)
1a	0	625.84205	-51.832613	-0.0078397	1	-1.0708881
1b	0	-659.23401	-36.001241	-0.0284933	1	-1.077619
1c	0	-906.68731	-38.951103	-0.0498585	1	-1.0497542
1d	0	-72.142209	-38.951103	-0.0811375	1	-1.1605997
1e	2	-1880.6691	-30.389263	-0.0206806	1	-1.1289626
1f	2	-2326.5688	-38.734764	-0.0439669	1	-1.0430077
1g	2	68.874231	-38.734764	-0.0712018	1	-1.3064016
1h	0	-143.46805	-43.875088	-0.0204115	1	-1.0638519
1i	0	-209.09382	-42.2832	-0.1047833	1	-1.1429537
1j	0	-141.41035	-22.775256	-0.1200234	1	-1.3074266
2a	0	711.20487	-41.178983	0.0546853	1	-1.1035081
2b	0	-296.67749	-26.120249	0.0241219	1	-1.1409188
2c	0	-553.66825	-29.070111	0.0126975	1	-1.1033951
2d	0	242.72699	-29.070111	-0.0127495	1	-1.2053186
2e	2	-1269.7916	-20.110447	0.0418849	1	-1.2113249
2f	2	-1737.5388	-28.455948	0.0287311	1	-1.1143123
2g	2	570.51472	-28.455948	0.0075466	1	-1.3636689
2h	0	63.38124	-34.085953	0.023075	1	-1.1188953
2i	0	-1.9947257	-31.966928	-0.0612063	1	-1.2018436
2j	0	101.6298	-15.00386	-0.0585098	1	-1.3353714
Donepezil	0	-645.05935	-24.83885	-0.03012158	1	-1.16306

10.5. DOCKING RESULTS:

20 ligands were docked against the acetylcholinesterase enzyme. The enzyme 4EY7 obtained from PDB is prepared by the procedure as discussed above. Also, the ligands were prepared for docking. The docking using the Autodock 1.5.6 software was carried out. The binding energy by ranking along with the ligand efficiency, inhibition constant, intermolecular energy, desolvation, electrostatic, torsional, and total internal energies of the ranked docking pose. All these energies were recorded for the best fit of the model for all the 20 compounds (Table. 10). The binding energies of the compounds ranged between -8.56 to -3.2 kcal/mol. The compound 1j shows the highest binding energy of -8.5 kcal/mol. The compounds 2a, 2b, 2c, 2d, and 2f exhibited the best binding energies of -8.28, -8.17, -8.07, -8.38, and -8.56 kcal/mol respectively. These compounds 1a, 1d, 1e, and 1f show more inhibition constant values of 728.45, 327.84, 210.31, and 221.54 respectively. The ligand efficiency of the compounds ranges from -0.28 to 29.77. The compound 1a with maximum inhibition constant binds AchE with the binding energy of -4.28 kcal/mol.

The interactions between the target AchE and the ligands visualized by BIOVIA Discovery Studio were recorded in the table 11. The interactions with the acetylcholinesterase were based on two main positions in the gorge of the target. The positions include the catalytic anionic site (CAS) and the peripheral anionic site (PAS). [48-51] (Figure. 8). The amino acids TRP 286, TYR 72, TYR 341, ASP 494, ASP 320, ASP 74, ASN 283, ASN 317, ASN 533, ASN 283, GLN 291, GLN 361, and GLN 527 constitute the anionic gorge at the peripheral position. The TRP 286 residue is attached with the ligands 1c, 1d, 2a, 2b, 2c, 2d, 2h, and 2g through stacking interaction of the pi bond, whereas in compounds 1a, 1e, 1g, 1i, and 1j bonded through Vander Waals interaction. The compounds 2d, 2g, 2h, 2i, 2j, and 1d were bonded to TYR 72 and TYR 341 through van der Waals interaction. The residues TYR 72 by vander waals and TYR 341 by stacking pi bonds to the ligands 1a, 2b, and 2c were observed. The aspartic acid and the asparagine residues were bonded by either van der Waals or hydrogen bonding. The GLN 291 residue is bonded by van der Waals interaction with the ligands 1a, 1c, 1d, 1g, 2a, 2d, and 2j. Most of the compounds that are involved in the PAS binding region were exhibited around the nitrogen atoms of the benzamide and the carbazide moieties of the compounds. The catalytic anionic site residues namely SER 293, HIS 287, and GLU 292 were bonded to the compounds 1g, 2g, 2j, and 2i by van der Waals interaction. This CAS binding is exhibited by the piperidone nucleus with the AchE. The binding of both CAS and PAS increases the ligand specificity. This kind of dual binding capacity is present in the

compounds 1g, 2g, 2j, and 2i (Figure. 9 - 12) which shows binding energies of -5.69, -7.2, -6.54, and -6.54 kcal/mol respectively. [49 – 52]

Table.10. Docking results of all the compounds using Autodock4.0 software.

Compound name	Binding energy (kcal/mol)	Ligand efficiency	Inhibition constant (μM)	Inter-molecular energy	Desolvation energy	Electro-static energy	Total internal energy	Torsional energy
1a	-4.28	-0.11	728.45	-6.67	-6.28	-0.38	2.32	2.39
1b	-6.17	29.77	-7.96	-7.96	-7.48	-0.48	-1.52	1.79
1c	-5.24	-0.15	143.37	-7.03	-6.41	-0.63	-2.61	1.79
1d	-4.75	-0.14	327.84	-6.54	-5.9	-0.64	-2.55	1.79
1e	-5.02	-0.15	210.31	-6.81	-6.26	-0.54	-2.46	1.79
1f	-4.99	-0.15	221.54	-6.78	5.73	-1.04	-1.42	1.79
1g	-5.69	-0.17	67.42	-7.48	-6.91	-0.57	-2.55	1.79
1h	-3.99	-0.12	1.19	-6.38	-5.43	-0.95	-4.15	2.39
1i	-3.2	-0.08	4.5	-6.18	-6.01	-0.18	2.97	2.98
1j	-8.5	-0.28	591.16nM	-10.29	-9.83	-0.46	-2.74	1.79
2a	-8.28	-0.22	852.53nM	-10.07	-9.32	-0.75	-1.26	1.79
2b	-8.17	-0.24	1.02	-9.37	-8.74	-0.62	-2.07	1.19
2c	-8.07	-0.24	1.22	-9.26	-8.66	-0.61	-1.08	1.19
2d	-8.38	-0.25	714.15nM	-9.58	-8.94	-0.64	-0.6	1.19
2e	-5.04	-0.15	200.72	-6.24	-5.83	-0.4	-2.54	1.19
2f	-8.56	-0.25	535.56nM	-9.75	-8.94	-0.81	-1.17	1.19
2g	-7.2	-0.21	5.29	-8.99	-8.37	-0.62	-2.65	1.79
2h	-7.54	-0.22	2.96	-9.33	-8.59	-0.75	-1.98	1.79
2i	-6.54	-0.17	16.04	-8.93	-8.16	-0.77	-2.42	2.39
2j	-6.54	-0.22	16.18	-7.73	-7.17	-0.56	-1.9	1.19
Donepezil	-5.72	-0.2	64.25	-7.51	-7.51	0	-1.92	1.79

Table.11. Docking interaction results of all the compounds using Biovia Discovery Studio 19.1.0 software.

COMPOUND NAME	VAN DER WAALS	CONVENTIONAL HYDROGEN BOND	CARBON HYDROGEN BOND	STACKED INTERACTION	OTHERS
DONEPEZIL	VAL A:294, ARG A:296, PHE A:297, TYR A:124, HIS A:447, GLY A:448,		TYR A:72, SER A:293	TRP A:86	TRP A:286, TYR A:341, PHE A:338, TYR A:337

	GLU A:202, SER A:203, GLY A:121				
1a	GLN A:291, TRP A:286, ASN A:283, TYR A:72, VAL A:340, GLY A:342		LEU A:289, VAL A:282	TYR A:341	LEU A:76, GLU A:292, HIS A:287
1b	SER A:371, ARG A:296, PRO A:368, TRP A:532, GLU A:313	GLN A:369			LEU A:540, VAL A:370, HIS A:405, PRO A:235, PRO A:537, LEU A:536
1c	GLN B:291, SER B:293, TYR B:341, VAL B:94, TYR B:7, LEU B:76, GLY B:342, PRO B:344			TRP B:286	GLU B:292, LEU B:289
1d	TYR B:12, TYR B:72, THR B:75, GLY B:342, VAL B:340, LEU B:76, SER B:293, GLU B:292, GLN B:291, VAL B:294, PHE B:295, PHE B:297	TYR B:341		TRP B:286	LEU B:289, PHE B:338
1e	TRP B:286, HIS B:287, LEU B:289, ALA B:361, PRO B:290	GLN B:291			GLU B:292, VAL B:365, ARG B:364
1f	ASN A:317, THR A:311, VAL A:303, GLU A:243, GLY A:242, THR A:238, PRO A:235	MET A:241	GLY A:240		GLU A:313, ALA A:314
1g	PRO A:290, GLU A:292, GLN A:291, TYR A:341, SER A:293	LEU A:289	HIS A:287		
1h	LEU A:518, LEU A:515, PRO A:498, TYR A:479, ASP A:494	GLU A:491, ARG A:478			PRO A:492, PRO A:517, ARG A:475

1i	HIS A:322, PHE A:321, LEU A:213, GLY A:319, PRO A:216, LEU A:214	ASP A:320	ARG A:219, GLY A:220		ALA A:318, LEU A:315
1j	GLN B:527, GLY B:523, TYR B:510, LYS B:332, VAL B:331, VAL B:330, LEU B:524, GLU B:431	ARG B:525, ARG B:522, ARG B:521			VAL B:429, VAL B:408, ALA B:526, LEU B:386
2a	PHE A:297, PHE A:338, PHE A:295, VAL A:294, ARG A:296, GLN A:291, LEU A:289, HIS A:287, GLY A:342, PHE A:346, VAL A:340, SER A:347, TYR A:77, TYR A:124	SER A:293	TYR A:124		GLY A:292, TRP A:286, TYR A:341, LEU A:76
2b	VAL B:340, LEU B:76, TYR B:72, PHE B:297, PHE B:338, PHE B:295, ARG B:296, LEU B:289, GLU B:292, SER B:293, GLY B:342			TYR B:124, TRP B:286, TYR B:341	VAL B:294
2c	PHE B:297, PHE B:295, TYR B:124, TYR B:72, ALA B:343, PHE B:346, VAL B:340, GLY B:342			TRP B:286	LEU B:289, TY B:341, LEU B:76
2d	LEU B:76, SER B:293, GLU B:292, GLN B:291, VAL B:294, PHE B:295, PHE B:297, TYR B:124, TYR B:72, GLY B:342, THR B:75, VAL B:340	TYR B:341		TRP B:286	LEU B:289
2e	ARG A:296, VAL A:370, PRO A:235, HIS A:405, TRP A:532, GLU A:313, ASN A:533				LEU A:540, LEU A:536, PRO A:537

2f	GLY B:342, TYR B:341, VAL B:294, PHE B:346, SER B:347, LEU B:76, GLU B:292, TYR B:77, VAL B:340	SER B:293		TRP B:286	LEU B:289
2g	GLY A:342, TYR A:341, VAL A:294, ARG A:296, PHE A:295, SER A:293, HIS A:287, LEU A:289, GLU A:292, TYR A:72, ASP A:74	THR A:75		TRP A:286	LEU A:76
2h	PHE B:338, PHE B:297, PHE B:295, VAL B:294, LEU B:289, GLU B:292, TYR B:72, GLY B:342, LEU B:76, VAL B:340	TYR B:341, ARG B:296		TRP B:286	SER B:293
2i	PRO A:344, VAL A:340 TRP A:286, LEU A:289, HIS A:287, GLU A:292, VAL A:294, TYR A:72	PHE A:346, GLY A:342, THR A:75, TYR A:341, SER A:293	ALA A:343		LEU A:76
2j	ASN A:283, VAL A:282, TYR A:72, HIS A:287, TYR A:341, PHE A:295, SER A:293, ARG A:296, GLU A:292		GLN A:291, TRP A:286		LEU A:289, VAL A:294

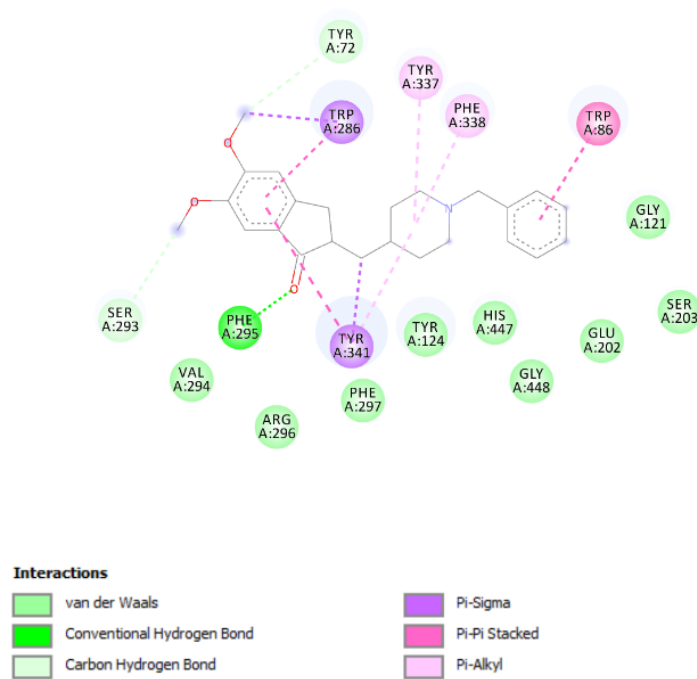


Figure 8. Interaction between standard donepezil and the acetylcholinesterase enzyme (PDB ID: 4EY7)

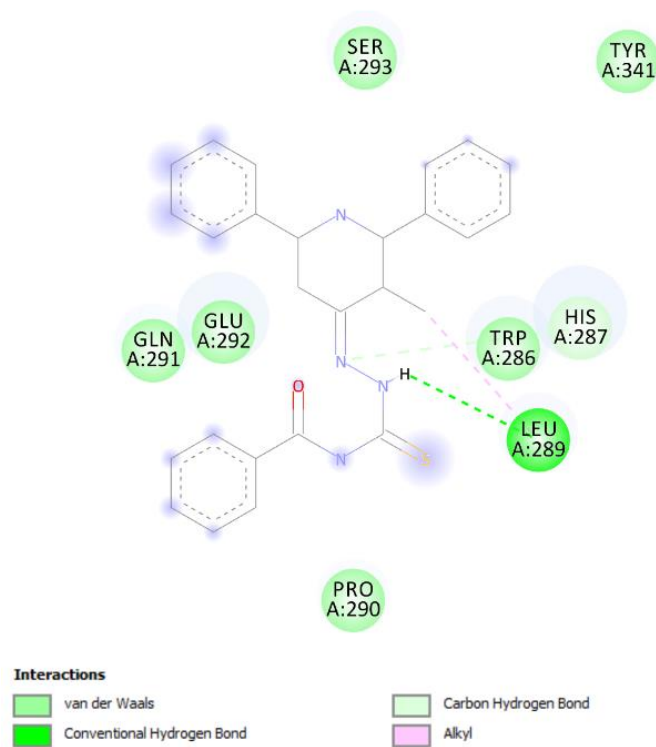


Figure 9. Interaction between compound 1g and the acetylcholinesterase enzyme (PDB ID: 4EY7)

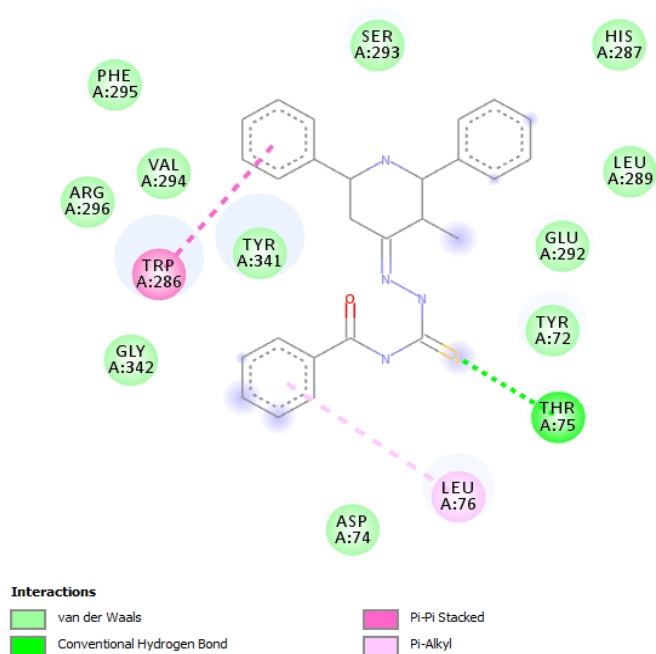


Figure 10. Interaction between compound 2g and the acetylcholinesterase enzyme (PDB ID: 4EY7)

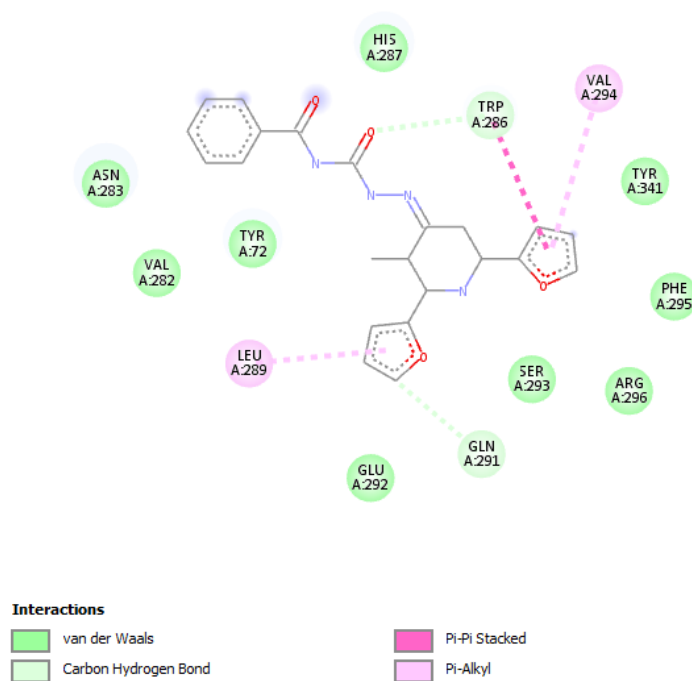


Figure 11. Interaction between compound 2j and the acetylcholinesterase enzyme (PDB ID: 4EY7)

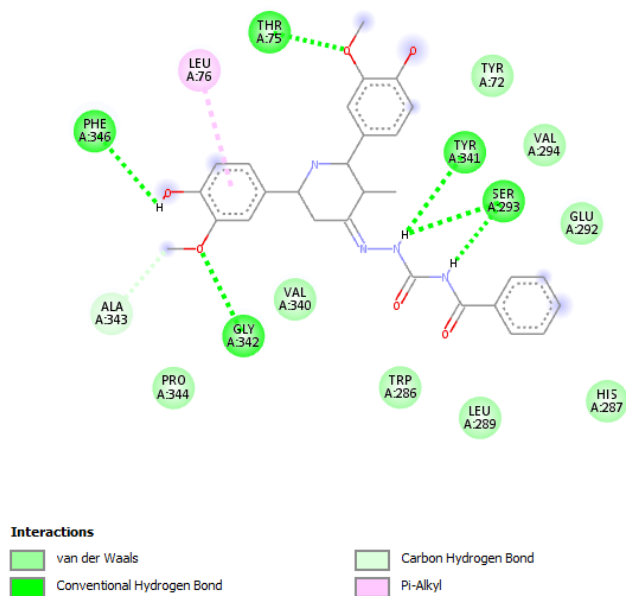


Figure 12. Interaction between compound 2i and the acetylcholinesterase enzyme (PDB ID: 4EY7)

10.6. SYNTHESIS:

The synthesis of 1a, 1b, 1d, 1i, and 1h compounds were carried out by the conventional procedure given in the scheme.1. All the chemicals were purchased from Sigma Aldrich in an analytical grade. Compounds contain benzamide fused with the 4-piperidone linked by thiosemicarbazide. The compounds produced a yield in the range of 72-91% (table.12). The products formed were confirmed by TLC. The R_f values were given in the table. 12. All the 5 compounds were characterized by FT-IR spectroscopy. The compounds 1a, 1d, 1i, and 1h were analyzed by ^1H and ^{13}C NMR spectroscopy. The compound 1d and 1i was confirmed by MASS spectroscopy.

Table.12. Properties of the synthesized compounds.

Compound no	Yield %	Melting point °C	R_f	Solubility				
				Water	Ethanol	DMSO	Ether	Chloroform
1a	78	252-263	0.63	-	+	++	+	++
1b	72	235-248	0.71	-	+	++	+	++
1d	91	245-267	0.82	-	+	++	+	++
1h	85	238-251	0.73	-	+	++	+	++
1i	89	249-265	0.72	-	+	++	+	++

Insoluble, + partially soluble, ++ soluble

10.7. CHARACTERISATION OF SYNTHESIZED COMPOUNDS:

Characterization of 1-benzoyl-3-[[**(4Z)**-2,6-bis[4-(dimethylamino)phenyl]-3-methylpiperidin-4-ylidene]amino}thiourea (**1a**)

Yield 78%, brown solid, FTIR (KBr, cm^{-1}) 3371 (-NH Stretching), 3150.20 (=C-H str, Aromatic), 1669.72 (C=O Amide), 1585.86 (C=C Aromatic), 1223.43 (C=S), 1062.25 (C-N Stretching), 816.27 (C-H bending)

Characterization of 1-benzoyl-3-[[**(4Z)**-2,6-bis(2-chlorophenyl)-3-methylpiperidin-4-ylidene]amino}thiourea (**1b**)

Yield 72%, white solid, FTIR (KBr, cm^{-1}) 3375.12 (-NH Stretching), 3169.77 (=C-H str, Aromatic), 1652.95 (C=O Amide), 1534.62 (C=C Aromatic), 1263.50 (C=S), 1107.90 (C-N Stretching), 828.39 (C-H bending), 748.26 (C-Cl)

Characterization of 1-benzoyl-3-[[**(4Z)**-2,6-bis(4-chlorophenyl)-3-methylpiperidin-4-ylidene]amino}thiourea (**1d**)

Yield 91%, yellow solid, FTIR (KBr, cm^{-1}) 3279.7 (-NH Stretching), 3162.31 (=C-H str, Aromatic), 2979.70 (C-H Stretching), 1718.17 (C=O Amide), 1597.04 (N-H bending), 1283.06 (C=S), 815.34 (C-H bending), 679 (C-Cl) M^+ peak for $\text{C}_{30}\text{H}_{36}\text{N}_6\text{OS}$ is found 511.28.

Characterization of 1-benzoyl-3-[[**(4Z)**-2,6-bis(2-hydroxyphenyl)-3-methylpiperidin-4-ylidene]amino}thiourea (**1h**)

Yield 85%, white solid, FTIR (KBr, cm^{-1}) 3441.82 (O-H Stretching), 3317.91 (-NH Stretching), 3157.36 (=C-H str, Aromatic), 2987.15 (C-H Stretching), 1619.41 (C=O Amide), 1265.36 (C=S), 1112.56 (C-N Stretching), 828.39 (C-H bending), 749.19 (C=C bending)

Characterization of 1-benzoyl-3-[[**(4Z)**-2,6-bis(4-hydroxy-3-methoxyphenyl)-3-methylpiperidin-4-ylidene]amino}thiourea (**1i**)

Yield 89%, reddish orange solid, FTIR (KBr, cm^{-1}) 3433.44 (O-H Stretching), 3153 (=C-H str, Aromatic), 2967.59 (C-H Stretching), 1653.88 (C=O Amide), 1596.12 (C=C Stretching), 1273.74 (C=S), 1025.91 (C-O Stretching), 814.41 (C-H bending) M^+ peak for $\text{C}_{30}\text{H}_{36}\text{N}_6\text{OS}$ is found 534.18.

11. REFERENCES:

1. Lombardino, J., Lowe, J. The role of the medicinal chemist in drug discovery — then and now. *Nat Rev Drug Discov* **3**, 853–862 (2004). <https://doi.org/10.1038/nrd1523>
2. Gao XH, Liu LB, Liu HR, Tang JJ, Kang L, Wu H, Cui P, Yan J. Structure–activity relationship investigation of benzamide and picolinamide derivatives containing dimethylamine side chain as acetylcholinesterase inhibitors. *Journal of enzyme inhibition and medicinal chemistry*. 2018 Jan 1; 33(1):110-4.
3. Mumtaz A, Shoaib M, Zaib S, Shah MS, Bhatti HA, Saeed A, Hussain I, Iqbal J. Synthesis, molecular modelling and biological evaluation of tetrasubstituted thiazoles towards cholinesterase enzymes and cytotoxicity studies. *Bioorganic chemistry*. 2018 Aug 1; 78:141-8.
4. Krátký M, Štěpánková Š, Hounghedji NH, Vosátka R, Vorčáková K, Vinšová J. 2-Hydroxy-N-phenylbenzamides and their esters inhibit acetylcholinesterase and butyrylcholinesterase. *Biomolecules*. 2019 Nov; 9(11):698.
5. Tuğrak M, Gül Hİ, Anil B, Gülçin İ. Synthesis and pharmacological effects of novel benzene sulfonamides carrying benzamide moiety as carbonic anhydrase and acetylcholinesterase inhibitors. *Turkish Journal of Chemistry*. 2020 Dec 16; 44(6):1601-9.
6. Raffa D, Daidone G, Plescia F, Schillaci D, Maggio B, Torta L. Synthesis and antifungal activity of new N-(1-phenyl-4-carboxypyrazol-5-yl)-, N-(indazol-3-yl)-and N-(indazol-5-yl)-2-iodobenzamides. *Il Farmaco*. 2002 Mar 1;57(3):183-7.
7. Tummino PJ, Harvey PJ, McQuade T, Domagala J, Gogliotti R, Sanchez J, Song Y, Hupe D. The human immunodeficiency virus type 1 (HIV-1) nucleocapsid protein zinc ejection activity of disulfide benzamides and benzisothiazolones: correlation with anti-HIV and virucidal activities. *Antimicrobial agents and chemotherapy*. 1997 Feb;41(2):394-400.
8. Yang X, Peng T, Yang Y, Li W, Xiong J, Zhao L, Ding Z. Antimicrobial and antioxidant activities of a new benzamide from endophytic *Streptomyces* sp. YIM 67086. *Natural product research*. 2015 Feb 16;29(4):331-5.
9. Vinitsky A, Michaud C, Powers JC, Orłowski M. Inhibition of the chymotrypsin-like activity of the pituitary multicatalytic proteinase complex. *Biochemistry*. 1992 Oct 1;31(39):9421-8.

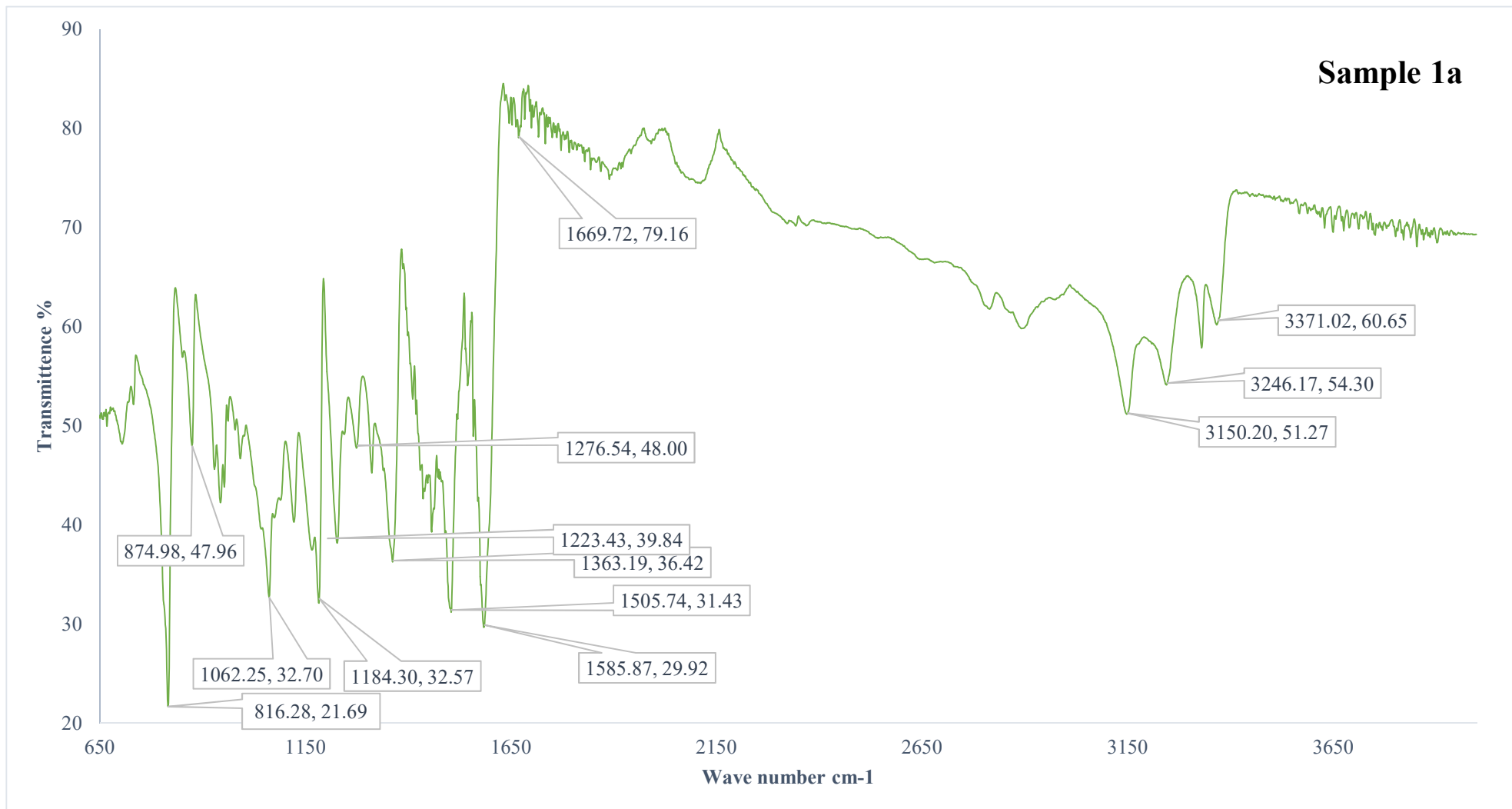
10. Ashton MJ, Cook DC, Fenton G, Karlsson JA, Palfreyman MN, Raeburn D, Ratcliffe AJ, Souness JE, Thurairatnam S, Vicker N. Selective type IV phosphodiesterase inhibitors as antiasthmatic agents. The syntheses and biological activities of 3-(cyclopentyloxy)-4-methoxybenzamides and analogs. *Journal of medicinal chemistry*. 1994 May;37(11):1696-703.
11. Bernstein PR. The Development of Cysteinyl Leukotriene Receptor Antagonists. Analogue-Based Drug Discovery III. 2012 Dec 19:211-39. Wilkerson WW, Akamike E, Cheatham WW, Hollis AY, Collins RD, DeLuca I, Lam PY, Ru Y. HIV protease inhibitory bis-benzamide cyclic ureas: a quantitative structure– activity relationship analysis. *Journal of medicinal chemistry*. 1996 Oct 11;39(21):4299-312.
12. Aliabadi A, Mohammadi-Farani A, Bistouni JR. Synthesis and acetylcholinesterase inhibitory assessment of benzamide derivatives incorporated piperazine moiety as potential anti-Alzheimer agents. *Journal of Pharmaceutical Sciences and Research*. 2017 Sep 1;9(9):1598.
13. Strange PG. The structure and mechanism of neurotransmitter receptors. Implications for the structure and function of the central nervous system. *Biochemical Journal*. 1988 Jan 15; 249(2):309.
14. Herlenius E, Lagercrantz H. Neurotransmitters and neuromodulators during early human development. *Early human development*. 2001 Oct 1; 65(1):21-37.
15. H Ferreira-Vieira T, M Guimaraes I, R Silva F, M Ribeiro F. Alzheimer's disease: targeting the cholinergic system. *Current neuropharmacology*. 2016 Jan 1; 14(1):101-15.
16. Taylor P, Brown JH. Synthesis, storage and release of acetylcholine. In *Basic Neurochemistry: Molecular, Cellular and Medical Aspects*. 6th edition 1999. Lippincott-Raven.
17. Lane RM, Potkin SG, Enz A. Targeting acetylcholinesterase and butyrylcholinesterase in dementia. *International Journal of Neuropsychopharmacology*. 2006 Feb 1; 9(1):101-24.
18. Colovic MB, Krstic DZ, Lazarevic-Pasti TD, Bondzic AM, Vasic VM. Acetylcholinesterase inhibitors: pharmacology and toxicology. *Current neuropharmacology*. 2013 May 1; 11(3):315-35.
19. Sharma K. Cholinesterase inhibitors as Alzheimer's therapeutics. *Molecular medicine reports*. 2019 Aug 1; 20(2):1479-87.

20. Radi Z, Taylor P. Structure and function of cholinesterases. In *Toxicology of Organophosphate & Carbamate Compounds* 2006 Jan 1 (pp. 161-186). Academic Press
21. Ballard CG, Greig NH, Guillozet-Bongaarts AL, Enz A, Darvesh S. Cholinesterases: roles in the brain during health and disease. *Current Alzheimer Research*. 2005 Jul 1; 2(3):307-18.
22. Ballinger EC, Ananth M, Talmage DA, Role LW. Basal forebrain cholinergic circuits and signaling in cognition and cognitive decline. *Neuron*. 2016 Sep 21; 91(6):1199-218.
23. Bartus RT, Dean R3, Beer B, Lippa AS. The cholinergic hypothesis of geriatric memory dysfunction. *Science*. 1982 Jul 30; 217(4558):408-14.
24. Mufson EJ, Counts SE, Perez SE, Ginsberg SD. Cholinergic system during the progression of Alzheimer's disease: therapeutic implications. *Expert review of neurotherapeutics*. 2008 Nov 1; 8(11):1703-18.
25. Whitehouse PJ, Price DL, Struble RG, Clark AW, Coyle JT, Delon MR. Alzheimer's disease and senile dementia: loss of neurons in the basal forebrain. *Science*. 1982 Mar 5; 215(4537):1237-9.
26. Chen XQ, Mobley WC. Exploring the pathogenesis of Alzheimer disease in basal forebrain cholinergic neurons: converging insights from alternative hypotheses. *Frontiers in neuroscience*. 2019 May 7; 13:446.
27. Schachter AS, Davis KL. Alzheimer's disease. *Dialogues Clin Neurosci*. 2000 Jun; 2(2):91-100. doi: 10.31887/DCNS.2000.2.2/asschachter. PMID: 22034442; PMCID: PMC3181599.
28. Nayak, Sanchika & Kumar, Shyama & Goyal, P & Vyas, Bhupendra & Chauhan, Chetan Singh. (2019). QSAR : An Approach To Develop New Drug Molecule In The Field Of Medicinal Chemistry.
29. Ferreira L, dos Santos R, Oliva G, Andricopulo A. Molecular docking and structure-based drug design strategies. *Molecules*. 2015;20(7):13384-421.
30. Parlar S. Synthesis and cholinesterase inhibitory activity studies of some piperidinone derivatives. *Organic Communications*. 2019 Oct 1;12(4):209.
31. Pavadai P, Ramalingam S, Panneerselvam T, Kunjiappan S, Perumal P, Mani V, Saravanan G, Alagarsamy V, Ammunje DN, Chimakurthy J. Synthesis of piperidine-4-one Derivative

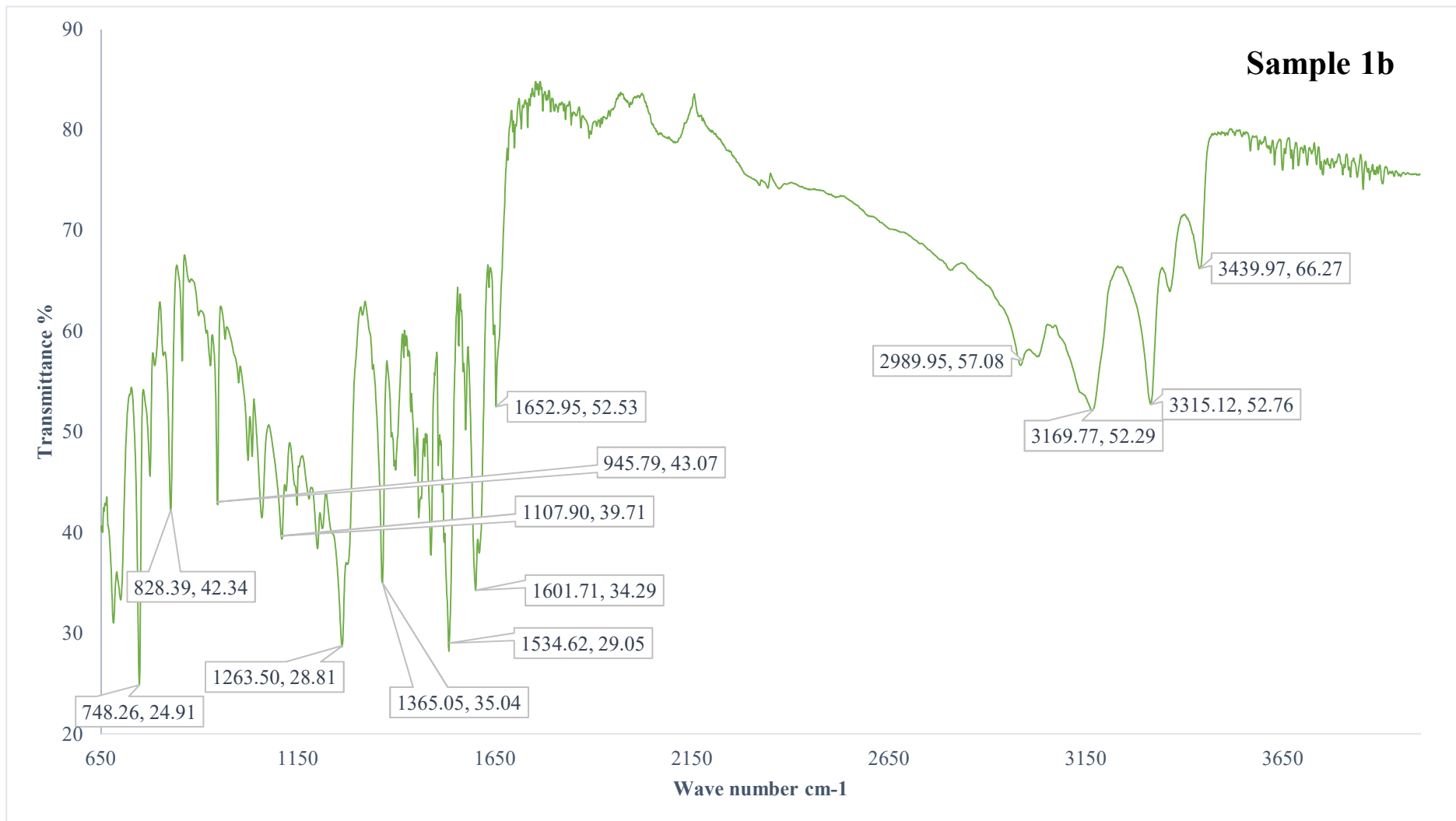
- Containing Dipeptide: An Acetyl cholinesterase and β -secretase Inhibitor. *Anti-Infective Agents*. 2020 Jun 1;18(2):160-8.
32. Caliendo G, Santagada V, Perissutti E, Severino B, Fiorino F, Warner TD, Wallace JL, Ifa DR, Antunes E, Cirino G, de Nucci G. Synthesis of substituted benzamides as anti-inflammatory agents that inhibit preferentially cyclooxygenase 1 but do not cause gastric damage. *European journal of medicinal chemistry*. 2001 Jun 1;36(6):517-30.
 33. Sonda S, Kawahara T, Murozono T, Sato N, Asano K, Haga K. Design and synthesis of orally active benzamide derivatives as potent serotonin 4 receptor agonist. *Bioorganic & medicinal chemistry*. 2003 Sep 15;11(19):4225-34.
 34. Asano T, Yoshikawa T, Usui T, Yamamoto H, Yamamoto Y, Uehara Y, Nakamura H. Benzamides and benzamidines as specific inhibitors of epidermal growth factor receptor and v-Src protein tyrosine kinases. *Bioorganic & medicinal chemistry*. 2004 Jul 1;12(13):3529-42.
 35. Anthwal A, Singh K, SM Rawat M, K Tyagi A, Haque A, Ali I, S Rawat D. Synthesis of 4-piperidone based curcuminoids with anti-inflammatory and anti-proliferation potential in human cancer cell lines. *Anti-Cancer Agents in Medicinal Chemistry (Formerly Current Medicinal Chemistry-Anti-Cancer Agents)*. 2016 Jul 1;16(7):841-51.
 36. Karthik N, Nithiya S, Jayabharathi J. Novel piperidone derivatives: synthesis, spectral and evaluation of antioxidant activity. *Int. J. Drug Devl. Res.* 2011 Apr;3(2):122-7.
 37. Krátký M, Štěpánková Š, Vorčáková K, Švarcová M, Vinšová J. Novel cholinesterase inhibitors based on O-aromatic N, N-disubstituted carbamates and thiocarbamates. *Molecules*. 2016 Feb;21(2):191.
 38. Canizares-Carmenate Y, Mena-Ulecia K, Perera-Sardiña Y, Torrens F, Castillo-Garit JA. An approach to identify new antihypertensive agents using Thermolysin as model: In silico study based on QSARINS and docking. *Arabian Journal of Chemistry*. 2019 Dec 1;12(8):4861-77.
 39. Molinspiration (2015) Calculation of Molecular Properties and Bioactivity Score. <http://www.molinspiration.com/cgi-bin/properties>
 40. Daina A, Michielin O, Zoete V. SwissADME: a free web tool to evaluate pharmacokinetics, drug-likeness and medicinal chemistry friendliness of small molecules. *Scientific reports*. 2017 Mar 3;7:42717.

41. S.K.Lee, G.S.Chang, I.H.Lee, J.E.Chung, K.Y.Sung, K.T.No, "[The PreADME: PC-BASED PROGRAM FOR BATCH PREDICTION OF ADME PROPERTIES](#)", EuroQSAR 2004, 2004, 9.5-10, Istanbul, Turkey.
42. S.K.Lee, I.H.Lee,H.J.Kim, G.S.Chang, J.E.Chung, K.T.No, "[The PreADME Approach: Web-based program for rapid prediction of physico-chemical, drug absorption and drug-like properties](#)", EuroQSAR 2002 Designing Drugs and Crop Protectants: processes, problems and solutions, 2003, pp. 418-420. Blackwell Publishing, Massachusetts, USA.
43. Banerjee P, Eckert AO, Schrey AK, Preissner R. ProTox-II: a webserver for the prediction of toxicity of chemicals. *Nucleic acids research*. 2018 Apr 30;46(W1):W257-63.
44. Michel F. Sanner. Python: A Programming Language for Software Integration and Development. *J. Mol. Graphics Mod.*, 1999, Vol 17, February. pp57-61
45. Rajesh P, Kumar MD, Kumar RS, Jamunarani R. Synthesis, Charecterization and Biological Activities Of N-(3-Methyl-2, 6-Diphenyl-Piperidin-4-Ylidine)-N'-Phenyl-Hydrazine. *J. Environ. Nanotechnol*. 2014;3(3):62-6.
46. Rastogi S, Rastogi H. An efficient synthesis of some substituted piperidin-4-one thiosemicarbazone derivatives as potential anticonvulsant under microwave irradiation.
47. <https://labmonk.com/synthesis-of-benzanilide-from-aniline>
48. Gramatica P, Chirico N, Papa E, Cassani S, Kovarich S. QSARINS: A new software for the development, analysis, and validation of QSAR MLR models.
49. H.M. Greenblatt, H. Dvir, I. Silman and J.L. Sussman, *Acetylcholinesterase*, *J. Mol. Neurosci*. 20 (2003), pp. 369–383.
50. Y. Bourne, P. Taylor, Z. Radić and P. Marchot, *Structural insights into ligand interactions at the acetylcholinesterase peripheral anionic site*, *EMBO J*. 22 (2003), pp. 1–12.
51. D. De Boer, N. Nguyen, J. Mao, J. Moore and E.J. Sorin, *A comprehensive review of cholinesterase modeling and simulation*, *Biomolecules*. 11 (2021), pp. 580.
52. F.J. Muñoz, R. Aldunate and N.C. Inestrosa, *Peripheral binding site is involved in the neurotrophic activity of acetylcholinesterase*, *Neuroreport*. 10 (1999), pp. 3621–3625

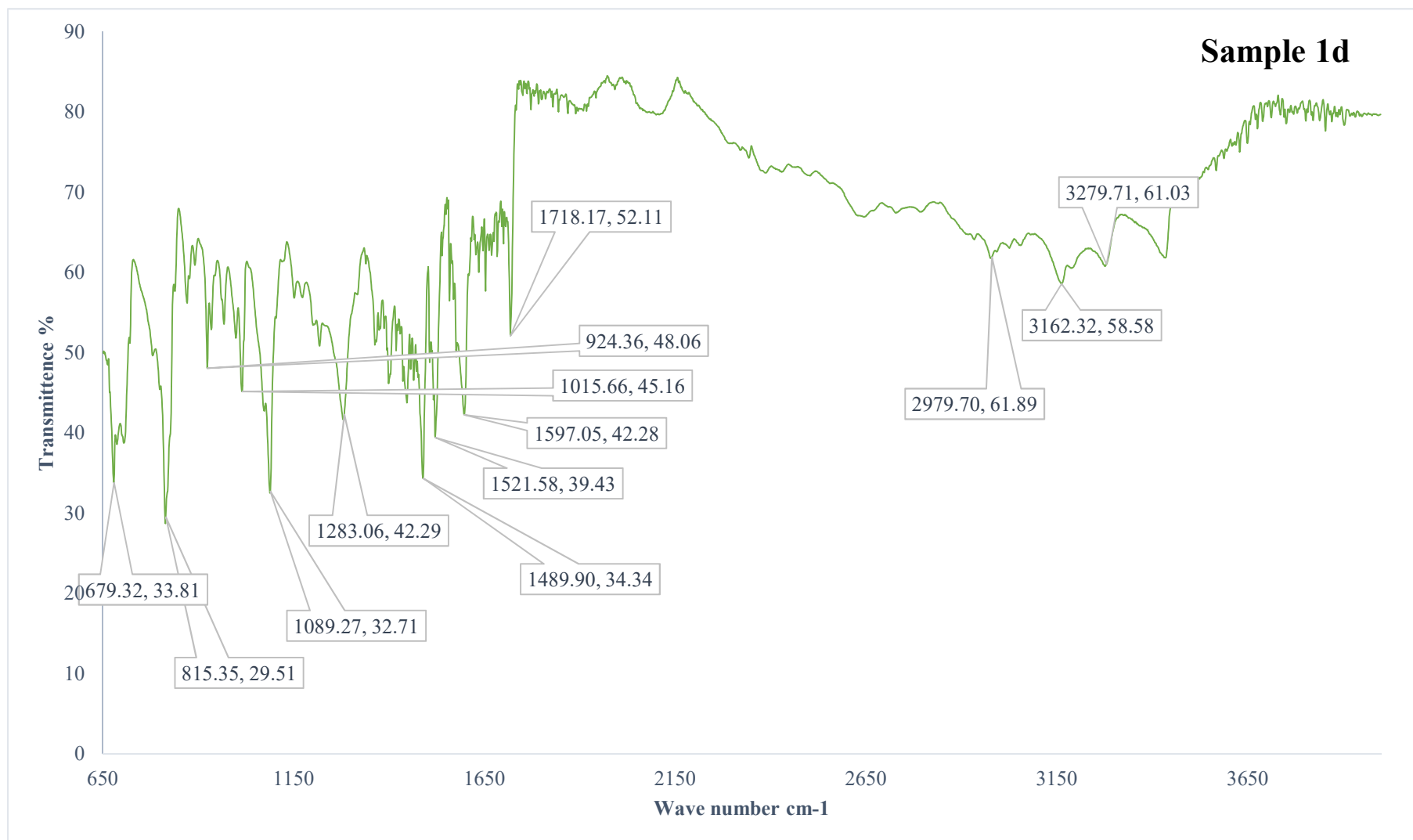
IR SPECTRUM – COMPOUND 1a



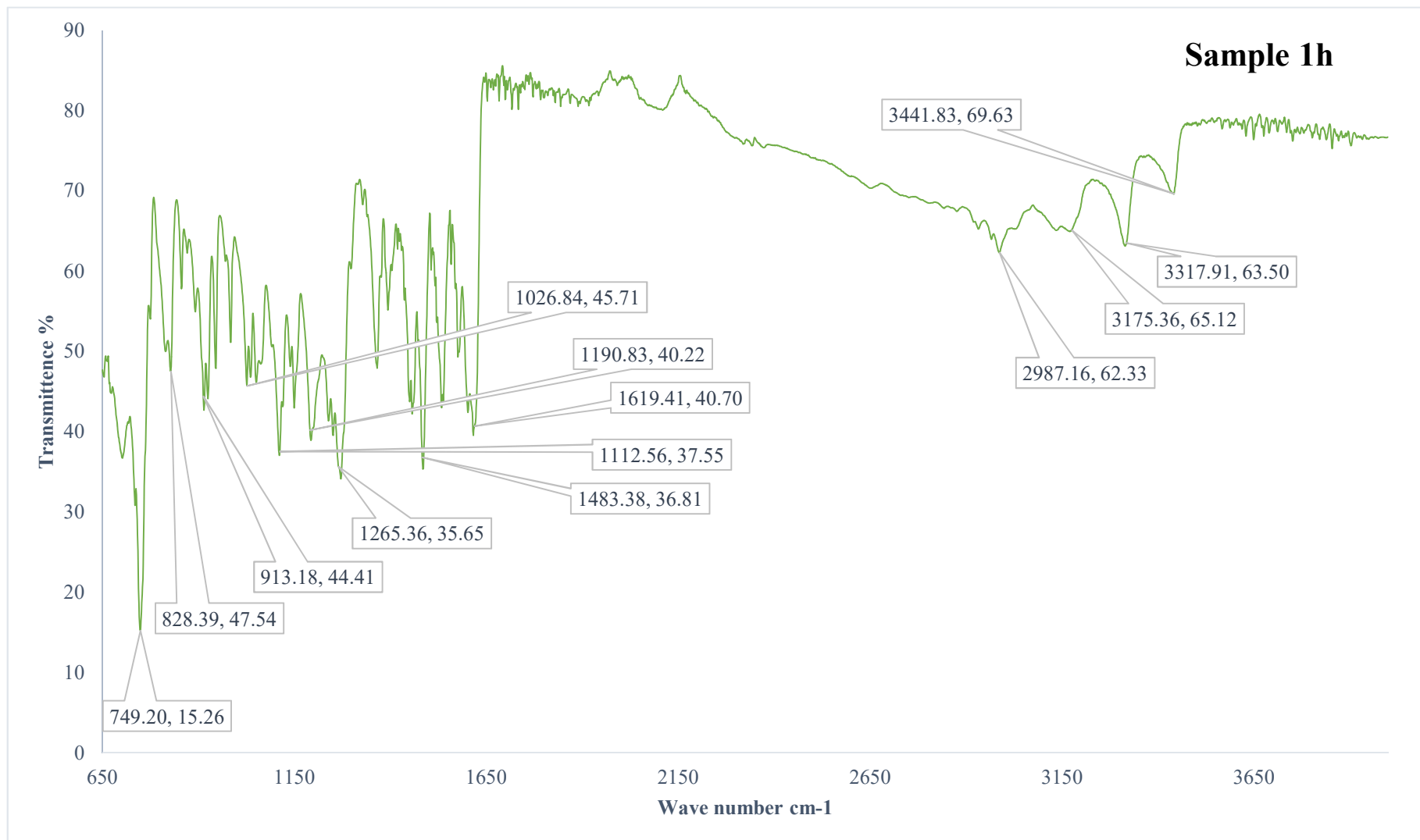
IR SPECTRUM – COMPOUND 1b



IR SPECTRUM – COMPOUND 1d



IR SPECTRUM – COMPOUND 1h



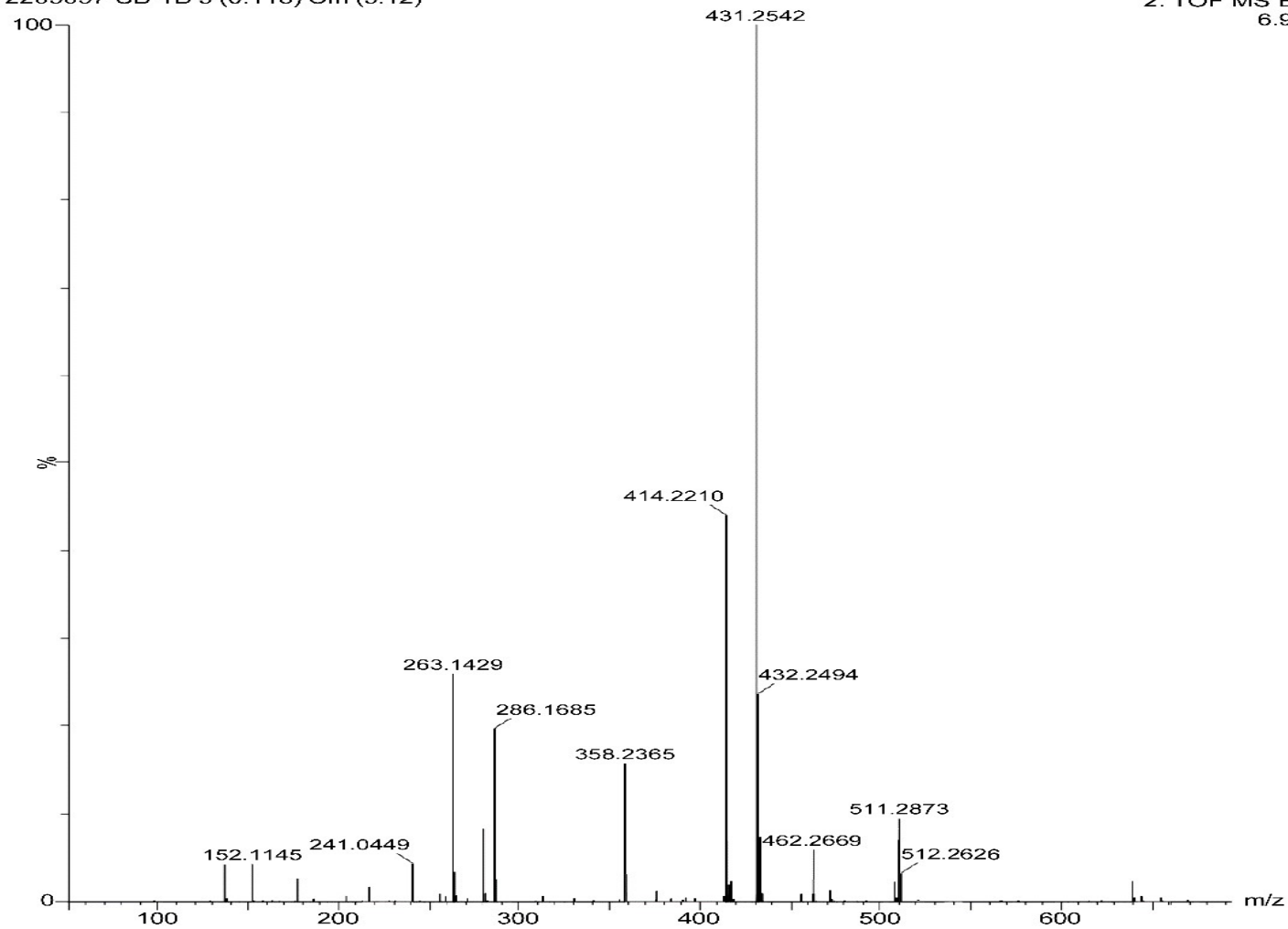
IR SPECTRUM – COMPOUND 1i



MASS SPECTRUM – COMPOUND 1d

2203057-SB-1D 3 (0.118) Cm (3:12)

2: TOF MS ES+
6.95e7



MASS SPECTRUM – COMPOUND 1i

2203057-SB-11 3 (0.118) Cm (3:12)

2: TOF MS ES+
6.95e7

